Actin Isoforms in Neuronal Structure and Function

A DISSERTATION
SUBMITTED TO THE FACULTY OF THE GRADUATE SCHOOL
OF THE UNIVERSITY OF MINNESOTA
BY

Thomas R. Cheever

IN PARTIAL FULFILLMENT OF THE REQUIREMENTS
FOR THE DEGREE OF
DOCTOR OF PHILOSOPHY

James M. Ervasti, Adviser

July, 2011

Acknowledgements

I would like to thank first and foremost my adviser Jim. Jim's support of me and this project has been unwavering the last five years. I will always be grateful for the opportunity to have worked with him and his willingness to let me follow my passion for studying neurons. I would also like to thank my undergraduate mentor Lihsia Chen. It was through Lihsia that I discovered my interest in neurons and axon guidance, and she has continued to be a mentor for me even in graduate school. Additionally, I would like to extend an extra special thanks to Lorene Lanier. Lorene has always been willing to answer my (many) questions and has been incredibly generous with her expertise and time. I am sincerely grateful for all the help and advice she has given me during my graduate work. Lastly, thank you to Emily Olson and Bin Li for sharing your brilliance and hard work with me. Your help was invaluable and means a lot to me.

I would also like to thank my friends both in and out of science. Kurt Prins has been a great friend both in and out of the lab. Brandon Goblirsch, Leah Randles, and Peder Cedervall have always been up for a lunch outing to ease the pain of failed experiments. I also have to thank my comrade in Gopher Hockey, Adam Engelhardt, for sticking it out the last couple of seasons and giving me something to look forward to on many cold Friday nights. To my incredible friends in rock n' roll, Jeff Williams and Tony Najm, thanks for giving this scientist the opportunity to shred guitars in addition to PCR tubes.

Finally, I have little doubt that I would not have survived the numerous setbacks, anxiety bouts, and broken ankles during graduate school without the incredible support of my family. It is difficult for me to express how grateful I am for their support and belief in me that I could do this even when on many days I was pretty sure I couldn't. Thank you from the bottom of my heart.

Dedication

I would like to dedicate this work to my grandparents, Bob, Char, Tom and Rosemary, and to my parents, Jeff and Colleen

Abstract

The actin cytoskeleton plays critical roles in nearly every aspect of neuronal development and function. During these processes, the localized polymerization of actin is one mechanism employed to carryout crucial tasks for normal neuronal function. While the activity of actin binding proteins is generally thought to be the primary mediator of spatially restricted actin polymerization, another prominent mechanism involves the local translation of β-actin, one of two actin isoforms expressed in neurons. The localized translation of β-actin has been shown previously to be essential for growth cone guidance in cultured neurons. Additionally, defects in the localization of β-actin have been implicated in the motor neuron disease Spinal Muscular Atrophy (SMA). However, no study to date has directly examined the role of β-actin in a mammalian *in vivo* system. Although the functions of β-actin were thought to be critical for all neurons, the work described in this thesis indicates that specific functions of β-actin are surprisingly confined to select populations in the central nervous system (CNS). β-actin is not required for motor axon regeneration or motor neuron function, but is required for the proper structure of the hippocampus, cerebellum, and corpus callosum, as well as hippocampal-associated behaviors. Thus, the work described here provides the first direct demonstration of specific roles for β-actin *in vivo* and presents a model to translate provocative findings in cell culture to the mammalian CNS.

Table of Contents

Table of Contents

Acknowledgements……..i

Dedication……ii

Abstract……...iii

Table of Contents……....iv

List of Figures……vi

Chapter 1 Introduction……1

Actin……2

Actin Isoforms……6

Distinct Regulation of Actin Isoforms……...11

Physiological Roles of Actin Isoforms……..15

Cytoplasmic Actin Isoforms in Neurons……15

Cytoplasmic Actin Isoforms in CNS Disease……23

Summary……27

Chapter 2 Axonal Regeneration and Neuronal Function are Preserved in Motor Neurons Lacking β-actin *in vivo*……..28

Introduction……30

Materials and Methods……...32

Results……39

Discussion……..60

Acknowledgements……62

Chapter 3 Ablation of β-actin in the Brain Causes Discrete Hippocampal Defects and Associated Behavioral Abnormalities……63

Introduction……65

Materials and Methods……...67

Results……74

Discussion……..94

Acknowledgements……98

Chapter 4 Conclusions and Future Directions……...99

References……111

Appendix

Actg1$^{-/-}$ Neurons do not Exhibit Morphological Abnormalities in Culture…….133

Localization of the Cytoplasmic Actin Isoforms in the Adult Mouse Brain…..136

Activity Levels of CNS-*Actb*KO Mice Over a 24-hour period……...141

Analysis of Olfactory Discrimination in CNS-*Actb*KO Mice…….143

References……146

List of Figures

Chapter 1

Figure 1.1: Actin filament properties *in vitro*……..4

Figure 1.2: The mammalian actin isoform family……...7

Figure 1.3: Attractive guidance cues induce zipcode-mediated local translation of β-actin in neuronal growth cones……...20

Chapter 2

Figure 2.1: Verification of β-actin ablation in motor neuron specific β-actin knock-out mice……48

Figure 2.2: β-actin is not required for motor neuron viability *in vivo.* ……..……..50

Figure 2.3: Neuromuscular junction development and morphology in *Actb*-MNsKO mice……52

Figure 2.4: *In vivo* muscle function of *Actb*-MNsKO mice……...……...54

Figure 2.5: Histological analysis of skeletal muscle in *Actb*-MNsKO mice…….55

Figure 2.6: Peripheral nerve regeneration is not impaired in *Actb*-MNsKO mice……57

Figure 2S.1: Characterization of motor neuron function in CNS-*Actb*KO mice……..59

Chapter 3

Figure 3.1: Conditional ablation of β-actin in the mouse central nervous system……81

Figure 3.2: Gross characterization of CNS-*Actb*KO mice…….83

Figure 3.3: Histological abnormalities in CNS-*Actb*KO brains…….85

Figure 3.4: CNS-*Actb*KO mice exhibit hyperactivity and decreased performance in the Morris water maze…….87

Figure 3.5: Characterization of primary hippocampal neurons from CNS-*Actb*KO mice and response to guidance cues ……..89

Figure 3S.1: Additional behavioral characterization of CNS-*Actb*KO mice……91

Figure 3S.2: Cortical layer histology in control and CNS-*Actb*KO mice…….93

Appendix

Figure A.1: *Actg1*$^{-/-}$ hippocampal neurons do not exhibit morphological abnormalities.....134

Figure A.2: Localization of cytoplasmic actin isoforms in the adult mouse brain…….139

Figure A.3: Activity of control and CNS-*Actb*KO over a 24-hour period……..142

Figure A.4: Analysis of Olfactory Discrimination in CNS-*Actb*KO mice……..145

Chapter 1

Introduction

Actin

Actin is one of the most abundant proteins in eukaryotic cells with critical direct or indirect roles in nearly every major cellular process. The protein actin itself is a 42 kilodalton ATPase composed of two symmetrical lobes with an adenine nucleotide and divalent cation binding cleft at the center (Kabsch et al., 1990). Actin has a higher affinity for ATP and Ca^{2+} than ADP and Mg^{2+}, however given the abundance of ATP and Mg^{2+} in the cytoplasm of most cells, ATP-actin with Mg^{2+} bound is the predominant species found in most cells (Wanger and Wegner, 1983; Carlier et al., 1986).

Actin Polymerization

Perhaps the best known property of actin is its ability to reversibly polymerize into double helical, polarized filaments with all subunits facing the same direction. The two ends of the actin filament are called the barbed and pointed end respectively. In an *in vitro* system, initiation of polymerization or nucleation of actin filaments is exceedingly slow due to the relatively weak interactions and instability of actin dimers. Only after the formation of an actin trimer does filament elongation become detectable, with elongation of filaments proceeding at a relatively rapid pace (Pollard, 1986a). Thus, actin nucleation via an actin trimer seed is the rate-limiting step in actin polymerization.

Once formed, actin filaments grow and shrink via the association and dissociation of monomers from both ends of the filaments. However, the rate of monomer association and dissociation differs at the two ends of the actin filament, and is dependent upon the nucleotide bound to actin (Pollard, 1986b). Association of ATP- or ADP actin is

diffusion limited at the barbed end, but ADP-actin dissociates nearly six times more rapidly than ATP-actin. Given the excess of ATP present in the cytoplasm of most cells, ATP-actin is thus the predominant species that polymerizes onto the barbed end. Association and dissociation of ATP- or ADP-actin at the pointed end occurs at relatively slower rates. Although generally regarded as dogma, recent studies have challenged the nucleotide-dependence of actin polymerization kinetics and suggest that the age of filaments may differentially affect their stability and rate of actin polymerization as well (Kueh et al., 2008).

One biochemical property of actin that is critical for understanding polymerization is the ratio of the dissociation rate constant (s^{-1}) to the association rate constant ($\mu M^{-1}s^{-1}$), a parameter best known as the critical concentration. When the concentration of free monomeric actin is at the critical concentration, the rate of actin monomer association and dissociation is equal, leading to no net filament growth. If the concentration of monomeric actin rises above or falls below the critical concentration, net polymerization or depolymerization results until the critical concentration of monomeric actin is reached. In a purified system and in the presence of ATP, the concentration of monomeric ATP-actin lies between the critical concentrations at the two ends of the filament, with the lower critical concentration at the barbed end (Pollard and Borisy, 2003). Thus, there is net polymerization at the barbed end and net depolymerization at the pointed end resulting in a phenomenon known as treadmilling. During treadmilling, individual actin monomers within a filament do not move relative to the substrate, but the filament as a whole advances due to continued polymerization of monomers onto the

barbed end and depolymerization at the pointed end. Following polymerization, the ATPase activity of actin is activated resulting in the rapid hydrolysis of ATP and relatively slower release of the γ-phosphate (Carlier et al., 1986; Blanchoin and Pollard, 2002). Because of the treadmilling of actin filaments, ADP-actin is thus the predominant species present and dissociating at the pointed end of filaments.

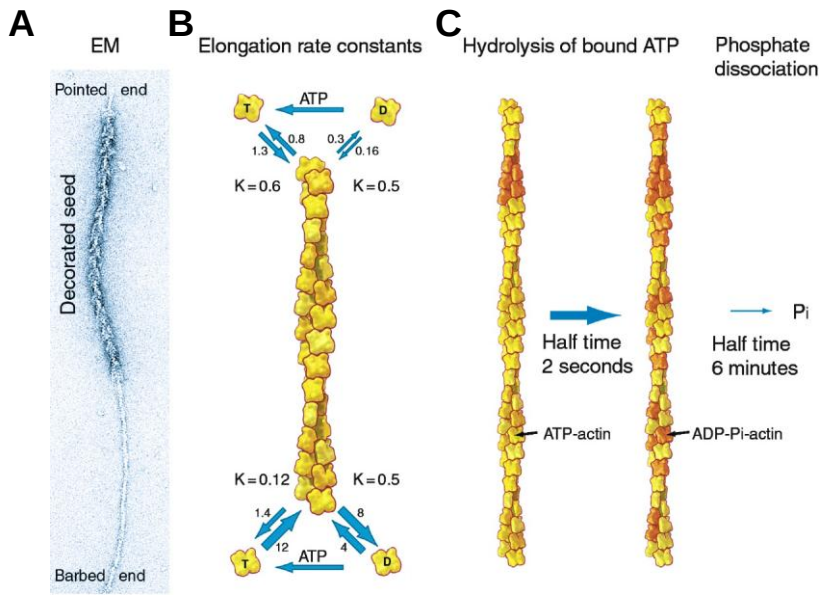

Figure 1.1: Actin filament properties *in vitro*. (A) Electron microscope image of an actin filament decorated with myosin subfragment 1 to reveal the intrinsic polarity of actin filaments. **(B)** Association ($\mu M^{-1}s^{-1}$) and dissociation (s^{-1}) rate constants for ATP- and ADP-actin at the barbed and pointed end of actin filaments. The ratio of the dissociation rate constant to the association rate constant gives the dissociation equilibrium constant, or critical concentration (K, in μM). **(C)** The ATPase activity of actin is activated upon polymerization, leading to rapid hydrolysis of ATP but significantly slower release of the γ-phosphate. From Pollard and Borisy, 2003.

Actin Polymerization in vivo

Intriguingly, the rate of actin treadmilling *in vitro* occurs nearly 100-times slower than that observed *in vivo* (Pantaloni et al., 2001). Given the need for cells to respond rapidly to various physiological stimuli, it is clear that the slow pace of actin dynamics *in vitro* is not sufficient to support the dynamic needs of cells. Thus, cells "catalyze" polymerization and actin dynamics by employing a number of different mechanisms. The first mechanism is to have a large excess of free, monomeric actin, most commonly referred to as globular actin or G-actin. Since the rate of actin filament elongation is directly proportional to the amount of free G-actin, by having a large supply of G-actin well above the critical concentration, cells can initiate rapid elongation of filaments when needed. Given that the concentration of free G-actin would greatly exceed the critical concentration however, G-actin would continue to polymerize uncontrollably until only the critical concentration of free monomers was left. Cells prevent this by sequestering free G-actin with G-actin binding proteins such as profilin or β-thymosin, thus permitting only the regulated polymerization of actin (Pollard and Borisy, 2003).

Cells also regulate actin polymerization with the use of actin capping proteins that bind to the barbed ends of actin filaments inhibiting further polymerization. In fact, given the large excess of G-actin in cells and the exceedingly slow formation of actin nucleation seeds, the availability of free barbed ends is the primary determinant of actin polymerization *in vivo*. Capping proteins are not the only class of proteins that regulate the availability of barbed ends however. Barbed ends can be generated by severing existing filaments through the action of proteins like ADF/cofilin, antagonizing barbed

end capping via proteins like Ena/Vasp, or initiating *de novo* formation of new filaments by nucleation factors such as Arp2/3 and formin (Condeelis, 1993; Zigmond, 1996; Zebda et al., 2000).

Actin Isoforms

Adding to the complexity of actin regulation in cells is the fact that actin is not a single homogenous protein species as commonly thought, but actually composed of six different isoforms encoded by six distinct genes in higher vertebrates (Vandekerckhove and Weber, 1978). Interestingly, no actin isoform differs from another in primary amino acid sequence by more than 7%, while the two most closely related actin isoforms, cytoplasmic β- and γ-actin, differ at only 4 of 375 amino acids clustered at the N-terminus. Perhaps even more striking is the fact that the six actin isoforms are completely conserved from birds to mammals, suggesting strong selective pressure has maintained these isoforms through 300 million years of evolution and that they likely perform distinct functions (Rubenstein, 1990).

The mammalian actin isoform family can be broken down into two groups: muscle actins, which are predominantly expressed in striated and smooth muscle, and cytoplasmic actins, which are expressed in all cells (McHugh et al., 1991; Tondeleir et al., 2009). While limited data is available directly comparing the biochemical properties of individual mammalian actin isoforms, a number of knock-out mouse models of different actin isoforms have been generated. These mouse models together with a small number of studies assessing rescue by transgenic overexpression of other actin isoforms

have begun to elucidate the functional overlap and potentially distinct functions of individual actin isoforms.

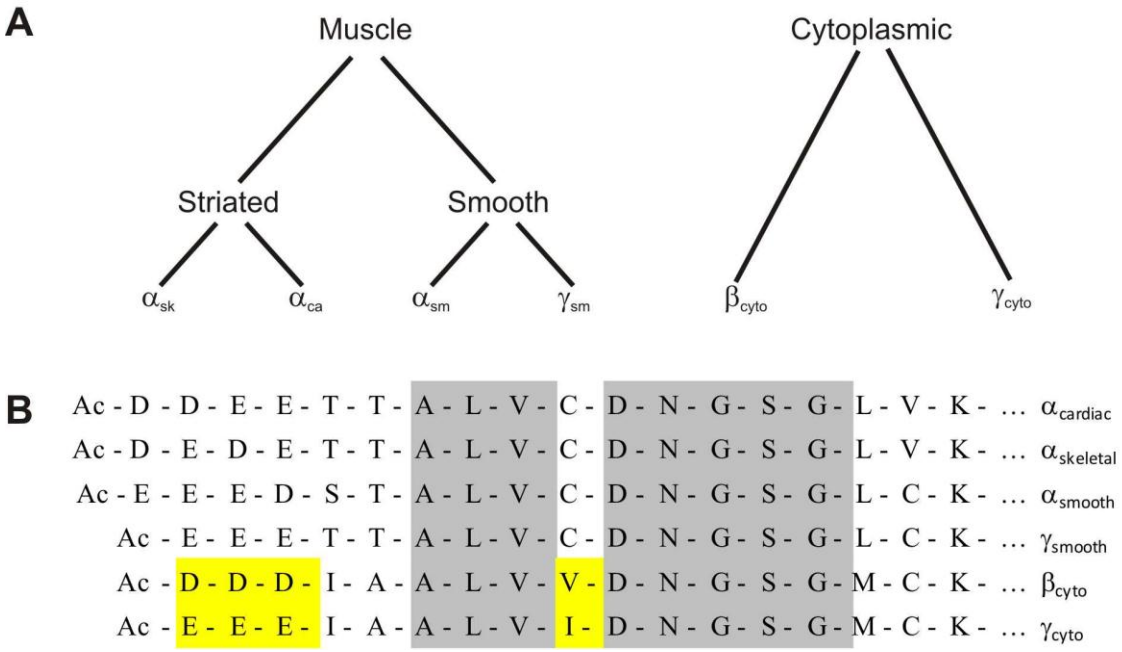

Figure 1.2: The mammalian actin isoform family. (A) Hierarchal organization of actin isoforms. Muscle actins are expressed in striated ($\alpha_{skeletal}$- and $\alpha_{cardiac}$-actin) and smooth muscle (α_{smooth}- and γ_{smooth}-actin), while the cytoplasmic actins (β_{cyto}- and γ_{cyto}-actin or β- and γ-actin) are expressed in all cells. **(B)** N-terminal primary amino acid sequences of muscle and cytoplasmic actins. Residues highlighted in gray are conserved across all isoforms. The four amino acids that differ between β- and γ-actin are highlighted in yellow. Ac indicates the position of the post-translational addition of an acetyl group. Modified from Rubenstein, 1990.

Striated Muscle Actin Isoforms

$\alpha_{skeletal}$-actin is the primary actin species composing the thin filaments of sarcomeres in skeletal muscle, upon which myosin motor proteins of the thick filaments pull on thereby generating contractile force. $\alpha_{cardiac}$-actin performs a similar function in cardiac muscle. Mice null for $\alpha_{skeletal}$-actin appear to develop normally possibly due to the upregulation of $\alpha_{cardiac}$- and the smooth muscle actin α_{smooth}-actin during development. However, these mice die perinatally due to profound muscle weakness inhibiting the procurement of nutrition (Crawford et al., 2002). Transgenic overexpression of the cytoplasmic γ-actin is not able to rescue the perinatal lethality in $\alpha_{skeletal}$-actin knock-out mice (Jaeger et al., 2009b). Mice null for $\alpha_{cardiac}$-actin exhibit embryonic/perinatal lethality due to developmental heart defects (Kumar et al., 1997). Interestingly however, $\alpha_{cardiac}$-actin overexpression in $\alpha_{skeletal}$-actin knock-out mice completely rescues the lethality in these mice, suggesting some functional overlap exists between the striated muscle but not cytoplasmic actin isoforms in skeletal muscle (Nowak et al., 2009).

Smooth Muscle Actin Isoforms

Smooth muscle provides involuntary contractile forces to the vascular, respiratory, gastrointestinal, and urogenital systems and differs fundamentally from striated muscle in appearance, regulation, and biochemical composition. α-smooth muscle actin (α_{smooth}-actin) is the predominate actin isoform found in vascular and respiratory smooth muscle, while γ-smooth muscle actin (γ_{smooth}-actin) predominates in

the gastrointestinal and urogenital tract, although it is present in low amounts in nearly all smooth muscles (McHugh and Lessard, 1988; Leslie et al., 1990; McHugh et al., 1991).

While little is known about γ_{smooth}-actin other than its expression patterns and ability to partially rescue $\alpha_{cardiac}$-actin null animals (Kumar et al., 1997), α_{smooth}-actin has relatively well described functions in normal and pathologic conditions (Chaponnier and Gabbiani, 2004). Although α_{smooth}-actin expression is the earliest expressed actin isoform in both smooth and some forms of striated muscle, α_{smooth}-actin knock-out mice present with a relatively mild phenotype with only minor deficits in vasculature contractility and blood pressure regulation (Schildmeyer et al., 2000). However, α_{smooth}-actin is also known to have a significant role in wound healing. During the process of wound healing, fibroblasts migrate into the wound where they encounter a number of cytokines, signaling molecules, and mechanical stress; all of which promote differentiation into a heterogeneous cell type called myofibroblasts (Chaponnier and Gabbiani, 2004). At present, myofibroblasts are best defined by their expression of α_{smooth}-actin which incorporates into the actin stress fibers of these cells and providing locomotive, structural, and contractile functions (Darby et al., 1990). Additional studies have shown that the amount of α_{smooth}-actin in myofibroblast-like cells is directly proportional to the cell traction force generated by these cells, while inhibiting α_{smooth}-actin function hinders wound closing *in vivo* (Hinz et al., 2002; Chen et al., 2007).

Cytoplasmic Actin Isoforms

The two cytoplasmic actins ($\beta_{cytoplasmic}$- and $\gamma_{cytoplasmic}$-actin, henceforth referred to as β- and γ-actin) represent the most closely related actin isoforms, differing at only four, biochemically similar amino acids out of 375 (with D substituted for E in positions 1-3, and V substituted for I in position 10 in γ-actin) (Rubenstein, 1990). The biochemical and cell biological roles of the individual cytoplasmic actins have only recently begun to be elucidated due to the prior lack of biochemical methods to purify or distinguish between the two nearly identical isoforms.

Despite their high degree of similarity, antibodies have been generated against β- and γ-actin which have revealed distinct localization patterns of the cytoplasmic actins in cells, with β-actin reported to be enriched at the leading edge of migrating fibroblasts while γ-actin was observed to accumulate in stress fibers and in the perinuclear region (Otey et al., 1986; Hoock et al., 1991; Kislauskis et al., 1997; Shestakova et al., 2001). Overexpression of β-actin in cultured myoblasts leads to an increase in cell surface area and motility whereas overexpression of γ-actin resulted in membrane retraction and a cell-rounding phenotype (Schevzov et al., 1992). Together, these studies suggest β-actin specifically may be important for cell motility and leading edge dynamics, while γ-actin may have a more static role in maintaining actin based structures.

Further evidence for a dynamic role of β-actin was recently demonstrated biochemically. Bergeron and colleagues (2010) used the baculovirus expression system to express biochemically relevant amounts of individual cytoplasmic actins which revealed ion-dependent polymerization differences between the two actin isoforms. When

Ca^{2+} was bound to the divalent cation binding cleft in insect cell expressed β- and γ-actin, filament nucleation, elongation, phosphate release, and depolymerization rates for β-actin were all significantly faster than γ-actin, suggesting β-actin is the more dynamic cytoplasmic actin isoform. Additionally, β- and γ-actin were shown to copolymerize, with mixed filament behavior reflective of their relative isoform composition. One caveat to the these findings however is that cytosolic Ca^{2+} levels in most cells are tightly controlled, with concentrations generally in the 2 μM range. Thus, actin in most cells is believed to be in the Mg^{2+} bound form, where the differences in polymerization kinetics between β- and γ-actin are far more similar. However, there are some instances where cytosolic Ca^{2+} concentrations could result in meaningful amounts of Ca^{2+} actin, such as in neuronal growth cones or dendritic spines where local Ca^{2+} transients can reach as high as 100 μM (Augustine et al., 2003). Collectively, these *in vitro* experiments lend further support to the idea that despite their considerable similarity, β- and γ-actin may have distinct properties and functions with β-actin being the more dynamic isoform.

Distinct Regulation of Actin Isoforms

Regulation of the actin cytoskeleton is largely responsible for the great diversity of actin functions within cells and occurs at the transcriptional, post-transcriptional, and post-translational levels. However, besides evidence that the transcription factor SRF regulates expression of a subset of actin isoforms (Alberti et al., 2005; Niu et al., 2005; Knoll et al., 2006; Knoll and Nordheim, 2009), there is little data at present on actin isoform-specific transcriptional regulation.

Post-transcriptional regulation of actin isoforms

Perhaps the most well characterized distinction between the cytoplasmic actins is in their post-transcriptional regulation. Studies from Robert Singer's group showed that enrichment of β-actin protein at the leading edge of motile fibroblasts was mediated in large part by a 54 nucleotide sequence in the 3' untranslated region of β-actin mRNA called the zipcode sequence (Kislauskis et al., 1994). Neither γ- nor any α-actin isoform contains an identifiable zipcode and neither is enriched at the leading edge of motile cell (Hill and Gunning, 1993; Kislauskis et al., 1993). At least two proteins were subsequently found that bind specifically to the β-actin zipcode sequence and were called zipcode binding protein 1 and 2 (ZBP1 and 2), with most studies focused on ZBP1 (Ross et al., 1997; Gu et al., 2002). Treatment of fibroblasts with anti-sense oligonucleotides to the zipcode sequence inhibited the localization of β-actin mRNA and protein, delocalized sites of actin polymerization, and reduced the directionality of cell movement in migrating fibroblasts (Kislauskis et al., 1997; Shestakova et al., 2001). Although indirect, these studies suggested a distinct role for β-actin in proper cell motility via a zipcode-mediated mRNA localization mechanism.

How might the localization of β-actin mRNA affect actin dynamics and promote directed cell motility and migration? The simplest explanation would suggest that the local translation of β-actin mRNA would result in a localized increase in available G-actin for polymerization. Since the rate of actin filament elongation depends on the concentration of G-actin, a localized increase in G-actin would make a plausible mechanism to promote directed cell motility. Alternatively, local synthesis of actin may

promote *de novo* nucleation of filaments. The cytosolic chaperone protein (CCT) is required for proper actin folding following translation, and has been shown to associate with filamentous actin (F-actin) and possibly act as a nucleation factor itself (Grantham et al., 2002; Pappenberger et al., 2006). Lastly, newly translated actin may be more readily polymerized than pre-existing actin. For example, post-translational glutathionylation of actin has been shown to negatively affect polymerization (Wang et al., 2001), and thus newly translated actin lacking this modification may promote actin filament polymerization and elongation required for cell motility.

Distinct post-translational regulation of actin isoforms

In addition to glutathionylation, actin can also be ubiquitinated (Burgess et al., 2004; Kudryashova et al., 2005), SUMOlyated (Hofmann et al., 2009), phosphorylated (Gu et al., 2003; Vandermoere et al., 2007), and acetylated (Rubenstein and Martin, 1983). However, besides small differences in how muscle and cytoplasmic actins are acetylated (Rubenstein, 1990), there have been no demonstrated differences in actin isoform post-translational modification. One intriguing exception however is the recent discovery that β-actin can be arginylated at its N-terminus by arginyltransferase 1 (*Ate1*) (Karakozova et al., 2006) . Intriguingly, γ-actin was not found to be arginylated in this experiment. *Ate1* null fibroblasts show migration and morphological defects that could be rescued by overexpression of β-actin with a genetically encoded arginine at the N-terminus (Karakozova et al., 2006). Subsequent studies determined that γ-actin could also be arginylated in cells, but that differences in translation speed owing to distinct RNA

secondary structures between β- and γ-actin exposed a lysine residue in γ-actin that is normally buried during rapid translation and folding (Zhang et al., 2010). This exposed lysine in γ-actin could be ubiquitinated leading to the rapid degradation of arginylated γ-actin, thus explaining why arginylated γ-actin was not previously detected.

Differential binding of actin isoforms by actin binding proteins

While the distinct regulatory mechanisms of β-actin just described are dependent on genomically encoded differences between β- and γ-actin, it is also possible that the primary amino acid sequence differences between the two cytoplasmic actins could influence interactions with actin regulatory proteins. The N-terminus containing the four divergent amino acids between β- and γ-actin is exposed on the surface of actin filaments (Oda et al., 2009), raising the possibility that actin binding proteins could differentially interact with the two cytoplasmic actins within filaments. The fact that antibodies can distinguish between β- and γ-actin and have been validated on knock-out tissue lends further support to this hypothesis (Gimona et al., 1994; Hanft et al., 2006; Sonnemann et al., 2006; Perrin et al., 2010; Cheever et al., 2011). However, no differential interactions of endogenous proteins with β- or γ-actin have been convincingly demonstrated. In a small number of studies, profilin (Larsson and Lindberg, 1988), L-plastin (Namba et al., 1992), ezrin (Yao et al., 1996), βcap73 (Shuster et al., 1996), and cofilin (De La Cruz, 2005) have been shown to interact with preparations rich in β-actin with higher affinity than muscle actin preparations. However, a direct demonstration of differential binding of these proteins between β- and γ-actin remains an enticing but so far elusive question.

Physiological Roles of the Cytoplasmic Actin Isoforms

Actin isoforms and their potential distinct functions have intrigued cell biologists for decades, yet studies of actin isoforms *in vivo*, and particularly the cytoplasmic actin isoforms, have been lacking mostly due to the unavailability of suitable reagents and the assumed essential nature of their functions. Although we now have evidence for unique functions and regulation of β- and γ-actin, only *in vivo* experiments can determine whether these often subtle distinctions are biologically meaningful. With the generation of conditional floxed *Actb* (encoding β-actin, Perrin et al., 2010) and *Actg1* (encoding γ-actin, Sonnemann et al., 2006) mouse lines, the door has now been opened for studies examining the functions of β- and γ-actin in mammalian tissues *in vivo*. Already we know that muscle specific ablation of β- and γ-actin both result in myopathies but to dramatically different extents, with ablation of γ-actin resulting in a more severe phenotype (Sonnemann et al., 2006; Prins et al., 2011). Ablation of β- and γ-actin in auditory hair cells both result in age related hearing loss, but again, to different extents and through apparently different mechanisms (Perrin et al., 2010).

Cytoplasmic Actin Isoform Functions in Neurons

The role of the cytoplasmic actins in neurons and the central nervous system (CNS) in general is relatively unexplored, especially in an *in vivo* context. Yet the significant amounts of β-and γ-actin expressed in the CNS, coupled with a number of critical roles for actin in CNS development and function, make it an attractive system to study potentially distinct physiological functions for the cytoplasmic actins. β- and γ-

actin are both present in brain lysates at ratios ranging from 1:1 to 2:1(Choo and Bray, 1978; Flanagan and Lin, 1979; Otey et al., 1987) . α-actin expression has not been reported in the brain. Interestingly, two studies have shown developmental downregulation of β-actin with localization generally confined to areas of the brain with a high capacity for remodeling such as synapses (Weinberger et al., 1996; Kaech et al., 1997; Micheva et al., 1998). Given previously described roles for β-actin in directed cell migration, one might predict that β-actin could play critical roles in the early directed cell migration that is required not only for neural tube formation (from which the brain and spinal cord are derived) (Copp et al., 2003), but also in the migration of newly generated neurons from sites of neurogenesis to their final positions throughout the brain (Ayala et al., 2007). Additionally, one recent study using newly generated antibodies to β- and γ-actin found β-actin to be exclusively enriched in the contractile ring of dividing cells in culture, while γ-actin was distributed all along the cortical cytoskeleton (Dugina et al., 2009). Thus, it is also possible that β-actin may be important in the proliferation and generation of the 100 billion neurons in the human brain. However, no reports to date have directly examined the role of β- or γ-actin in the early stages of CNS specification, neurogenesis, or neuronal migration.

Actin isoform functions in axon guidance

Significant research has been conducted however on a possible distinct role for β-actin in in the initial wiring of the nervous system via axon guidance. Axons of developing neurons are capped by highly specialized structures known as growth cones,

which are responsible for detecting extracellular guidance cues and guiding axons to their proper synaptic targets. Growth cones accomplish this by receiving and transducing extracellular guidance information into cytoskeletal changes that underlie growth cone turning and extension towards targets (Tessier-Lavigne and Goodman, 1996; Lowery and Van Vactor, 2009). The peripheral growth cone cytoskeleton is predominantly composed of bundles and dendritic arrays of actin with barbed ends oriented towards the plasma membrane, while microtubules are the major cytoskeletal component in the central domain but also transiently explore the periphery (Dent and Gertler, 2003). Depolymerization of growth cone actin by treatment with cytochalasin B leads to misguided axon growth (Marsh and Letourneau, 1984; Lafont et al., 1993), while disrupting microtubule dynamics impairs axon outgrowth and actin-dependent guidance (Letourneau and Ressler, 1984; Buck and Zheng, 2002). Thus, while actin is not essential for axonal elongation in general, it is essential for the guided growth of axons.

Growth cones send out protrusions in search of guidance cues or synaptic targets that are driven by the retrograde flow of actin filaments. Retrograde flow describes the process whereby actin filaments are pushed and pulled from the periphery of the growth cone to the central region in part by myosin motor proteins (Forscher and Smith, 1988; Medeiros et al., 2006). Retrograde flow can thus antagonize filament elongation, leading to no net membrane protrusion. However, when actin filaments are coupled to a substrate via a molecular "clutch" of still undefined protein components, retrograde flow can be attenuated allowing for continued actin filament elongation promoting membrane protrusion and growth cone extension (Lowery and Van Vactor, 2009; Suter and

Forscher, 2000). In the case of an elongating axon in the absence of guidance cues, actin polymerization and substrate adhesion are uniformly distributed across the growth cone, leading to straight growth of the axon. However, when an attractive guidance cue is encountered at one side of the growth cone, retrograde flow can be locally attenuated. If actin filaments can be locally polymerized or elongated in that region, then asymmetric membrane protrusion will occur causing the growth cone to turn (O'Connor and Bentley, 1993; Lin et al., 1994). Invasion by microtubules further stabilizes the asymmetric protrusion of the growth cone and is followed by consolidation of the axon shaft around the advancing microtubules, resulting in the turning of the axon towards the attractive cue (Dent and Gertler, 2003). Axonal branching occurs by a similar mechanism of localized actin polymerization and microtubule invasion (Dent et al., 2003). During nervous system development, there are many examples of axons branching to innervate multiple targets or collateral axon branches innervating targets while the primary axon retracts (Bagri et al., 2003; Schmidt and Rathjen, 2010; Gibson and Ma, 2011).

The local polymerization of actin at sites proximal to attractive guidance cues could be mediated by a number of mechanisms. Local activity of actin regulatory proteins such as cofilin, formin, and Ena/Vasp represent the most likely candidates to promote localized actin polymerization necessary for growth cone turning (Dent and Gertler, 2003; Pak et al., 2008) . Alternatively, the local translation of β-actin could also promote increased actin polymerization in response to attractive guidance cues. Similar to fibroblasts, β-actin mRNA and protein have been reported to be enriched at the leading edge of growth cones (Bassell et al., 1998). This enrichment can be enhanced following

exposure to attractive guidance cues such as neurotrophin-3 or netrin-1 (Zhang et al., 2001; Leung et al., 2006). Seminal work by James Zheng and Christine Holt's groups showed that β-actin mRNA and protein become asymmetrically localized to the side of the growth cone proximal to an attractive guidance cue, and this localization correlated with attractive turning (Leung et al., 2006; Yao et al., 2006). Anti-sense oligonucleotides directed at the zipcode sequence of β-actin mRNA prevented the asymmetric localization of β-actin protein and abolished the turning response, suggesting that zipcode and ZBP1-mediated localization of β-actin mRNA may be critical for growth cone guidance. In order for the localization of β-actin mRNA to result in only local synthesis of β-actin protein, the mRNA must be translationally silent during transit. Work by Robert Singer's group showed this is indeed the case and that β-actin mRNA is translationally silenced when bound to ZBP1 (Huttelmaier et al., 2005). This inhibition can be relieved following phosphorylation of tyrosine 396 in ZBP1 by Src kinase, which can also be activated locally in response to attractive guidance cues (Yao et al., 2006; Sasaki et al., 2010). Thus, asymmetric exposure of growth cones to an attractive guidance cue leads to the local translation of β-actin which likely promotes increased actin polymerization, membrane protrusion, and growth cone turning.

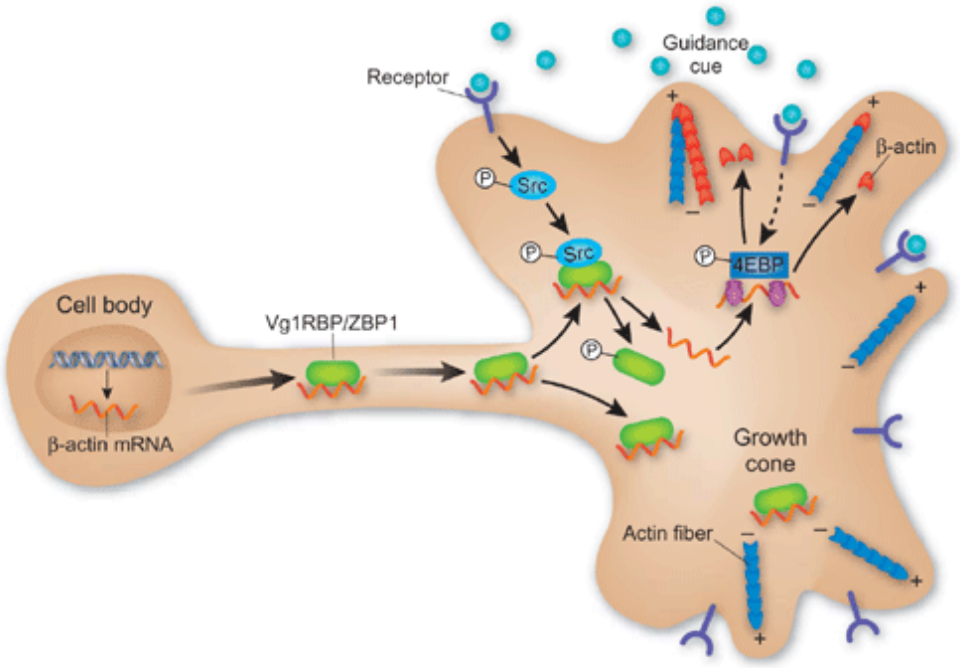

Figure 1.3: Attractive guidance cues induce zipcode-mediated local translation of β-actin in neuronal growth cones. ZBP1 transports β-actin mRNA from the neuronal cell body to the growth cone while also inhibiting translation. When attractive guidance cues are received by one side of the growth cone, Src kinase is locally activated and can phosphorylate ZBP1, resulting in the release and local translation of β-actin mRNA. The net effect of this process is the local accumulation of newly translated β-actin at the side of the growth cone closest to the attractive guidance cue. From Ming, 2006.

While the role for local translation of β-actin has been convincingly demonstrated in *Xenopus* neurons from the aforementioned studies, it is unclear if this mechanism is conserved in higher vertebrates. Experiments where growth cones from chick and mouse neurons were locally exposed to protein synthesis inhibitors with the aid of

compartmentalized culture dishes revealed that these growth cones responded normally to attractive and repulsive cues (Roche et al., 2009). In addition, protein synthesis inhibitors did not prevent localized increases in F-actin in response to attractive guidance cues. Finally, although β-actin protein was redistributed to the periphery of the growth cone, a net increase in β-actin protein was not observed following exposure of growth cones to attractive guidance cues. The conflicting observations of this study may be partially explained by intrinsic differences between *Xenopus* and higher vertebrate growth cones. *Xenopus* growth cones were found to constitutively express significantly lower amounts of β- and γ-actin than their chick counterparts (Marsick et al., 2010). Thus, local translation of β-actin in *Xenopus* growth cones may be critical for growth cone guidance while higher vertebrate growth cones may contain sufficient actin to facilitate cytoskeletal remodeling in response to guidance cues. Additional studies in higher vertebrate *in vivo* systems will likely prove helpful in resolving these conflicting *in vitro* findings.

Functions of actin isoforms in synapse formation

Although the initial wiring of the nervous system is mostly complete in the perinatal period, the nervous system is by no means done forming and fine-tuning synaptic connections. In fact, synapses are constantly being added, subtracted and modified throughout life which is essential for our ability to learn and remember (Holtmaat and Svoboda, 2009). In the mammalian brain, most excitatory synapses occur at tiny structures along dendrites called dendritic spines (Nimchinsky et al., 2002; Sheng

and Hoogenraad, 2007). Synapses at dendritic spines can be formed when immature dendritic filopodia encounter an axon (Holtmaat and Svoboda, 2009). The dendrites of mature neurons are studded by dendritic filopodia composed of small bundles of actin filaments (Hotulainen and Hoogenraad, 2010). These dendritic filopodia are highly dynamic and stochastically appear and disappear in cultured neurons (Yoshihara et al., 2009). However, certain neurotrophic factors or chemical stimuli can induce an increase in dendritic filopodia, which can be stabilized if filopodia are in close apposition to axons (Shimada et al., 1998; Tiruchinapalli et al., 2003). In the case of synapse formation, increased actin polymerization in dendritic filopodia can lead to an expansion of the filopodia, generating a mushroom shaped structure that is characteristic of a mature, functional dendritic spine (Hotulainen and Hoogenraad, 2010; Okamoto et al., 2004; Honkura et al., 2008).

How dendritic filopodia dynamics and maturation are regulated remains a lingering question in the synaptic development field. Like in growth cones, dendritic filopodia and spine formation requires localized actin polymerization in response to stimuli. It is perhaps no surprise then that local translation of β-actin has also been implicated in dendritic filopodia formation. ZBP1 and β-actin mRNA colocalize throughout the dendrites of mature neurons in culture, and this colocalization can be enhanced following KCl-mediated depolarization (Tiruchinapalli et al., 2003). Knock-down of ZBP1 reduced dendritic levels of β-actin mRNA and also reduced the density of dendritic filopodia in response to stimulation (Eom et al., 2003). Overexpression of β-actin constructs with the zipcode and intriguingly the zipcode alone dramatically

increased the density of dendritic filopodia over expression of β-actin alone (Eom et al., 2003). Thus, the zipcode mediated localization of β-actin appears to not only be important in growth cone guidance, but also in the continued synaptic remodeling of mature neurons.

Cytoplasmic Actin isoforms in CNS disease

A number of human neurological diseases have known or suspected pathologies involving neuronal migration, axon guidance, and synaptic remodeling/regulation (Ayala et al., 2007; Engle, 2010; Penzes et al., 2011). While actin has significant roles in all of these processes, there have been no studies to date that have examined actin isoform-specific contributions to these pathologies *in vivo*. Perhaps the best evidence for an actin isoform specific role in CNS disease comes from a prominent study which reported that β-actin levels were decreased in the growth cones of motor neurons cultured from a mouse model of spinal muscular atrophy (SMA) (Rossoll et al., 2003).

Spinal Muscular Atrophy

Spinal muscular atrophy (SMA) is an autosomal recessive genetic disorder with an incidence of 1 in 10,000. SMA is characterized by the loss of lower α-motor neurons, the neurons which innervate and regulate skeletal muscle contraction. The subsequent loss of motor neurons leads to hypotonia, muscle atrophy, and in its most severe form death within the first two years of life (Monani, 2005; Lunn and Wang, 2008). There is currently no treatment available for SMA patients. Although the genetic cause of SMA

has been linked to mutations in the survival motor neuron 1 (SMN1) gene (Lefebvre et al., 1995), how loss of the ubiquitously expressed SMN protein causes disease primarily in motor neurons remains an important unanswered question. Initial studies localized SMN to the nucleus of cells where it is involved in RNA processing and snRNP biogenesis (Monani, 2005). The identification of SMN outside the nucleus and throughout neuronal processes however suggested that SMN has additional functions in neurons beyond its more established role in RNA processing (Tizzano et al., 1998; Pagliardini et al., 2000; Fan and Simard, 2002). In support of this hypothesis, knock-down of SMN in a number of neuronal cell lines and in zebrafish results in decreased neurite outgrowth and branching defects, arguing for a role of SMN specifically in regulating the neuronal cytoskeleton responsible for neurite elongation and axon guidance (McWhorter et al., 2003; Bowerman et al., 2007; van Bergeijk et al., 2007; Oprea et al., 2008; Tadesse et al., 2008).

β-actin in SMA pathogenesis

SMN directly interacts with the human homologue of ZBP2, a homolog of ZBP1 which is also known to bind the zipcode sequence of β-actin mRNA (Tadesse et al., 2008). Additionally, SMN associates with heterogeneous ribonucleoprotein R (hnRNP-R) *in vivo*, yet another protein that binds the zipcode sequence of β-actin mRNA and mediates its localization to growth cones (Rossoll et al., 2002; Rossoll et al., 2003). Studies by Zheng and colleagues (2003) revealed that SMN undergoes fast, bi-directional transport between the neuronal cell body and growth cone, making SMN a likely

candidate for mediating the localization of β-actin mRNA to the periphery of motor neuron growth cones.

Given that SMN knock-down in neuronal cell lines and zebrafish results in defective axonal outgrowth, an intriguing hypothesis to explain SMA pathogenesis is that decreased levels of SMN in motor neurons results in defective transport of β-actin mRNA to growth cones leading to impaired neurite elongation and guidance to targets (Jablonka et al., 2004; Briese et al., 2005; Dahm and Macchi, 2007). In support of this hypothesis, primary motor neurons from a mouse model of SMA were found to have decreased β-actin at growth cones (Rossoll et al., 2003). The mislocalization of β-actin correlated with a reduction in the size of growth cones and axon elongation defects similar to those observed in neuronal cell lines and zebrafish. Two studies of SMA mouse models however failed to reveal any gross abnormalities in nerve elongation and guidance *in vivo* (Kariya et al., 2008; McGovern et al., 2008). Yet, these reports are in contrast to a more recent study in another SMA mouse model showing that axons innervating the diaphragm are significantly longer than wild type controls (Kariya et al., 2009). This data was interpreted as motor axons "overshooting" the post-synaptic motor end plate and indicative of a failure of growth cones to properly respond to target-derived guidance cues. Collectively, the conflicting data on the status of axon guidance and elongation in SMA mouse models indicates that potential axon guidance defects in SMA cannot be ruled out.

A number of SMA mouse models also exhibit defects in the maturation or maintenance of the neuromuscular junction (NMJ), the highly specialized synapse

between motor neurons and skeletal muscle. Accumulations of neurofilament protein accompanied by poor branching in nerve terminals are observed at the pre-synaptic side of the NMJ in numerous SMA mouse models, while retention of the embryonic γ-subunit of the acetylcholine receptor and unoccupied or aberrantly folded motor end plates are evident at the post-synaptic side (Cifuentes-Diaz et al., 2002; Murray et al., 2008; Kariya et al., 2008; McGovern et al., 2008). NMJ formation and maintenance is dependent on bidirectional signaling between the motor neuron and skeletal muscle, and thus is a possible target of SMA molecular pathogenesis (Sanes and Lichtman, 1999; Fox and Umemori, 2006). For example, the direct interaction between the pore subunit of the pre-synaptic voltage gated calcium channel (VGCC) and the post-synaptic β2 subunit of laminin is known to be important for proper maturation of the NMJ (Nishimune et al., 2004). Interestingly, delocalized VGCCs correlate with decreased β-actin at growth cones in cultured motor neurons from SMA mice, suggesting that an actin cytoskeletal scaffold is crucial for ensuring the proper positioning of VGCCs in the growth cone (Jablonka et al., 2007). In addition to being essential for NMJ maturation and maintenance, the VGCC-laminin β2 interaction also serves as a "stop" signal for elongating motor axons by inhibiting their outgrowth (Porter et al., 1995). Such a mechanism may explain the findings of Kariya et al. (2009) which showed that axons from the phrenic nerve in an SMA mouse model were significantly longer than controls and appeared to "overshoot" the motor end plate. When considered together, these studies suggest that decreased β-actin expression or localization within growth cones of motor neurons may contribute to the pathologies associated with SMA.

Summary

The primary goal of my thesis research was to assess the role of cytoplasmic actins in CNS development, function, and disease with mammalian *in vivo* models. While there is evidence to suggest that β-actin may have unique and essential roles in the initial wiring and remodeling of the nervous system, none of these models have been thoroughly tested in a mammalian *in vivo* system. The first chapter of this thesis details an analysis of the role of β-actin in motor neuron development and function. In the second chapter, the role of β-actin in the brain is presented. Collectively, these studies have identified novel roles for β-actin in brain morphogenesis and regulation of behavior while demonstrating that β-actin-specific functions in the mammalian CNS are significantly more restricted than previously thought.

Chapter 2

Axonal regeneration and neuronal function are preserved in motor neurons lacking β-actin *in vivo*

This chapter is unmodified from the published article:

Cheever, T.R., Olson, EA. and Ervasti, J.M. (2011). Axonal regeneration and neuronal function are preserved in motor neurons lacking β-actin *in vivo*. *PLoS One* 6(3):e17768

Emily Olson assisted with skeletal muscle histology. Tom Cheever performed all other experiments and wrote the manuscript.

SUMMARY

The proper localization of β-actin mRNA and protein is essential for growth cone guidance and axon elongation in cultured neurons. In addition, decreased levels of β-actin mRNA and protein have been identified in the growth cones of motor neurons cultured from a mouse model of Spinal Muscular Atrophy (SMA), suggesting that β-actin loss-of-function at growth cones or pre-synaptic nerve terminals could contribute to the pathogenesis of this disease. However, the role of β-actin in motor neurons *in vivo* and its potential relevance to disease has yet to be examined. We therefore generated motor neuron specific β-actin knock-out mice (*Actb*-MNsKO) to investigate the function of β-actin in motor neurons *in vivo*. Surprisingly, β-actin was not required for motor neuron viability or neuromuscular junction maintenance. Skeletal muscle from *Actb*-MNsKO mice showed no histological indication of denervation and did not significantly differ from controls in several measurements of physiologic function. Finally, motor axon regeneration was unimpaired in *Actb*-MNsKO mice, suggesting that β-actin is not required for motor neuron function or regeneration *in vivo.*

INTRODUCTION

The cytoskeletal protein actin has well characterized roles in many aspects of neuronal development and function from growth cone dynamics to the remodeling of dendritic spines (Dent and Gertler, 2003; Cingolani and Goda, 2008). Although neurons of higher vertebrates express two nearly identical actin isoforms, β- and γ-actin (Choo and Bray, 1978), β-actin is thought to be the primary mediator of neuronal actin dynamics based on its unique post-transcriptional regulation. In cultured neurons, β-actin is enriched at the leading edge of growth cones via an mRNA localization and local translation mechanism (Bassell et al., 1998; Huttelmaier et al., 2005). The 3'-UTR of β-actin mRNA contains a 54 nucleotide sequence called the zipcode which is bound co-transcriptionally by zipcode binding protein 1 (ZBP1, also known as IMP1 in humans, mIMP or CRD-BP in mice) (Kislauskis et al., 1994; Ross et al., 1997; Huttelmaier et al., 2005; Yisraeli, 2005). ZBP1 facilitates the transport of β-actin mRNA from the cell body to the growth cone while also inhibiting its translation (Huttelmaier et al., 2005). Attractive guidance cues received by the growth cone initiate a signaling cascade that results in the release and translation of β-actin mRNA, thereby generating a localized increase of newly translated β-actin which is hypothesized to be an underlying mechanism behind growth cone turning (Leung et al., 2006; Yao et al., 2006).

Although extensively characterized in cell culture models, less is known regarding the significance of β-actin mRNA and protein localization in mammalian neurons *in vivo*. The most compelling evidence comes from a mouse model of Spinal Muscular Atrophy (SMA), a genetic disorder resulting from the selective loss of lower

motor neurons (Burghes and Beattie, 2009). Rossol and colleagues (2003) observed a dramatic decrease in β-actin mRNA and protein in the growth cones of cultured motor neurons from a mouse model of SMA, which correlated with a decrease in axonal elongation, growth cone size, and mislocalization of voltage gated calcium channels (Jablonka et al., 2007). Interestingly, survival motor neuron (SMN), the protein depleted in SMA, interacts with two proteins known to bind the zipcode sequence of β-actin mRNA: hnRNP-R and KSRP, the human homologue of a ZBP family member (Rossoll et al., 2002; Rossoll et al., 2003; Tadesse et al., 2008; Glinka et al., 2010). These observations led to the hypothesis that reduced levels of β-actin at growth cones in SMN-deficient motor neurons may cause axon guidance or nerve terminal defects ultimately resulting in motor neuron death.

A number of recent studies however have now shown motor neuron axon guidance and elongation is unperturbed in SMA mouse models, suggesting that decreased levels of β-actin in motor neuron growth cones likely does not hinder axon guidance or elongation (Kariya et al., 2008; McGovern et al., 2008; Murray et al., 2010). Yet, this data does not rule out whether β-actin may play a role later in the development or maintenance of the neuromuscular junctions (NMJ), the specialized synapse between motor neurons and skeletal muscle. Given that previous studies have shown a mislocalization of voltage gated calcium channels in SMA motor neurons that correlated with the decrease of β-actin in growth cones (Jablonka et al., 2007), one intriguing hypothesis is that β-actin plays a crucial role in pre-synaptic NMJ structure and function, a potential pathogenic mechanism more in line with current *in vivo* findings from SMA

mouse models (Cifuentes-Diaz et al., 2002; Kariya et al., 2008; McGovern et al., 2008; Murray et al., 2008; Kong et al., 2009).

We therefore set out to determine the function of β-actin in mature motor neurons by conditionally ablating its expression with a floxed β-actin mouse line (Perrin et al., 2010) and the motor neuron specific Cre line, Mnx1-Cre (Yang et al., 2001, see additional references in materials and methods). Surprisingly, motor neuron specific β-actin knock-out (*Actb*-MNsKO) mice exhibited no overt phenotype, with motor neuron viability, NMJ, and muscle performance all preserved in comparison to controls. Peripheral nerve axonal regeneration was also unimpaired in *Actb*-MNsKO mice, indicating that β-actin is dispensable for motor neuron function and regeneration *in vivo*.

MATERIALS AND METHODS

Ethics Statement

The experimental protocols in this study were reviewed and approved by the University of Minnesota Institutional Animal Care and Use Committee (IACUC) and approved on August 13th, 2010 (IACUC Protocol #0907A69551).

Mouse Lines

Motor neuron specific β-actin knock-out mice (*Actb*-MNsKO) were generated by crossing $Actb^{flox/flox}$ (Perrin et al., 2010) mice with the Mnx1 (also known as HB9, Hlxb9) – Cre line (Stock# 006600, Jackson Labs, Bar Harbor, ME) to generate mice homozygous for the *Actb* floxed allele and hemizygous for the Mnx1-Cre allele. Mice homozygous for the *Actb* floxed allele but lacking Cre were used for controls ($Actb^{flox/flox}$). Mnx1-Cre

expression in all or nearly all motor neurons has been previously verified by crossing to ROSA26 reporter strains (Hess et al., 2007; Luria and Laufer, 2007; Li et al., 2008; Kramer et al., 2006) and used to target Cre recombinase expression in gene knock-out or motor neuron ablation studies starting at embryonic day 9.25-9.5 (E9.25-E9.5) (Yang et al., 2001; Bolis et al., 2005; Hess et al., 2007; Luria and Laufer, 2007; Li et al., 2008; Chipman et al., 2010; Mende et al., 2010; Jevsek et al., 2006; Franz et al., 2008; Kim and Burden, 2008). CNS-*Actb*KO mice were generated in a similar fashion to the *Actb*-MNsKO mice but with the Nestin-Cre line instead (Stock# 003771, Jackson Labs, Bar Harbor, ME). Nestin-Cre is expressed throughout the nervous system with Cre expression beginning at E10.5 (Tronche et al., 1999; Graus-Porta et al., 2001). Genotyping for the *Actb* allele and Cre transgene were performed as described (Sonnemann et al., 2006; Perrin et al., 2010). For timed matings, the morning a vaginal plug was found was designated E0.5.

β-galactosidase Staining

Mnx1-Cre expression and activity were confirmed by crossing control and *Actb*-MNsKO mice to a ROSA26 reporter line (Stock# 003474, Jackson Labs, Bar Harbor, ME). Staining of E12.5 embryos for β-galactosidase activity was performed on whole mounts or cryosections as described previously (Chow et al., 2006). Cross sections were counterstained with 0.1% Neutral red.

Spinal Cord Immunofluorescence and Histology

Mice at 6 (6-8) and 12 (12-14) months of age were anesthetized and transcardially perfused with cold phosphate buffered saline (PBS) followed by 4% paraformaldehyde

(PFA, Electron Microscopy Sciences, Hatfield, PA) in PBS. The spinal cord was isolated by laminectomy and post-fixed in 4% PFA for 2 hours at 4ºC. Isolated spinal cords were then cryoprotected for 2-3 days in 30% sucrose in PBS at 4ºC. The lumbar enlargement of spinal cords were finally frozen in liquid nitrogen cooled isopentane and embedded in OCT (TissueTek, Torrance, CA). For immunofluorescence, 20 μm cryosections were cut and post-fixed in 4% PFA for 10 minutes, washed briefly in PBS, and post-fixed in ice cold 100% methanol for 10 minutes. Fixed sections were then washed in wash buffer (PBS + 0.3% Triton X-100 (Sigma, St. Louis, MO)) followed by blocking in blocking buffer (3% bovine serum albumin (BSA, Sigma) in PBS + 0.3% Triton X-100) for 1 hour at room temperature. Goat anti-choline acetyltransferase (AB144P; Millipore, Billerica, MA, 1:10) was incubated overnight in 1% BSA + 0.3% Triton X-100 at 4ºC, while FITC-conjugated mouse anti-β-actin (ab6277; Abcam, Cambridge, MA, 1:75)) was incubated with 2º antibody (anti-goat Alexa Fluor 568; Invitrogen, Carlsbad, CA, 1:500) the following day for 1-2 hours at room temperature. Sections were washed in wash buffer and mounted in SlowFade Gold antifade reagent with DAPI (S36938; Invitrogen). Images of control, *Actb*-MNsKO, and CNS-*Actb*KO sections were obtained and processed under identical conditions at the Biomedical Image Processing Laboratory with an Olympus FluoView FV1000 laser scanning confocal microscope and processed equivalently with Adobe Photoshop.

Fluorescent Nissl staining was performed on 20 μm cryosections using a 1:100 dilution of NeuroTrace (N21480; Invitrogen) following the manufacturer's instructions. At least 10 sections > 150 μm apart were used for quantification of Nissl stained motor

neurons that met the following criteria used previously (Palazzolo et al., 2009): 1) Located below a horizontal line drawn tangent to the bottom of the central canal, 2) visible and distinct nucleolus with robust, globular cytoplasmic staining, and 3) diameter at the largest point > 20 μm. Motor neuron size was assessed on the same sections by measuring the diameter at the largest point of all motor neurons with a minimum diameter of > 20 μm using ImagePro software. Three mice per genotype per time point were characterized.

Whole Mount Muscle Immunostaining

E16.5 diaphragms were dissected in 1X PBS and fixed in 4% PFA in 0.1M PBS (0.019 M monobasic sodium phosphate, 0.081 M dibasic sodium phosphate heptahydrate, pH 7.4) for 30 minutes at room temperature. Fixed muscles were briefly washed in 0.1M PBS followed by incubation in 0.1M glycine in 0.1M PBS for 1 hour. Diaphragms were then blocked in blocking buffer (4% BSA + 0.5% Triton X-100 in 0.1M PBS) overnight at 4ºC. Mouse anti-neurofilament 1º antibody (2H3; Developmental Studies Hybridoma Bank, Iowa City, IA, 1:200) was incubated in blocking buffer overnight at 4ºC. Diaphragms were then washed in wash buffer (0.1M PBS + 0.5% Triton X-100) and incubated with anti-mouse 2º antibodies conjugated to Alexa Fluor 568 (A11031; Invitrogen, 1:200) and α-bungarotoxin conjugated to Alexa Fluor 488 (B13422; Invitrogen, 1:200) overnight at 4ºC. After washing in wash buffer, diaphragms were flat mounted on slides with SlowFade Gold antifade reagent (S36936; Invitrogen).

Adult (4 month old) diaphragms were stained as described (Mejat et al., 2009) with slight modification. 1% PFA was used as a fixative while 2H3 antibody and fluorescent α-bungarotoxin were used as described above.

In vivo Muscle Performance and EMG

In vivo muscle performance was assessed at 6 and 12 months of age ($n \geq 3$ mice per genotype per time point). Forelimb grip strength measurements were made using a computerized grip strength meter (Columbus Instruments, Columbus, OH) following standard protocols (Van Damme et al., 2003; Whittemore et al., 2003). For each subject at each time point, five trials were conducted with the top three averaged and normalized to body mass. Maximal exercise performance was assessed using a Columbus instruments treadmill as reported previously (Jaeger et al., 2009a). Whole-body tension analysis was performed as described previously (Prins et al., 2008). Data are reported as the maximum pulling force generated (WBT_{Max}), and the average of the top five pulls ($WBT_{Ave(1-5)}$). Electromyography (EMG) recordings were made using a TECA Synergy EMG monitoring system (Viasys Healthcare, San Diego, CA) with a 27 gauge disposable needle electrode (Medtronic, Minneapolis, MN). Six month old *Actb*-MNsKO and control mice were anesthetized with ketamine (100 mg/kg body weight [BW]) and xylazine (10 mg/kg BW) and maintained on a heating pad. A subdermal ground was placed subcutaneously on the back. The recording electrode was inserted into the gastrocnemius muscle and spontaneous electrical activity was recorded for 20 seconds in at least three different positions within the muscle.

Muscle Histology

Fiber typing was performed at 6 and 12 months on the gastrocnemius muscle as described previously ($n \geq 3$ mice per genotype per time point) (Jaeger et al., 2009). Fiber typing of gastrocnemius and soleus muscles following nerve crush was performed on muscles harvested 6 weeks post-crush ($n = 3$ mice of each genotype). For all experiments, three non-overlapping images were acquired with an Olympus FluoView FV1000 laser scanning confocal microscope and quantified using ImagePro software. For assessment of fiber diameter, hematoxylin and eosin stained sections were prepared and analyzed as described previously (Prins et al., 2008) with minor modification. Sections were analyzed from at least three different mice of each genotype at both 6 and 12 months. Three non-overlapping images were captured with a Zeiss Axiovert 25 microscope and >1000 fibers were analyzed for each genotype in all experiments.

Nerve Crush

Twelve week old control and *Actb*-MNsKO mice ($n = 4$ for each genotype) were first anesthetized with 0.2% isofluorane. Under aseptic conditions, a 15 mm incision was made distal and parallel to the femur of the left leg through the skin and biceps femoris muscle. The tibial nerve was located and dissected away from musculature and fat. Upon isolation, the tibial nerve was crushed with a fine tip hemostat (13020-12; Fine Science Tools, Foster City, CA) clamped to the first notch for exactly 30 seconds. After verification of crush under a dissecting microscope, the bicep femoris and skin were closed with 6-0 sterile silk suture. The left tibial nerve of all mice was crushed while the

right served as an inter-animal control. Mice were administered buprenorphine (0.05 mg/kg BW) immediately and then daily for three days post-surgery.

Print Length Factor

Functional recovery after tibial nerve crush was assessed via determination of the Print Length Factor (PLF) as described previously (George et al., 2003) with slight modification. The hind paws of mice were dipped in black India Ink and mice were allowed to walk down a corridor lined with white paper. Three trials at each time point were conducted per mouse, and four sets of prints from the same stride were measured and averaged for each time point.

***In vivo* Muscle Torque Analysis**

Maximal isometric torque of the plantarflexors (i.e., posterior muscles gastrocnemius, soleus, plantaris) was measured *in vivo* using a muscle-lever servomotor (model 300B-LR, Aurora Scientific, Aurora, Ontario,Canada). Mice were anesthetized with a cocktail of fentanyl citrate (10 mg/kg BW), droperidol (0.2 mg/kg BW), and diazepam (5 mg/kg BW). The left hindlimb was shaved, aseptically prepared, and each mouse was positioned on a heated platform with its left foot placed in a metal foot plate attached to the servomotor and knee clamped to maintain positioning throughout the experiment. Two platinum electrodes (model E2-12, Grass Technologies, West Warwick, RI, USA) were inserted subcutaneously on either side of the sciatic nerve. To ensure that sciatic nerve stimulation would not elicit anterior muscle contractions the peroneal nerve was cut. A plantar-flexion contraction was elicited by electrical stimulation of the sciatic nerve via a stimulator and stimulus unit (models S48 and SIU5, respectively, Grass Technologies,

West Warwick, RI, USA). The parameters for stimulation were set at a 200 ms contraction duration consisting of 0.5 ms square-wave pulses at 250 Hz. The voltage was adjusted from 3.0 to 9.0 V until maximal isometric torque was achieved.

Statistical Analysis

All data are presented as mean ± standard error of the mean and calculated with GraphPad Prism 5 software (GraphPad Software, Inc.). T-tests were conducted to determine statistical significance when only two groups were compared while one-way ANOVA was used for groups of three or more accompanied by a Tukey post hoc test or Bonferroni post-test in the case of the regeneration fiber diameter analysis. A p-value of <0.05 was considered significant.

RESULTS

Generation of a motor neuron specific β-actin knock-out mouse model (*Actb*-MNsKO)

In order to circumvent the early embryonic lethality observed in previous β-actin knock-out mouse models (Shawlot et al., 1998; Shmerling et al., 2005), floxed β-actin mice (Perrin et al., 2010) were crossed to the Mnx1-Cre transgenic mouse line to specifically ablate β-actin in motor neurons. The floxed *Actb* line has been used to successfully ablate β-actin from hair cells of the inner ear (Perrin et al., 2010) while the Mnx1-Cre line has been used extensively to generate a number of motor neuron specific knock-out mouse lines (Bolis et al., 2005; Hess et al., 2007; Luria and Laufer, 2007; Li et al., 2008; Chipman et al., 2010; Mende et al., 2010). We first confirmed the spatial and

temporal expression of Mnx1-Cre by crossing *Actb*-MNsKO mice with a ROSA26 reporter line containing the β-galactosidase gene with a floxed stop codon cassette. Thus, β-galactosidase activity is present only in tissues where Cre recombinase is expressed and functional. At embryonic day 12.5 (E12.5), Cre recombinase activity was present throughout the ventral horns along the entire length of the developing spinal cord, confirming robust expression of Mnx1-Cre in motor neurons in *Actb*-MNsKO embryos (Figure 2.1A-C). Successful recombination of the *Actb* locus was confirmed by PCR of genomic DNA from embryonic spinal cord tissue at E12.5 (Figure 2.1E). Furthermore, spinal cord sections from control and *Actb*-MNsKO mice were stained for β-actin protein and choline acetyltransferase (ChAT), a marker for motor neurons. β-actin expression was ubiquitous throughout the spinal cord, although it was relatively weak in the cell bodies of control motor neurons (Figure 2.1F top), consistent with previous reports indicating that β-actin is present in neuronal cell bodies only at low levels *in vivo* (Weinberger et al., 1996; Micheva et al., 1998). However, no detectable β-actin signal was present in motor neuron cell bodies from *Actb*-MNsKO mice, confirming motor neuron specific ablation of β-actin (Figure 2.1F bottom). Finally, no detectable β-actin signal was present in motor neuron cell bodies from a second line of β-acitn knock-out mice generated with the Nestin-Cre transgenic line (Figure 2S.1A), which expresses Cre in motor neurons and other cells of the central nervous system (CNS-*Actb*KO) ((Tronche et al., 1999; Graus-Porta et al., 2001; Schwander et al., 2004). Thus, we have verified selective and robust motor neuron specific Cre expression by the Mnx1-Cre transgenic mouse line, recombination of the floxed *Actb* locus, and loss of β-actin signal from motor

neuron cell bodies in two independent lines by immunofluorescence, collectively establishing conditional ablation of β-actin in motor neurons.

β-actin is not required for motor neuron viability

Motor neuron viability in *Actb*-MNsKO mice was assessed by quantifying Nissl stained motor neurons in the ventral horns of spinal cord sections. At 6 and 12 months of age, no significant differences were observed in the number of motor neurons per section in *Actb*-MNsKO compared to controls, indicating that β-actin is not required for motor neuron viability *in vivo* (Figure 2. 2A-C). Motor neuron size was also examined to quantitatively assess cell structure in motor neurons deficient for β-actin. At both 6 and 12 months of age, motor neuron diameter was comparable between control and *Actb*-MNsKO mice (Figure 2.2D). Although we did observe a significant difference ($p = 0.03$) in motor neuron diameter at 12 months of age, the difference of less than 1 μm is likely not biologically relevant.

NMJ maturation and maintenance in *Actb*-MNsKO mice

We next examined motor axon patterning and maintenance in *Actb*-MNsKO mice. Motor axon transit to target muscles occurs between E9 and E11-12, although NMJs are not fully mature until approximately two weeks after birth (Sanes and Lichtman, 1999; Mantilla and Sieck, 2008). Because of the rapid outgrowth of axons shortly after motor neuron birth and Mnx1-Cre expression, we were not able to conclude that β-actin protein was completely eliminated from motor neurons prior to motor axons reaching their final targets. However, we were interested in examining motor axon morphology and positioning following DNA recombination of the *Actb* locus, and thus the role of new β-

actin transcripts in late motor axon patterning. Given that recombination of the *Actb* locus occurs shortly after Mnx1-Cre expression at E12.5 (Figure 2.1D), synthesis of β-actin from mRNA transcribed after E12.5 cannot occur.

We used the developing mouse diaphragm as a model for assessing axonal guidance, where motor axons first reach the diaphragm between E11-12, but continue to branch and respond to guidance cues up to E15, when the mature innervation pattern is reached (Allan and Greer, 1997; Greer et al., 1999). Whole-mount E16.5 diaphragms from control and *Actb*-MNsKO embryos were stained with antibodies against neurofilament to label motor axons and fluorescently conjugated α-bungarotoxin to mark acetylcholine receptors at the motor end plate. Previous studies have shown defects in motor axon guidance can result in excessive motor axon branching or axons that fail to halt at the motor endplate (Lin et al., 2000; Brandon et al., 2003; Fu et al., 2005). We observed no indication of excessive motor axon branching (Figure 2.3A) or axons that extended beyond the motor end plate (Figure 2.3B). These results indicate that translation of β-actin mRNA transcribed after E12.5 is not required for the late stages of motor axon guidance and elongation in the diaphragm.

Actin is also hypothesized to be an important component of the pre-synapse at mature NMJs, with roles in synaptic vesicle organization and endocytosis (Wang et al., 1996; Cole et al., 2000; Shupliakov et al., 2002; Bloom et al., 2003). Using anti-neurofilament antibodies and α-bungarotoxin to label motor axons and acetylcholine receptors respectively, we stained whole-mount diaphragms from 4 month old control and *Actb*-MNsKO mice to assess NMJ stability and morphology. Nerve terminals were

highly branched and overlapped extensively with acetylcholine receptors (Figure 2.3C), with no indication of retraction bulbs or neurofilament aggregation as seen in SMA mouse models (Kariya et al., 2008; McGovern et al., 2008; Cifuentes-Diaz et al., 2002; Murray et al., 2008). Post-synaptic acetylcholine receptors exhibited a highly folded morphology consistent with normal motor endplates (Figure 2.3C). Thus, the observation of mature motor endplates together with morphologically normal nerve terminals indicates that β-actin is not required for the stability or long-term maintenance of NMJs.

In vivo muscle function of *Actb*-MNsKO mice

Although morphologically normal, subtle defects in pre-synaptic organization not visible by light microscopy could preclude normal NMJ synaptic transmission. In order to assess NMJ function in *Actb*-MNsKO mice, we used three physiological assessments of motor neuron function *in vivo*. Control and *Actb*-MNsKO mice at 6 and 12 months of age were subjected to grip strength, treadmill, and whole-body tension analyses to assess muscle performance and endurance. No significant differences were observed at either time point in any of the assays, suggesting that NMJ physiological function was not impaired in *Actb*-MNsKO mice (Figure 2.4A-D). CNS-*Actb*KO mice also presented with unimpaired motor function (Figure 2S.1B-C) comparable to the *Actb*-MNsKO mice, thus providing independent confirmation of our findings in the *Actb*-MNsKO line (Figure 2.4A-D). Because a mild mouse model of SMA presented with EMG abnormalities (Monani et al., 2003), we also examined 6 month old control and *Actb*-MNsKO mice for spontaneous muscle depolarization consistent with motor neuron degeneration. No

fibrillations or fasciculations were detected in *Actb*-MNsKO mice, further confirming the functional integrity of NMJs with β-actin deficient motor neurons.

Actb-MNsKO skeletal muscle does not show indications of atrophy or denervation

We next examined the histological properties of skeletal muscle from *Actb*-MNsKO mice for subtle or early signs of denervation. In a number of motor neuron diseases, selective loss of a particular fiber type or fiber type clustering can occur and is consistent with early motor neuron degeneration (Telerman-Toppet and Coers, 1978; Ben Hamida et al., 1994; Baloh et al., 2007). We stained gastrocnemius muscle sections from control and *Actb*-MNsKO mice at 6 and 12 months of age with antibodies to fast and slow myosin heavy chain to label fast and slow twitch muscle fibers respectively. No indication of fiber type clustering was observed in *Actb*-MNsKO mice and percent fiber type composition of the gastrocnemius up to 12 months of age was comparable to controls (Figure 2.5 A-B, E-F). Muscle fiber diameter was analyzed to determine whether any indication of muscle atrophy was present. Although significant differences were observed in fiber diameter between controls and *Actb*-MNsKO mice at both 6 and 12 months (Figure 2.5C-D, G-H), the small differences of approximately 2 μm are unlikely to be of physiological relevance, consistent with no significant differences observed in muscle performance at either 6 or 12 months in *Actb*-MNsKO mice (Figure 2.4A-D). Thus, β-actin is not essential for the long-term stability and function of motor neurons and NMJs as revealed by histological analysis of skeletal muscle.

β-actin is not required for functional motor axon regeneration

Because β-actin protein is estimated to have a half-life of 2-3 days (Dugina et al., 2009), it remains possible that the normal motor axon outgrowth observed in *Actb*-MNsKO embryos was due to persistence of β-actin expressed prior to gene recombination. To address the role of β-actin in axonal elongation more directly, we used a tibial nerve crush model to examine motor axon regeneration in mice at 12 weeks of age, long after recombination of the *Actb* locus between E9.5 and 12.5 (Yang et al., 2001) and Figure 2.1E).

Analysis of the print length factor (PLF) was used as a real-time readout for functional recovery and has been previously validated in mice (Inserra et al., 1998; George et al., 2003; Varejao et al., 2004). Before nerve crush, the PLF of control and *Actb*-MNsKO mice did not significantly differ from each other and approached zero, consistent with an uninjured, normal PLF (Figure 2.6A-B). One week after tibial nerve crush, both control and *Actb*-MNsKO mice demonstrated a significant increase in PLF compared to pre-injury values ($p < 0.05$), but did not significantly differ from each other, indicating that the level of injury was functionally equivalent between genotypes (Figure 2.6A-B). Both control and *Actb*-MNsKO mice followed a similar trend in functional recovery and did not significantly differ from each other up to 5 weeks post-crush (Figure 2.6A-B).

To complement the PLF recovery analysis, we also assessed motor neuron regeneration and reinnervation via nerve stimulation and analysis of muscle performance *in vivo*. At six weeks post-crush, the left (crushed-side) paw of sedated mice was placed

on a lever to measure torque generated by neuronal activation of the gastrocnemius/soleus complex. Both control and *Actb*-MNsKO mice generated equivalent amounts of maximal plantarflexion torque, providing further evidence that β-actin is not required for functional reinnervation of skeletal muscle following nerve crush (Figure 2.6C).

Finally, muscle histology was analyzed as in Figure 2.5 to determine whether any subtle indications of reinnervation defects were present. Fiber type composition did not significantly differ between the crushed side gastrocnemius of control and *Actb*-MNsKO, and neither significantly differed from their respective contralateral side, further indicating functional innervation was restored (Figure 2.6D-E). The same was true for the soleus, where fiber type composition was comparable between the crushed and contralateral sides with no indication of significant fiber type grouping (Figure 2.6H-I).

Fiber diameter analysis showed a moderate decrease in fiber diameter of the crushed side gastrocnemius in both control and *Actb*-MNsKO mice as compared to the contralateral side, indicative of temporary denervation and subsequent reinnervation following motor axon regeneration (Figure 2.6G). Although fiber diameter significantly differed between the crushed side gastrocnemius of control and *Actb*-MNsKO mice, the difference of 1.29 μm is not likely biologically relevant. Muscle fiber atrophy due to denervation was less pronounced in the soleus, with no significant difference in fiber diameter between the crushed and contralateral side of control solei muscles (Figure 2.6K). For reasons that are not clear, the contralateral soleus of *Actb*-MNsKO mice deviated significantly from that of the control contralateral soleus, although we would

expect a larger decrease in fiber diameter if atrophy was occurring due to muscle denervation. Additionally, fiber diameter of the crushed side and fiber type composition and distribution of both sides did not differ between controls and *Actb*-MNsKO mice (Figure 2.6H-K), further suggesting that this observed difference is not likely due to aberrant reinnervation.

Figure 2.1

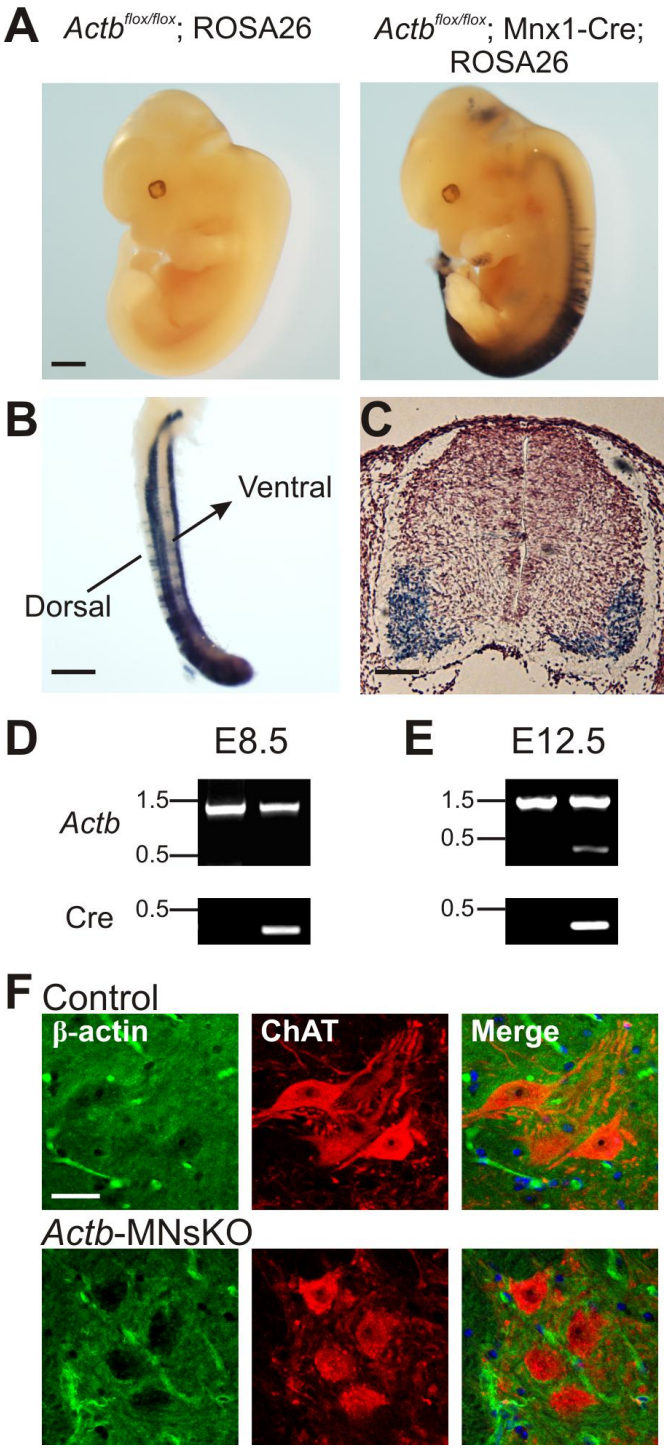
A
Actb flox/flox; ROSA26
Actb flox/flox; Mnx1-Cre; ROSA26
B
Ventral
Dorsal
C
D
E8.5
Actb
1.5
0.5
Cre
0.5
E
E12.5
1.5
0.5
0.5
F
Control
β-actin
ChAT
Merge
Actb-MNsKO

Figure 2.1: Verification of β-actin ablation in motor neuron specific β-actin knock-out mice. **(A)** *Actb* $^{flox/flox}$ and *Actb* $^{flox/flox}$; Mnx1-Cre (*Actb*-MNsKO) mice were crossed to the ROSA26 reporter strain and stained for β-galactosidase activity at E12.5. No background β-galactosidase activity was noted in Mnx1-Cre (-) controls. In Mnx1-Cre (+) embryos, β-galactosidase activity was present throughout the entire length of the spinal cord as seen in whole embryos **(A)** and isolated spinal cord **(B).** Scale bar 1mm. **(C)** Stained cross sections through the spinal cord showed β-galactosidase activity throughout the ventral horns confirming that Mnx1-Cre is expressed selectively in motor neurons in the developing spinal cord. Sections were counterstained with 0.1% neutral red. Scale bar 25μm. **(D-E)** PCR genotyping of spinal cord DNA extracts from control and *Actb*-MNsKO embryos. One day prior to Mnx1-Cre expression at E8.5, no recombination product was detected in embryos with the Cre transgene **(D)**. Following Cre expression and recombination at E12.5, the recombined *Actb* allele was present only in spinal cord DNA extracts from embryos harboring the Cre transgene and not in control embryos **(E)**. **(F)** Twenty micron cryosections from the ventral horn of the lumbar enlargement of 6 month old control and *Actb*-MNsKO mice stained with antibodies against β-actin and choline acetyltransferase (ChAT) to label motor neurons. Merged image also includes DAPI to label nuclei. Scale bar 30 μm.

Figure 2.2

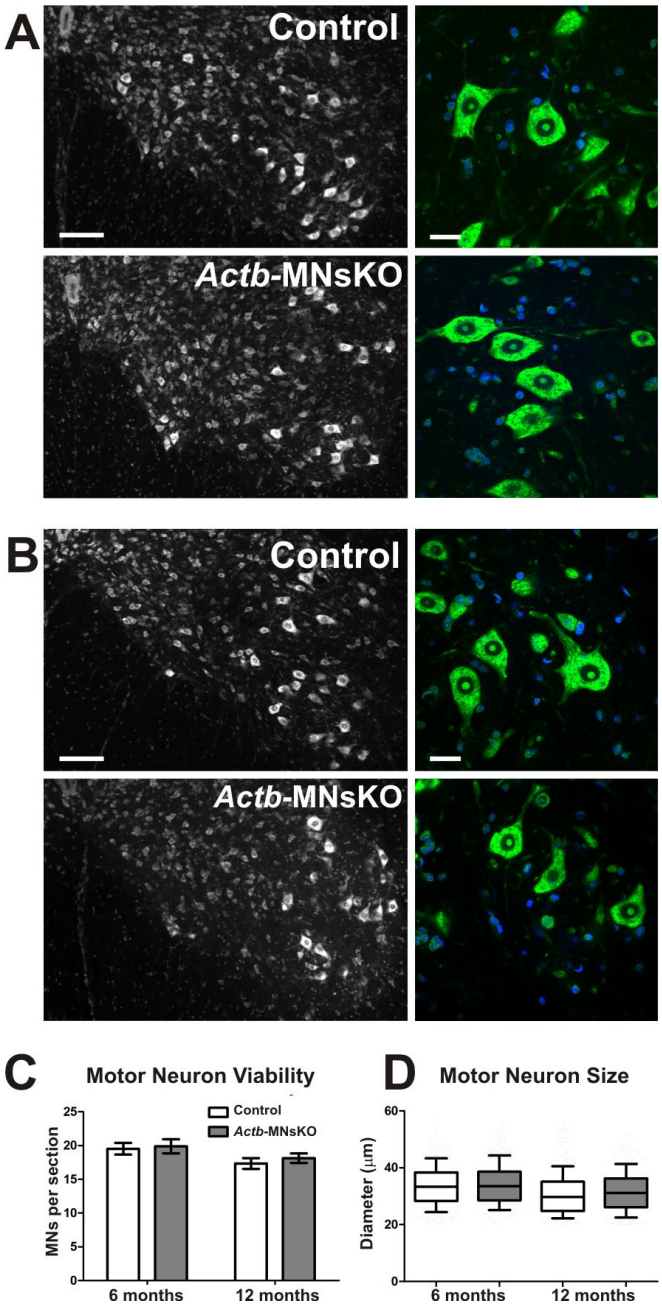
A
Control
Actb-MNsKO
B
Control
Actb-MNsKO
C
Motor Neuron Viability
Control
Actb-MNsKO
MNs per section
25
20
15
10
5
0
6 months
12 months
D
Motor Neuron Size
Diameter (μm)
60
40
20
0
6 months
12 months

Figure 2.2: β-actin is not required for motor neuron viability *in vivo.* (A) Representative images of Nissl stained spinal cord sections from the lumber enlargement of 6 and **(B)** 12 month old mice. Magnified images at right show no indication of chromatolysis in motor neurons. DAPI staining is in blue. Scale bar 100 μm left, 30 μm right. **(C)** Quantification of motor neurons per section at 6 and 12 months of age (n = 3 for each genotype per time point). No statistically significant differences were observed between control and *Actb*-MNsKOs at either time point. **(D)** Quantification of motor neuron size at 6 and 12 months of age. Data plotted as mean ± standard error of the mean.

Figure 2.3

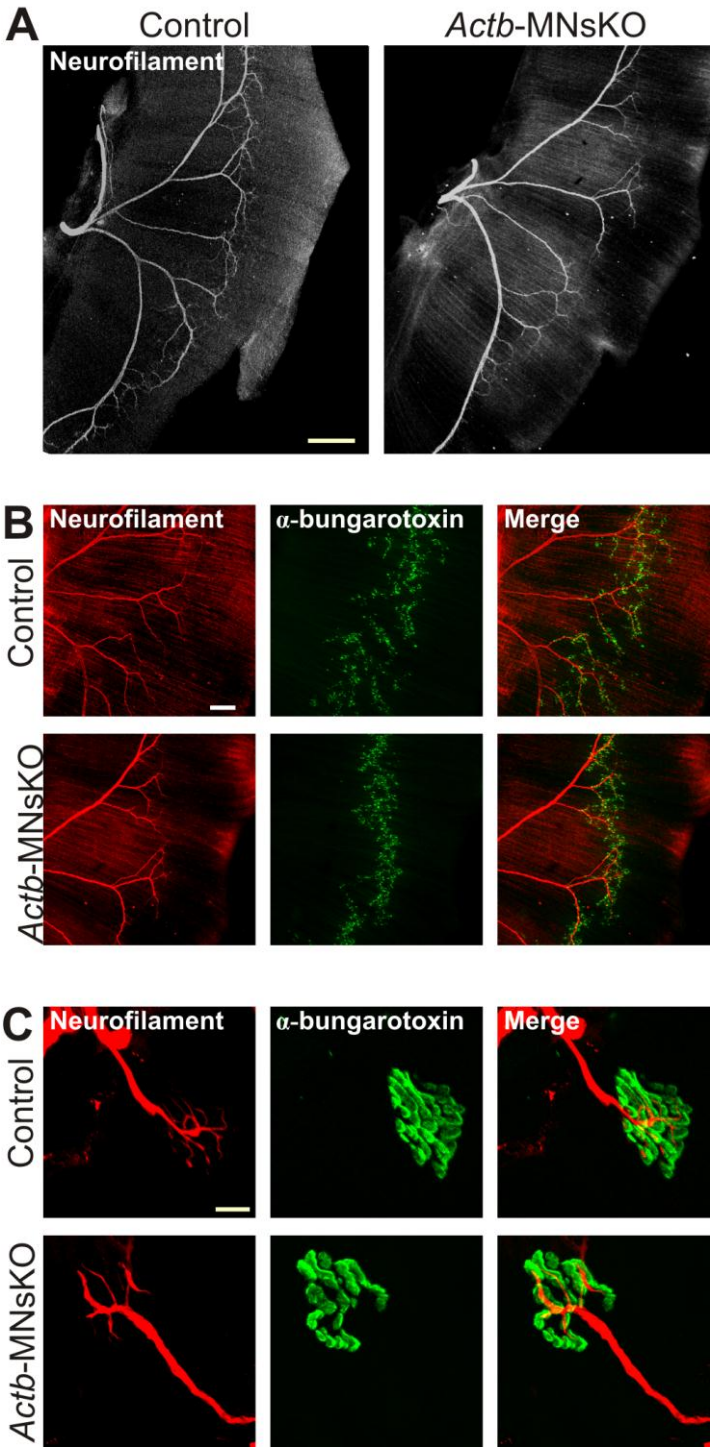
A
Control
Actb-MNsKO
Neurofilament
B
Neurofilament
α-bungarotoxin
Merge
Control
Actb-MNsKO
C
Neurofilament
α-bungarotoxin
Merge
Control
Actb-MNsKO

Figure 2.3: Neuromuscular junction development and morphology in *Actb*-MNsKO mice. (A) E16.5 left diaphragms stained with an anti-neurofilament antibody to label motor axons. Scale bar 300 μm. **(B)** Magnified images of E16.5 diaphragms stained with anti-neurofilament antibodies and Alexa 488 conjugated α-bungarotoxin. No indication of excessive branching or axons extending beyond the motor endplate was observed. Scale bar 150 μm. **(C)** Neurofilament and α-bungarotoxin staining of NMJs in the diaphragms of adult mice with no morphological defects observed. Scale bar 10 μm.

Figure 2.4

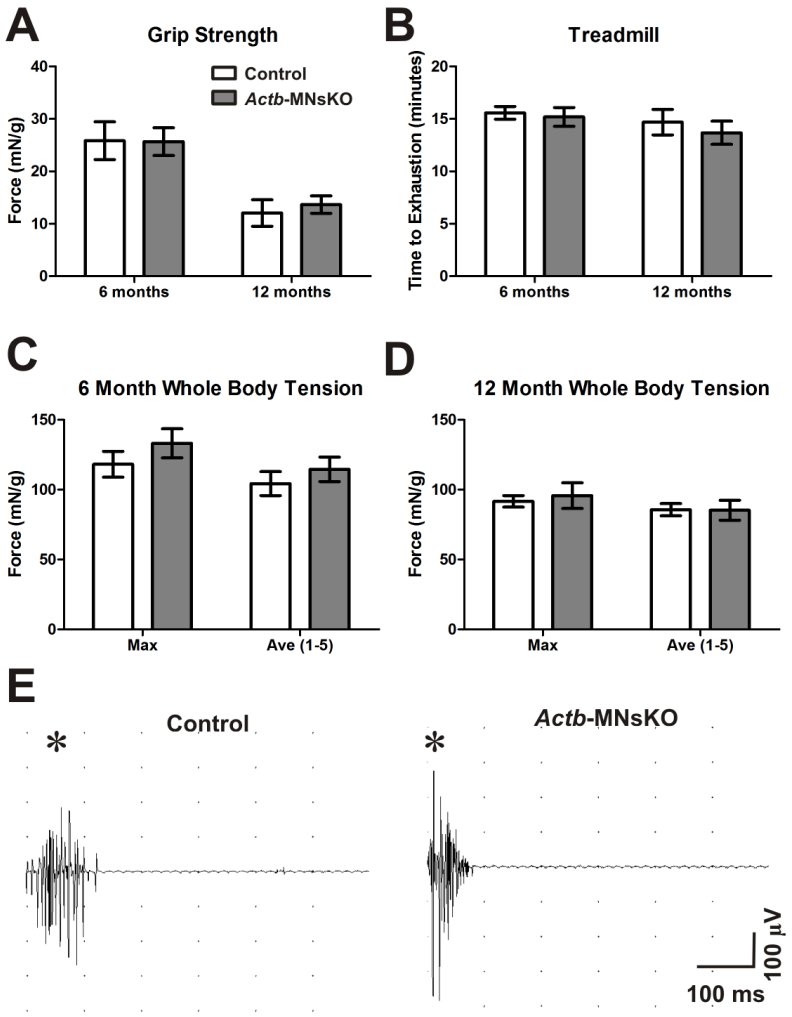

Figure 2.4: ***In vivo*** **muscle function of** ***Actb*****-MNsKO mice. (A)** Grip strength, **(B)** treadmill, and **(C)** whole-body tension analysis performed on 6 and 12 month old control and *Actb*-MNsKO mice. $n \geq 3$ animals per genotype per time point for all experiments. No significant differences were observed between control and *Actb*-MNsKO mice in any assay at either time point. Error bars represent standard error of the mean. **(D)** Electromyography of 6 month old control and *Actb*-MNsKO mice showed no indication of fibrillation or fasciculation ($n = 3$ mice per genotype). Asterisks indicate depolarization due to initial needle insertion.

Figure 2.5

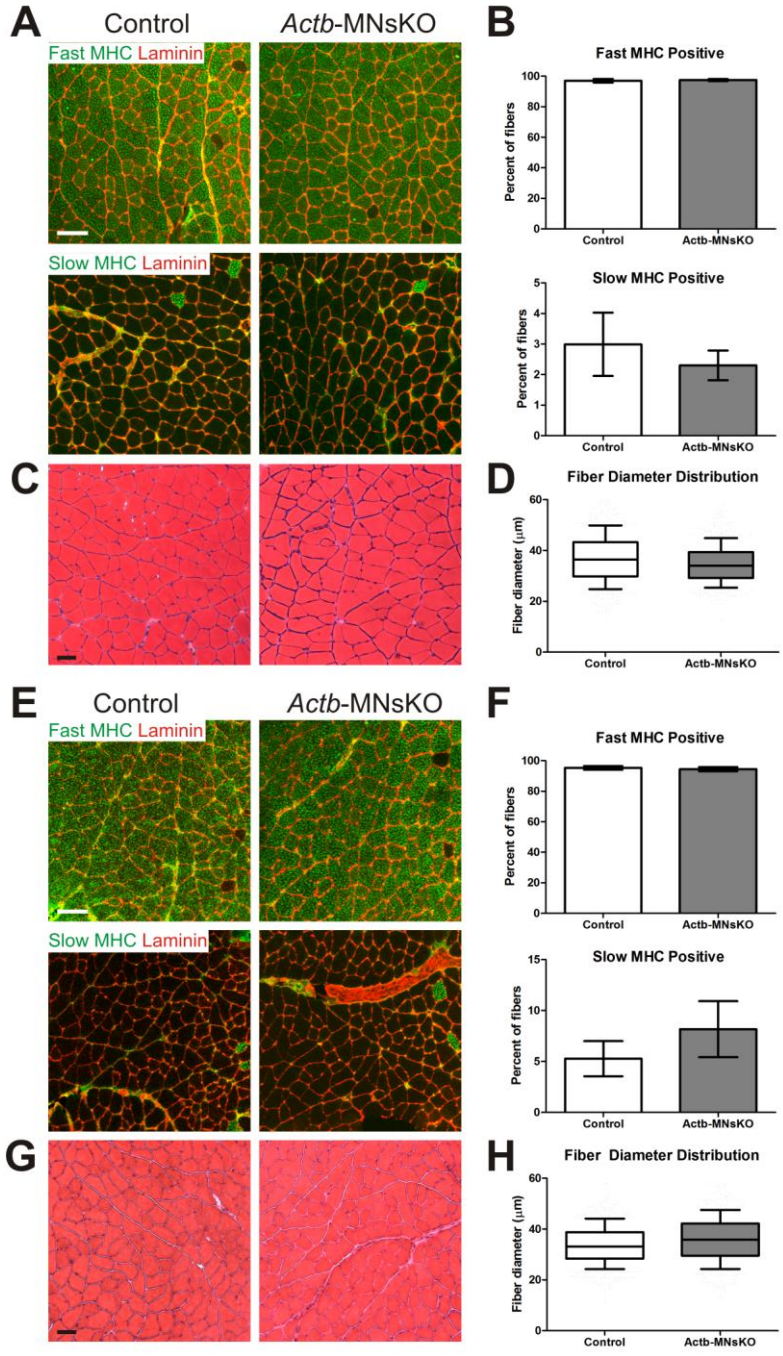
A
Control
Actb-MNsKO
Fast MHC Laminin
Slow MHC Laminin
B
Fast MHC Positive
Percent of fibers
Control
Actb-MNsKO
Slow MHC Positive
C
D
Fiber Diameter Distribution
Fiber diameter (μm)
E
F
G
H

Figure 2.5: Histological analysis of skeletal muscle in *Actb*-MNsKO mice. Fiber type composition and distribution was assessed in the gastrocnemius muscle of 6 and **(A-B)** and 12 month old **(E-F)** control and *Actb*-MNsKO mice. Antibodies to fast and slow myosin heavy chain were used to identify fast and slow twitch fibers respectively. Anti-laminin staining was used to delineate the borders of muscle fibers. Scale bar 100 μm. Fiber diameter was analyzed from hematoxylin and eosin stained sections of the gastrocnemius muscle at 6 **(C)** and 12 months **(G)** of age. Scale bar 50 μm. Box and whisker plots of fiber diameter distribution at 6 **(D)** and 12 **(H)** months of age.

Figure 2.6

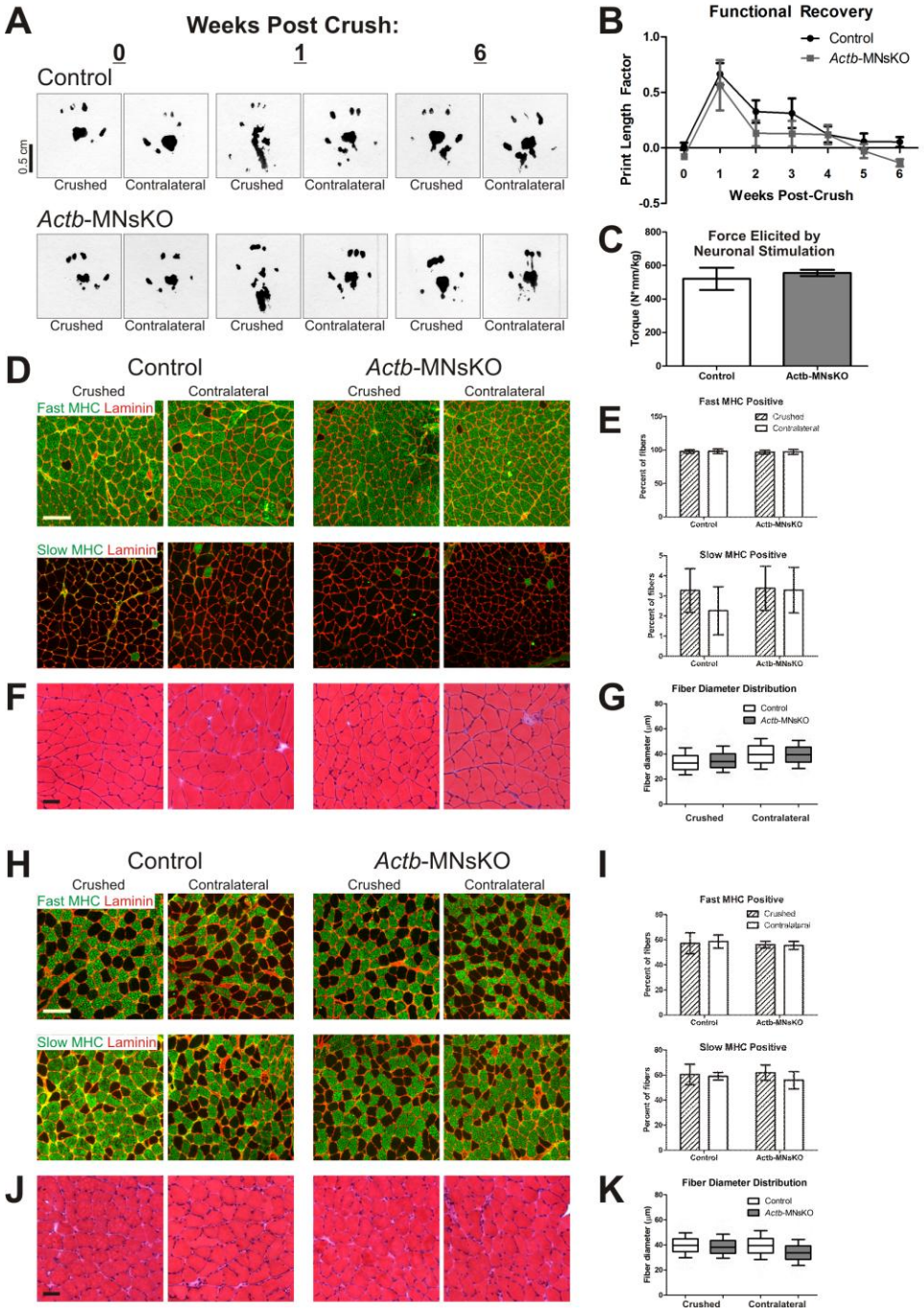
A
Weeks Post Crush:
0
1
6
Control
0.5 cm
Crushed
Contralateral
Actb-MNsKO
B
Functional Recovery
Control
Actb-MNsKO
Print Length Factor
Weeks Post-Crush
C
Force Elicited by Neuronal Stimulation
Torque (N*mm/kg)
Control
Actb-MNsKO
D
Control
Actb-MNsKO
Fast MHC Laminin
Slow MHC Laminin
E
Fast MHC Positive
Slow MHC Positive
Percent of fibers
F
G
Fiber Diameter Distribution
Fiber diameter (um)
H
I
J
K

Figure 2.6: Peripheral nerve regeneration is not impaired in *Actb*-MNsKO mice. (A) Representative paw prints from the crushed and contralateral side of control and *Actb*-MNsKO mice at 0, 1 and 6 weeks post-crush. **(B)** Quantification of PLF functional recovery (n = 4 mice per genotype). No significant differences were observed between control and *Actb*-MNsKO mice up to 5 weeks post-crush. **(C)** Force elicited by neuronal stimulation did not differ in *Actb*-MNsKO as compared to controls, indicating that axonal function had been restored (n = 3 mice per genotype). Fiber type composition and distribution in the crushed and contralateral side of the gastrocnemius **(D-E)** and soleus **(H-I)** muscle at 6 weeks post-crush. Scale bars 100μm. Fiber diameter distribution in the crushed and contralateral side of the gastrocnemius **(F-G)** and soleus **(J-K)** muscles at 6 weeks post-crush. Scale bar 50 μm. Three mice per genotype were analyzed for muscle histology.

Figure 2S.1

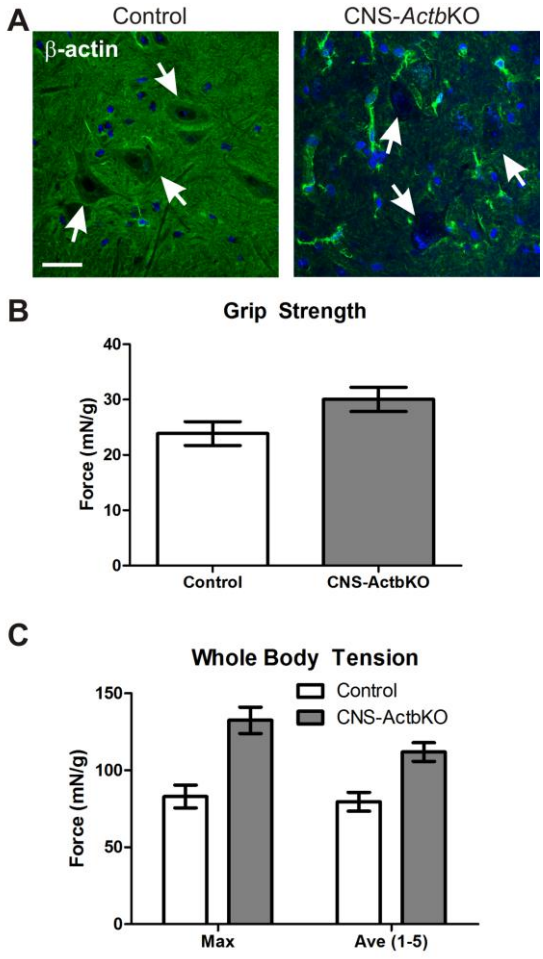

Figure 2S.1: Characterization of motor neuron function in CNS-*Actb*KO mice. (A) Ventral horns from cross sections of the lumbar enlargement of the spinal cord from adult control and CNS-*Actb*KO mice stained with a β-actin specific antibody and DAPI to label nuclei. Arrows indicate motor neuron cell bodies. Scale bar 30 μm. **(B-C)** Eight-10 month old CNS-*Actb*KO mice do not present with deficits in motor function compared to controls as determined by grip strength **(B)** and whole-body tension assays **(C)**. $n \geq 4$ mice per genotype. Data plotted as mean ± standard error of the mean.

DISCUSSION

Here we report the first *in vivo* characterization of β-actin function in motor neurons using a motor neuron specific β-actin knock-out mouse. β-actin deficient motor neurons were viable and formed morphologically and functionally normal NMJs based on immunofluorescence and *in vivo* muscle performance assays. Skeletal muscle histology supported these findings and revealed no indication of denervation up to 12 months of age. Finally, motor axon regeneration proceeded normally in the absence of β-actin, which altogether suggests that β-actin plays a non-essential role in mature motor neurons *in vivo*.

The dispensability of β-actin in motor neurons *in vivo* was surprising given that deficits in β-actin mRNA and protein localization correlated strongly with growth cone and axon elongation defects observed in cultured SMA motor neurons (Rossoll et al., 2003). However, a number of additional studies on SMA mouse models have not identified similar defects *in vivo*, suggesting that SMA is not likely caused by aberrant motor axon elongation or guidance (Kariya et al., 2008; McGovern et al., 2008; Murray et al., 2010). Instead, defects in NMJ maturation were reported in these SMA mouse models, with abnormalities in pre-synaptic architecture and delayed maturation of the post-synaptic motor endplate (Cifuentes-Diaz et al., 2002; Kariya et al., 2008; McGovern et al., 2008; Murray et al., 2008; Kong et al., 2009). The finding that voltage gated calcium channel delocalization correlated with the misregulation of β-actin in cultured SMA motor neurons suggests that an improperly formed pre-synaptic actin cytoskeleton could contribute to synaptic transmission defects, thus hindering NMJ maturation in

SMA mice (Jablonka et al., 2007). However, we have shown that NMJ maturation proceeds normally in *Actb*-MNsKO mice (Figure 2.3C), indicating that the NMJ maturation defects observed in SMA mice are not likely due to a loss-of-function of β-actin in the nerve terminal. Yet, we cannot rule out the possibility that the mislocalization of β-actin contributes to SMA pathogenesis by some other mechanism, perhaps by disrupting the subcellular localization of other proteins or that some compensatory mechanism occurring in *Actb*-MNsKO mice does not also occur in SMA mouse models.

While studies in SMA mice have not revealed axon guidance or elongation defects *in vivo*, the hypothesis that the localization and local translation of β-actin is important for normal motor neuron development cannot be ruled out. Although the timing of Cre expression limited our ability to assess early motor axon guidance and elongation in *Actb*-MNsKO mice, analysis of axonal regeneration following nerve crush allowed us to study axonal elongation in a system that recapitulates many properties of axonal development. Additionally, previous studies suggested that β-actin has an important role in peripheral nerve regeneration with reports indicating that β-actin expression is upregulated in response to sciatic nerve crush *in vivo*, and that β-actin localization is required for growth cone formation and axon elongation in injury-conditioned dorsal root ganglion cultures (Lund and McQuarrie, 1996; Vogelaar et al., 2009). However, β-actin deficient motor neurons had no functional defects or delays in axonal regeneration following nerve crush *in vivo* (Figure 2.6), suggesting that other actin isoforms or components of the cytoskeleton such as microtubules are likely sufficient for functional axonal regeneration and motor neuron function *in vivo*.

The dispensability of β-actin in mature motor neurons is also surprising given that loss of β-actin in hair cells of the inner ear and skeletal muscle results in mice with distinct phenotypes (Perrin et al., 2010; Prins et al., 2011). Thus, the requirement for β-actin *in vivo* likely varies in a tissue dependent fashion. Given the enormous diversity of neurons in the central nervous system, it remains possible that expression of β-actin may only be required by some neurons and not others. Additional studies using Cre lines expressed by distinct populations of neurons besides motor neurons will be required to determine the relative importance of β-actin to neuronal function *in vivo*.

Chapter 3

Ablation of β-actin in the brain causes discrete hippocampal defects with associated behavioral abnormalities

Bin Li performed the quantitative Western blotting in Figure 3.1A-B and neuronal morphology measurements in Figure 3.5. Tom Cheever performed all other experiments and wrote the manuscript.

SUMMARY

The local translation of β-actin is one mechanism proposed to regulate spatially-restricted actin polymerization crucial for nearly all aspects of neuronal development and function. However, the physiological significance of localized β-actin translation in neurons has not yet been demonstrated *in vivo*. To investigate the role of β-actin in the mammalian central nervous system (CNS), we characterized brain structure and function in a CNS-specific β-actin knock-out mouse (CNS-*Actb*KO). β-actin was rapidly ablated in the embryonic mouse brain, but total actin levels were maintained through upregulation of other actin isoforms during development. CNS-*Actb*KO mice exhibited significant perinatal lethality while survivors presented with restricted hippocampal and cerebellar morphological abnormalities that correlated with hyperactivity, maternal behavior defects, and decreased performance in the Morris water maze. Finally, we identified partial agenesis of the corpus callosum in CNS-*Actb*KO mice, which was likely due to neuronal extrinsic factors as hippocampal neurons in culture responded normally to attractive guidance cues. Altogether, we identified novel roles for β-actin in promoting complex CNS tissue architecture which have consequences for brain function when perturbed.

INTRODUCTION

The actin cytoskeleton has critical functions in gene expression, cell division, cell migration, force generation, and endocytosis (Bettinger et al., 2004; Hofmann et al., 2004; Pollard and Cooper, 2009). Additionally, the regulated polymerization of actin is of particular importance in neurons where it contributes to almost every stage of neuronal development (Luo, 2002). Following neurogenesis, the localized polymerization of actin filaments in the leading process of migrating neurons is crucial for the final positioning of neurons throughout the brain (Ayala et al., 2007). The localized polymerization of actin is also critical in the initial wiring of the nervous system, where actin filaments in axonal growth cones are locally remodeled in response to guidance cues, facilitating the proper formation of synapses in the developing CNS (Dent and Gertler, 2003). Finally, actin polymerization in dendritic spines of mature neurons is thought to be important in mediating synaptic plasticity and learning (Cingolani and Goda, 2008).

Although the mechanisms regulating localized actin polymerization in neurons remain incompletely understood, current data support two models that are not necessarily mutually exclusive. The first model relies on the regulated activity of a plethora of actin binding proteins to promote local actin polymerization, while the second model focuses on local synthesis of β-actin to mediate localized actin polymerization in neurons. β-actin is one of six actin isoforms expressed in mammalian cells and is the only isoform thought to be locally translated (Rubenstein, 1990; Hill and Gunning, 1993; Kislauskis et al., 1993). The molecular mechanism of the latter model has been extensively characterized in various cell culture models and is dependent on a 54 nucleotide sequence in the 3'

untranslated region of β-actin mRNA called the "zipcode"(Kislauskis et al., 1994). The zipcode sequence of β-actin mRNA is bound cotranscriptionally by zipcode binding protein-1 (ZBP1; also known as IMP1 in humans, mIMP or CRD-BP in mice, Vg1RBP in Xenopus) which mediates the transport of β-actin mRNA from the cell body to the growth cone while also inhibiting its translation (Ross et al., 1997; Huttelmaier et al., 2005; Yisraeli, 2005). When attractive guidance cues are received at one side of the growth cone, a signaling cascade is initiated leading to the phosphorylation of ZBP1 and release of β-actin mRNA, thus freeing it for local translation (Huttelmaier et al., 2005; Leung et al., 2006; Yao et al., 2006; Sasaki et al., 2010). However, growth cones are believed to constitutively express high concentrations of monomeric actin, and a general role for local translation in early growth cone guidance is controversial (Devineni et al., 1999; Roche et al., 2009). Furthermore, the significance of this mechanism *in vivo* has yet to be established. A knock-out of the mouse ZBP1ortholog *Imp1* exhibited high perinatal lethality but no reported brain pathology, while motor neuron specific β-actin knock-out mice presented with no defects in motor neuron function or axonal regeneration (Hansen et al., 2004; Cheever et al., 2011).

In order to investigate the role of β-actin in the development and function of the mammalian CNS, we generated a central nervous system specific β-actin knock-out mouse (CNS-*Actb*KO). β-actin was rapidly and efficiently ablated from the brains of CNS-*Actb*KO mice while γ- and α_{sm}-actin isoforms were upregulated to maintain total actin levels during development. However, nearly two thirds of these mice died postnatally, demonstrating an important role for β-actin in the developing CNS. Animals

that did survive were significantly smaller and presented with hind-limb contractures. Closer examination of the brain revealed specific defects in the morphology of the cerebellum and hippocampus that correlated with hyperactivity, poor performance in the Morris water maze, and maternal behavior defects. CNS-*Actb*KO mice also exhibited partial agenesis of the corpus callosum, raising the possibility of impaired axon guidance in growth cones unable to locally translate β-actin. However, cultured hippocampal neurons from CNS-*Actb*KO embryos exhibited only limited morphological defects and responded normally to guidance factors, suggesting that the corpus callosum agenesis had a non-neuronal component. Together, our study reveals a previously unreported role for β-actin in the morphogenesis of the hippocampus, corpus callosum, and cerebellum, while demonstrating that the local translation of β-actin may have a more restricted role in nervous system development and function than previously thought.

MATERIALS AND METHODS

Mouse Lines, Breeding, and Ethics Statement

CNS-*Actb*KO mice were generated by crossing a floxed *Actb* mouse line (Perrin et al., 2010) to the Nestin-Cre transgenic line (Stock# 003771, Jackson Labs, Bar Harbor, ME) as described previously (Cheever et al., 2011). Homozygous floxed animals lacking the Cre transgene were used as controls. Because of the scarcity of CNS-*Actb*KO animals and a maternal behavior defect in CNS-*Actb*KO females, breeding of *Actb flox/+*; Nestin-cre animals to *Actb flox/flox* animals was required. For timed matings, the morning a

vaginal plug was found was designated E0.5. The experimental protocols in this study were reviewed and approved by the University of Minnesota Institutional Animal Care and Use Committee (IACUC) and approved on August 13th, 2010 (IACUC Protocol #0907A69551).

Brain Lysate Preparation and Quantitative Western Blot Analysis

Control and CNS-*Actb*KO embryo and adult (6-9 month old) mouse brains were snap frozen and pulverized in liquid nitrogen. Pulverized tissue was solubilized in a 1:10 (m:V) dilution of SDS lysis buffer (1% SDS, 5 mM EGTA, 1 mM Benzamadine, 10 µM Leupeptin, 0.2 mM PMSF) at 100°C for 5 minutes. Lysates were then cleared by centrifugation at 25,000 × g for 2 minutes. The resulting supernatant was collected and analyzed with the Bio-Rad D_C protein assay kit to determine protein concentration. 25 mg of control and CNS-*Actb*KO brain lysates were then run side by side and in duplicate on 8-16% SDS-polyacrylamide gels, transferred to PVDF membrane, and blocked for 1 hour in 5% milk. The following primary antibodies were used: C4, a pan-actin antibody that recognizes all actin isoforms (LMAB-C4, Seven Hills Bioreagents, Cincinatti, OH, 1:1000), anti-β-actin antibody AC15 (A1978, Sigma Aldrich, St. Louis, MO, 1:1000), anti-γ-actin antibody 2-4 ((Hanft et al., 2006), 1:1000) and anti-α_{sm}-actin antibody 1A4 (A5228, Sigma Aldrich, 1:500). All membranes were also incubated with an anti-GAPDH antibody (G9545, Sigma Aldrich, 1:2000) as a loading control. Infrared dye conjugated secondary antibodies were purchased from Li-Cor Biosciences. The infrared signals from duplicate blots were quantitatively measured with the Li-Cor Odyssey

Imager system (Li-Cor Biosciences, Lincoln, NE, USA), normalized to the loading control signal and averaged.

Brain Isolation, Histology and Immunofluorescence

Brains for histology were isolated from age matched adult (4-18 month old) control and CNS-*Actb*KO mice and perfused, post-fixed and cryoprotected as described previously (Cheever et al., 2011). Brains were then blocked in the desired orientation and frozen in OCT (TissueTek, Torrance, CA) on dry ice. Sixteen micron cryosections were cut and stored at -20°C until processing for histology or immunofluorescence. For histology, sections were equilibrated to room temperature and stained with 0.1% Cresyl Violet acetate (C1791, Sigma Aldrich, St. Louis, MO) following standard protocols. Stained sections were mounted with Eukitt (03989, Sigma Aldrich).

For immunofluorescence with actin isoform-specific antibodies, sections were post-fixed in 100% Methanol and processed as described previously (Cheever et al., 2011). For β- and γ-actin staining, sections were co-labeled with directly conjugated anti-β-actin AC15 (ab6277; Abcam, Cambridge MA, 1:75) and directly conjugated mouse monoclonal anti-γ-actin (Clone 1-37-Alexa568; Hanft et al., 2006; Perrin et al., 2010), 1:50). Anti-α_{sm}-actin 1A4 was used to localize α_{sm}-actin in brain sections (A5228; Sigma Aldrich, 1:400) with an anti-mouse Alexa Fluor 488 conjugated secondary antibody (Invitrogen, Carlsbad, CA, 1:500). Coverslips were mounted with SlowFade Gold antifade reagent with DAPI (S36938; Invitrogen). Images were acquired on an Olympus FluoView FV1000 laser scanning confocal microscope at the Biomedical Image

Processing Laboratory with identical settings between control and CNS-*Actb*KO sections. Images were further processed identically with Adobe Photoshop.

Behavioral Assays

Rotarod

An accelerating Rotarod apparatus (Accelerating Model, Ugo Basile Biological Research Apparatus, Varese, Italy) was used to assess motor coordination in gender matched 6 month old control and CNS-*Actb*KO mice (*n*=8 controls and 6 CNS-*Actb*KO mice). The Rotarod was configured to accelerate from 4-40 RPM in five minutes, and continue at the maximal speed for another five minutes. Mice were tested for four consecutive days with four trials per day and 10 minute rest intervals between each trial.

Open Field Activity Assay

Activity of age matched adult (6-9 month old) male control (*n*=4) and CNS-*Actb*KO (*n*=4) mice in a 50 x 50 x 40cm test cage was videotaped and analyzed using the Topscan System (Clever System). Mice were allowed to explore the cage for 15 minutes while their activity was tracked.

Water Maze

A water maze analysis was conducted in a 1.2 m diameter opaque pool with water maintained at 24 ± 0.5°C. The testing room was decorated with posters and other fixtures to serve as spatial cues. Age matched adult (6-9 month old) male control (*n*=4) and CNS-*Actb*KO (*n*=4) mice were trained to locate a 10cm platform submerged 0.5 cm under the

water in an arbitrary quadrant during 90 second training trials. On the first day, the platform was raised to the surface of the water and fitted with a 15 cm flag to serve as a cued control for possible visual differences between control and CNS-*Actb*KO animals. Hidden platform learning sessions were conducted on the following nine days, where mice performed two 90 second trials per day separated by 30 minutes. Mice were started from randomized positions approximately equidistant from the hidden platform. For the probe trial, the platform was removed and mice were started from a novel starting position for a 30 second probe trial. Video data was analyzed with the Topscan Video Analysis System (Clever System).

Food Consumption

Food consumption from adult (4-6 month old) male control and CNS-*Actb*KO mice (*n*=4 for each genotype) was analyzed by weighing the amount of food initially placed in the cage and the amount consumed per 24 hours for three consecutive days. The data from the three days was then averaged.

Culturing Primary Hippocampal Neurons

Primary hippocampal neurons from E15.5 embryos were isolated and cultured individually as described previously (Strasser et al., 2004) with modifications listed below. Embryos were genotyped from tail snip lysates following protocols described previously (Cheever et al., 2011). 80,000 neurons were plated in 35 mm dishes containing acid washed coverslips coated with Poly-D-Lysine (100 μg/ml) and laminin (4 μg/ml). Neurons were plated in neuronal plating media (MEM with Earle's salts, 10 mM

HEPES, 10 mM sodium pyruvate, 0.5 mM glutamine, 12.5 μM glutamate, 10% FBS, and 0.6% glucose). Four to six hours after plating, the media was replaced with neuronal growth media (Neurobasal media with B27 supplement, 0.5 mM glutamine, 12.5 mM glutamate, 1X penicillin/streptomycin (P433, Sigma Aldrich)). For netrin-1 bath application experiments, 250 ng/ml mouse netrin-1 (R&D Systems, Minneapolis, MN) was added to the neuronal growth media at the time of media change as described previously (Popko et al., 2009). An equivalent volume of PBS was added to control cultures.

For all experiments, neurons were cultured for three days *in vitro* and then fixed in 4% PFA in PBS warmed to 37°C for 15 minutes. The coverslips were then rinsed in PBS, permeabilized for 10 minutes in 0.2% Triton X-100 in PBS, rinsed again in PBS, and blocked with 3% BSA in PBS for 30 minutes. Coverslips to be used for morphological analysis were then stained with a mouse monoclonal anti-βIII tubulin (G712A; Promega, Madison, WI, 1:2000) followed by an anti-mouse Alexa 488 fluor conjugated secondary antibody (Invitrogen). Coverslips were finally washed again in PBS and mounted in SlowFade Gold antifade reagent with DAPI (Invitrogen, S36938). For cultures stained with actin isoform specific antibodies, coverslips were post-fixed in ice cold 100% Methanol at -20°C for 10 minutes, rinsed for 5 minutes in PBS, and then processed as described above. The directly labeled anti-β-actin antibody described above was used along with a rabbit polyclonal anti-γ-actin 7577 (Hanft et al., 2006) and an anti-rabbit Alexa 568 conjugated secondary antibody. Images were acquired on an Olympus

FluoView FV1000 laser scanning confocal microscope or a Zeiss Axiovert 25 micrscope under identical conditions for control and CNS-*Actb*KO coverslips.

Stage 3 neurons were characterized for morphological analysis where the axon was specified as the primary neurite at least twice as long as the next longest primary neurite. All measurements were made with the NeuronJ ImageJ plugin (Meijering et al., 2004). Data for analysis of morphological parameters in control (n=127 neurons) and CNS-*Actb*KO neurons (n=149) was collected from at least two independent cultures. Analysis of cultured neuron response to netrin-1 was conducted on control (n=120) and CNS-*Actb*KO (n=113) neurons gathered from two independent experiments. Axonal branches were defined as processes extending at orthogonal angles to the axon, while distal axon segments were identified as the process that remained parallel to the axonal segment proximal to the branch point as described previously (Dent et al., 2004).

Statistics

All data are presented as mean ± standard error of the mean and calculated with GraphPad Prism 5 software (GraphPad Software, Inc.). T-tests were conducted to determine statistical significance when only two groups were compared while one-way ANOVA was used for groups of three or more accompanied by a Tukey post hoc test. A p-vale of <0.05 was considered significant.

RESULTS

Actin isoform expression in CNS-*Actb*KO brains

In order to examine the role of β-actin in the CNS, floxed *Actb* mice (Perrin et al., 2010) were crossed to the transgenic Nestin-Cre line (Tronche et al., 1999; Graus-Porta et al., 2001) to generate CNS-specific β-actin knock-out mice (CNS-*Actb*KO). Brains from embryonic day (E) 13.5, E18.5, and adult control and CNS-*Actb*KO mice were analyzed via quantitative Western blot analysis to confirm β-actin ablation (Figure 3.1A-B). At E13.5, approximately three days after Cre expression and DNA recombination, β-actin levels in CNS-*Actb*KO brains were decreased 53.8% and further reduced to 30% of controls at E18.5. Adult CNS-*Actb*KO mice exhibited a 90.9% reduction of β-actin relative to controls, with the remaining β-actin likely due to the presence of non-CNS derived cells (Figure 3.1C). Using a pan-actin antibody that recognizes all actin isoforms, we measured similar levels of total actin in CNS-*Actb*KO and control embryos throughout development. However, brains from adult CNS-*Actb*KO mice revealed a 19.8% decrease in total actin, demonstrating that adult CNS-*Actb*KO brains were unable to completely compensate for the loss of β-actin. The most closely related actin isoform to β-actin, γ-actin, was upregulated on average 19.5% at all time points analyzed. Surprisingly, the most dramatic increase in actin isoform expression was measured for vascular smooth muscle α-actin (α_{sm}-actin). Although the expression of α_{sm}-actin in E13.5 CNS-*Actb*KO embryos did not differ from controls, at E18.5 α_{sm}-actin was upregulated 35-fold. This significant increase in α_{sm}-actin expression was reduced to only

a 3.4-fold increase in adults however, likely due to increased α_{sm}-actin expression in controls as a result of the increased vasculature in mature brains.

To examine the localization of actin in CNS-*Actb*KO brains, we performed immunofluorescence microscopy with actin isoform-specific antibodies on sections from E18.5 control and CNS-*Actb*KO embryos. While β-actin was expressed throughout the hippocampal region in control embryos, signal from CNS-*Actb*KO sections in the hippocampus was absent (Figure 3.1C). The pattern of γ–actin staining in CNS-*Actb*KO sections was indistinguishable from β- and γ-actin staining in control sections (Figure 3.1C). α_{sm}-actin was only detectable around vasculature in controls (Figure 3.1C arrows), but was surprisingly found in select populations of cells throughout the hippocampus in CNS-*Actb*KO embryos (Figure 3.1C bottom right panel and inset).

Perinatal lethality and gross morphological phenotypes in CNS-*Actb*KO mice

We next determined whether the increased expression of γ- and α_{sm}-actin was able to compensate for the ablation of β-actin and maintain the viability of CNS-*Actb*KO mice. The expected number of CNS-*Actb*KO embryos were found immediately prior to birth at E18.5, but nearly two thirds were lost before weaning at postnatal day 21 (P21) due to unknown causes (Figure 3.2A). E18.5 CNS-*Actb*KO embryos were morphologically indistinguishable from controls and of a similar mass (Figure 3.2B). The small number of CNS-*Actb*KO mice that escaped perinatal lethality were on average 32.4% smaller than control littermates and maintained this decreased mass throughout adulthood despite having a caloric intake two times greater than controls (Figure 3.2C

and 3S.1B). Surviving CNS-*Actb*KO mice also exhibited hind-limb clasping or contractures (Figure 3.2D) which are generally indicative of neuromuscular dysfunction. Adult CNS-*Actb*KO mice were otherwise morphologically unremarkable however, and lived normal lifespans. Isolated brains of CNS-*Actb*KO mice revealed no obvious abnormalities other than a slightly decreased size which was proportional with their reduced body size (Figure 3.2E).

Histopathology in brains from CNS-*Actb*KO Mice

Although surviving CNS-*Actb*KO mice presented with only limited gross phenotypes, examination of CNS-*Actb*KO brains histologically revealed several morphological abnormalities in select areas of the brain. Midsaggital sections through the adult cerebellum and stained with Cresyl violet revealed abnormal foliation patterns (denoted by asterisks in Figure 3.3A) that varied from extensive (Figure 3.3A-left panel), to the aberrant positioning of only a single folia (Figure 3.3A-middle panel). Interestingly, lamination of the cerebellum appeared unperturbed in the absence of β-actin, with no gross derangement of the molecular or granule cell layer.

Examination of the hippocampus in adult CNS-*Actb*KO mice also revealed prominent abnormalities. In saggital sections of the hippocampus, the dorsal arm of the dentate gyrus was abnormally positioned and approached the CA1 pyramidal cell layer (Figure 3.3B). In addition, the hippocampal fissure (denoted by arrows in Figure 3.3B) intersected with a portion of the CA1 pyramidal cell layer correlating spatially with the invasion of the dentate gyrus (delineated by dashed lines in Figure 3.3B). A dramatic decrease in cell body staining in the CA1 pyramidal cell layer was also apparent in the

region invaded by the dentate gyrus and hippocampal fissure (area between dashed lines). Interestingly, these abnormalities appeared to be more severe rostrally, with the derangement of the dorsal arm of the dentate gyrus (black arrow in Figure 3.3C) and decreased staining in the CA1 cell layer (red arrow in Figure 3.3C) more prominent rostrally compared to more caudal sections.

CNS-*Actb*KO mice also presented with partial agenesis of the corpus callosum. While the callosal axons from control mice completely crossed the midline (Figure 3.3D left panel, arrow), axons from CNS-*Actb*KO mice stopped short and appeared to assemble into probst bundles (arrows in Figure 3.3D, right panel) indicative of growth cone aggregation due to an inability to traverse a substrate. The callosal axons in more rostral sections however crossed the midline normally (Figure 3.3E). Interestingly, the agenesis of the corpus callosum appeared to occur at levels that overlay the hippocampus, suggesting a possible interaction between the aberrant morphology of the hippocampus and corpus callosum. No other features of the brain appeared disturbed, including the cortex which was laminated properly into the six cortical layers (Figure 3S.2). Thus, abnormal tissue architecture in CNS-*Actb*KO brains was apparent only in a subset of brain structures.

Behavioral abnormalities in CNS-*Actb*KO mice

CNS-*Actb*KO mice exhibited no overtly abnormal cage behaviors with one striking exception. No pups born to a CNS-*Actb*KO mother survived longer than one day regardless of genotype (Figure 3S.1D). This maternal behavior defect correlated with an apparent pup retrieval deficit (Figure 3S.1E, left), which may explain the pup mortality.

Importantly, the maternal behavior defect observed was not due to the pups themselves, as pups born to CNS-*Actb*KO mothers can be fostered to control females where they were retrieved and survived (Figure 3S.1E, right).

In order to determine if the observed cerebellar histological anomalies resulted in behavioral phenotypes, cerebellar function was assessed using the Rotarod apparatus. CNS-*Actb*KO mice performed similarly to controls however, suggesting cerebellar functions in motor performance are largely intact (Figure 3S.1C). We also conducted an Open Field activity assay to examine motor function and basal activity levels of CNS-*Actb*KO mice. Surprisingly, CNS-*Actb*KO mice exhibited a profound hyperactive phenotype. Representative traces of mouse activity from the first five minutes of a fifteen minute trial are shown in Figure 3.4A. CNS-*Actb*KO mice traveled significantly farther and at a significantly greater average velocity than control mice (Figure 3.4B-C). The profound hyperactivity may explain the significant increase in caloric demand observed in CNS-*Actb*KO mice (Figure 3S.1A-B) and the reduced size of these animals throughout their lifetime (Figure 3.2C). Interestingly, the hippocampus has also been implicated in the regulation of mouse basal activity, suggesting that the morphological abnormalities in the hippocampus could contribute to the hyperactive phenotype observed (Viggiano, 2008; Mignogna and Viggiano, 2010).

In order to more directly examine hippocampal function, CNS-*Actb*KO and control mice were subjected to a Morris water maze. CNS-*Actb*KO mice performed similarly to controls with a cued platform, suggesting that vision is not likely impaired in these animals (Figure 3.4G). During a nine day hidden platform training series, CNS-

*Actb*KO mice appeared to perform comparably to controls until the last day, at which time CNS-*Actb*KO mice took significantly longer than controls to find the platform (Figure 3.4G). Traces from the probe trial revealed that CNS-*Actb*KO mice employed an unusual search pattern (Figure 3.4Fand 3S.1D) and spent a significantly smaller percentage of time in the platform quadrant compared to controls (Figure 3.4H). This was also corroborated by quantification of distance traveled in the platform quadrant (Figure 3.4I) and platform area crosses (Figure 3.4J), both of which were significantly decreased in CNS-*Actb*KO mice. The abnormal performance of CNS-*Actb*KO mice suggests these mice suffer from cognitive dysfunction with a possible basis in aberrant hippocampal organization.

CNS-*Actb*KO hippocampal neurons are comparable to controls in culture

While the restricted nature of histological abnormalities in CNS-*Actb*KO brains was unexpected, agenesis of the corpus callosum is often linked to axon guidance defects where β-actin is believed to have an essential role (Richards et al., 2004). In order to investigate whether the corpus callosum agenesis was due to defective neuronal development, we cultured primary hippocampal neurons from control and CNS-*Actb*KO embryos to examine neuronal morphology and response to guidance cues *in vitro*. Hippocampal neurons derived from E15.5 CNS-*Actb*KO embryos and cultured three days *in vitro* were null for β-actin by immunofluorescence (Figure 3.5A). Immunolocalization of β- and γ–actin in control neurons revealed that both cytoplasmic actin isoforms colocalized throughout the neuronal cell body (Figure 3.5A) and growth cone (Figure 3.5B).

We next analyzed morphological parameters in hippocampal neurons to determine if the absence of β-actin adversely affected neuritogenesis or differentiation *in vitro*. Quantification of neurons labeled with a βIII-tubulin antibody revealed no significant differences in the length of axon or axon branches, number of axonal branches, number of dendrites or dendritic branches, or length of dendritic branches (Figure 3.5C-D). However, we did observe a small but significant decrease in the length of primary dendrites (Figure 3.5D). The number of dendritic branches was also reduced in CNS-*Actb*KO neurons, but did not reach statistical significance (Figure 3.5D).

Finally, we assessed how β-actin deficient hippocampal neurons respond to guidance cues using a bath application of netrin-1, an attractive guidance cue that promotes axon branching in hippocampal neurons and has also been shown to induce localization of β-actin in *Xenopus* neurons (Leung et al., 2006; Popko et al., 2009). Interestingly, neurons from CNS-*Actb*KO embryos showed a significant increase in axonal branching following exposure to netrin-1 that was comparable to controls (Figure 3.5E-F). Because axonal branching and growth cone turning in response to attractive guidance cues utilize similar mechanisms (Dent et al., 2003; Dent et al., 2004), the equivalent increase in axonal branching of CNS-*Actb*KO hippocampal neurons suggests β-actin deficient neurons can respond normally to guidance cues. Thus, the agenesis of the corpus callosum *in vivo* is likely due to neuronal extrinsic factors and not an inability to locally translate β-actin.

Figure 3.1

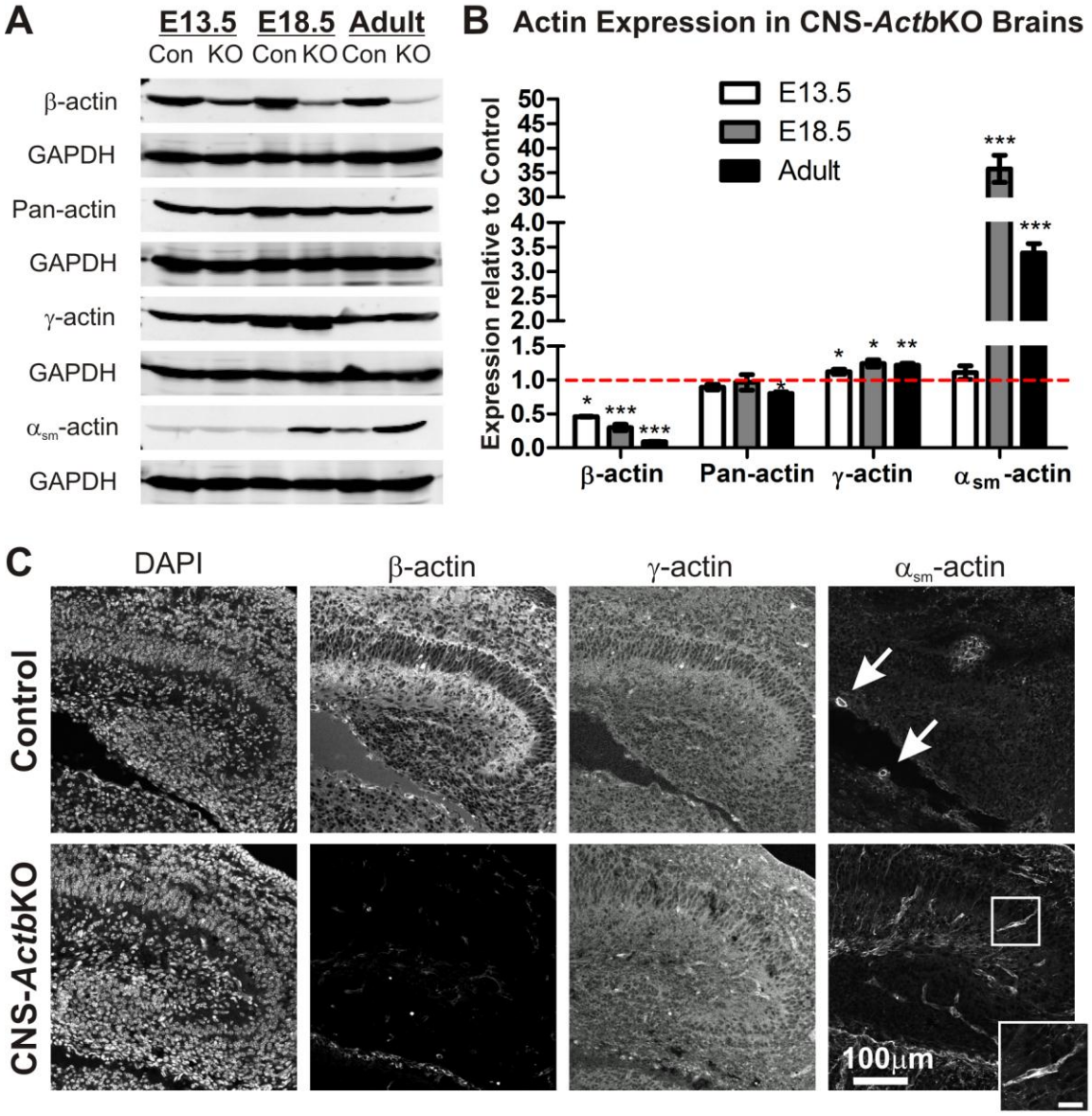
A
E13.5 E18.5 Adult
Con KO Con KO Con KO
β-actin
GAPDH
Pan-actin
GAPDH
γ-actin
GAPDH
αsm-actin
GAPDH
B
Actin Expression in CNS-ActbKO Brains
E13.5
E18.5
Adult
Expression relative to Control
β-actin
Pan-actin
γ-actin
αsm-actin
C
DAPI
β-actin
γ-actin
αsm-actin
Control
CNS-ActbKO
100μm

Figure 3.1: Conditional ablation of β-actin in the mouse central nervous system. (A-B) Western blot analysis of whole brain lysates revealed β-actin protein levels are decreased 53.8% at E13.5 and 70% at E18.5 in CNS-*Actb*KO embryos. Adult animals (6-9 months) have only 9.08% of the β-actin protein found in controls. A pan-actin isoform antibody indicated that total actin levels were conserved throughout development but decreased 19.8% in CNS-*Actb*KO adult mice. γ-actin was upregulated approximately 10-20% in embryos and adults while α_{sm}-actin was upregulated 35-fold in E18.5 embryos. α_{sm}-actin expression in adult CNS-*Actb*KO brains was increased 3.4-fold. Data plotted as mean ± standard error of the mean with an $n \geq 3$ for each genotype per age point. **(C)** Immunofluorescence with actin isoform-specific antibodies on saggital sections of the hippocampus at E18.5. β-actin staining was dramatically reduced in CNS-*Actb*KO brain sections. γ-actin staining gave a similar localization pattern to β-actin on co-labeled control sections and was still present in CNS-*Actb*KO embryos. α_{sm}-actin was restricted to blood vessels in control brains (arrows) but was prominent in select cells in CNS-*Actb*KO brain sections (see inset, inset scale bar 25μm). Scale bar 100μm. * indicates $p<0.05$, ** indicates $p<0.01$, *** indicates $p<0.001$.

Figure 3.2

A

Age	*n*	*flox/flox*	*flox/+*	*flox/+* ; Cre	*flox/flox* ; Cre (CNS-ActbKO)
E18.5	65	26.2%	24.6%	24.6%	24.6%
P21*	433	31.2%	31.6%	29.3%	7.9%

*p<0.05, χ^2 analysis

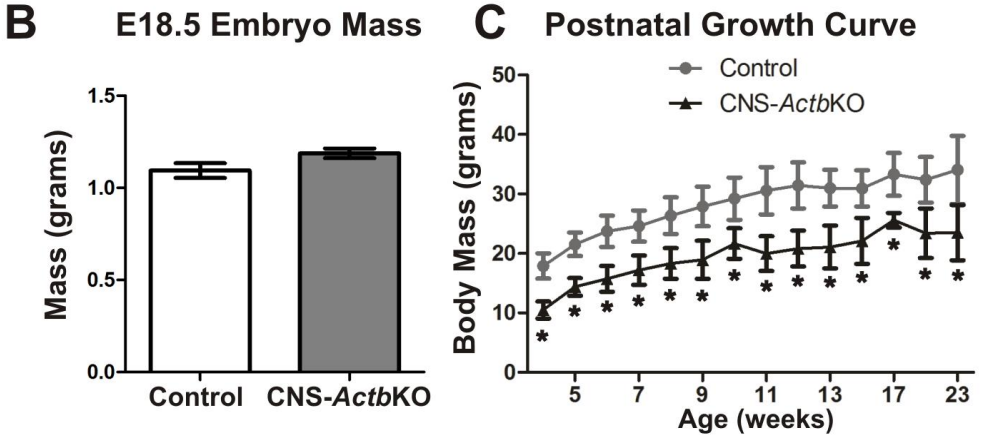

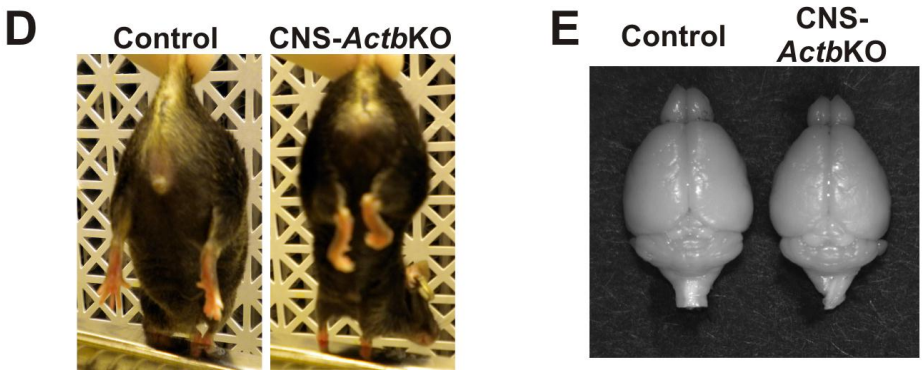

Figure 3.2: Gross characterization of CNS-*Actb*KO mice. (A) While the expected number of CNS-*Actb*KO embryos were present at E18.5, nearly 2/3's die between birth and weaning at P21. **(B)** Immediately prior to birth at E18.5, CNS-*Actb*KO embryos were indistinguishable from control littermates and have similar masses. **(C)** However, CNS-*Actb*KO mice were significantly smaller than control littermates from weaning at P21 through adulthood, although they followed a similar trend in growth. Data plotted as mean ± standard error of the mean. $n \geq 3$ male mice per genotype per age point. **(D)** Of the CNS-*Actb*KO mice that survived past weaning, hind-limb clasping/contractures were present indicating neurological dysfunction. **(E)** Brains from CNS-*Actb*KO mice appeared grossly normal and were proportionate in size to the smaller body mass of CNS-*Actb*KO mice. * indicates $p<0.05$.

Figure 3.3

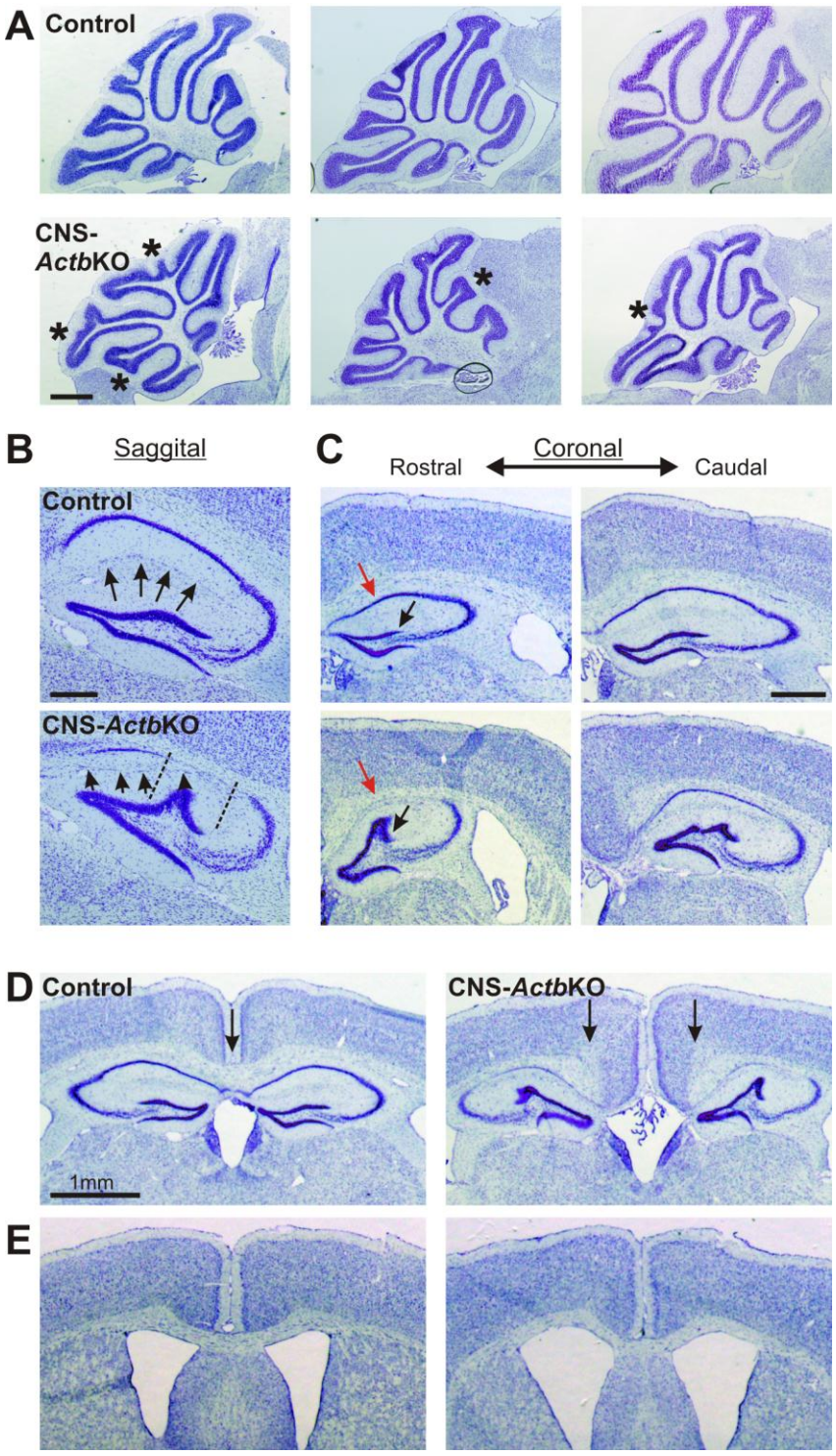
A
Control
CNS-
ActbKO
B
Saggital
Control
CNS-ActbKO
C
Rostral
Coronal
Caudal
D
Control
CNS-ActbKO
1mm
E

Figure 3.3: Histological abnormalities in CNS-*Actb*KO brains. **(A)** Midsaggital sections through the cerebellum revealed variable abnormalities in the foliation pattern of the cerebellum. Aberrantly positioned folia are marked by asterisks. Scale bar 1mm. **(B)** Morphological abnormalities in the hippocampus as seen in saggital sections. Arrows indicate the position of the hippocampal fissure normally found between the dentate gyrus and CA1 pyramidal layer. In CNS-*Actb*KO mice, the hippocampal fissure was displaced (arrows), which correlated with an abnormal invagination of the dentate gyrus. The region corresponding to this displacement is indicated by dashed lines which also reveals a dramatic decrease in cell body staining in the CA1 pyramidal cell layer. Scale bar 0.5mm. **(C)** The abnormal morphology of the hippocampus in CNS-*Actb*KO mice is further illustrated in coronal sections from rostral and caudal portions of the brain. The abnormal histology of the hippocampus was most prominent rostrally, where the dentate gyrus is displaced (black arrow). Directly above the dentate gyrus, dramatic decreases in cell body staining in the CA1 region were apparent (red arrows). The defects were less prominent caudally. Scale bar 0.5mm. **(D)** CNS-*Actb*KO mice also presented with partial agenesis of the corpus callosum. Whereas the corpus callosum completely crossed the midline in control mice (arrow, left panel), it failed to cross the midline in CNS-*Actb*KO mice, instead stopping just short (arrows, right panel). **(E)** More rostrally however, the corpus callosum crossed the midline and appeared similar to controls. Scale bars in D-E, 1mm.

Figure 3.4

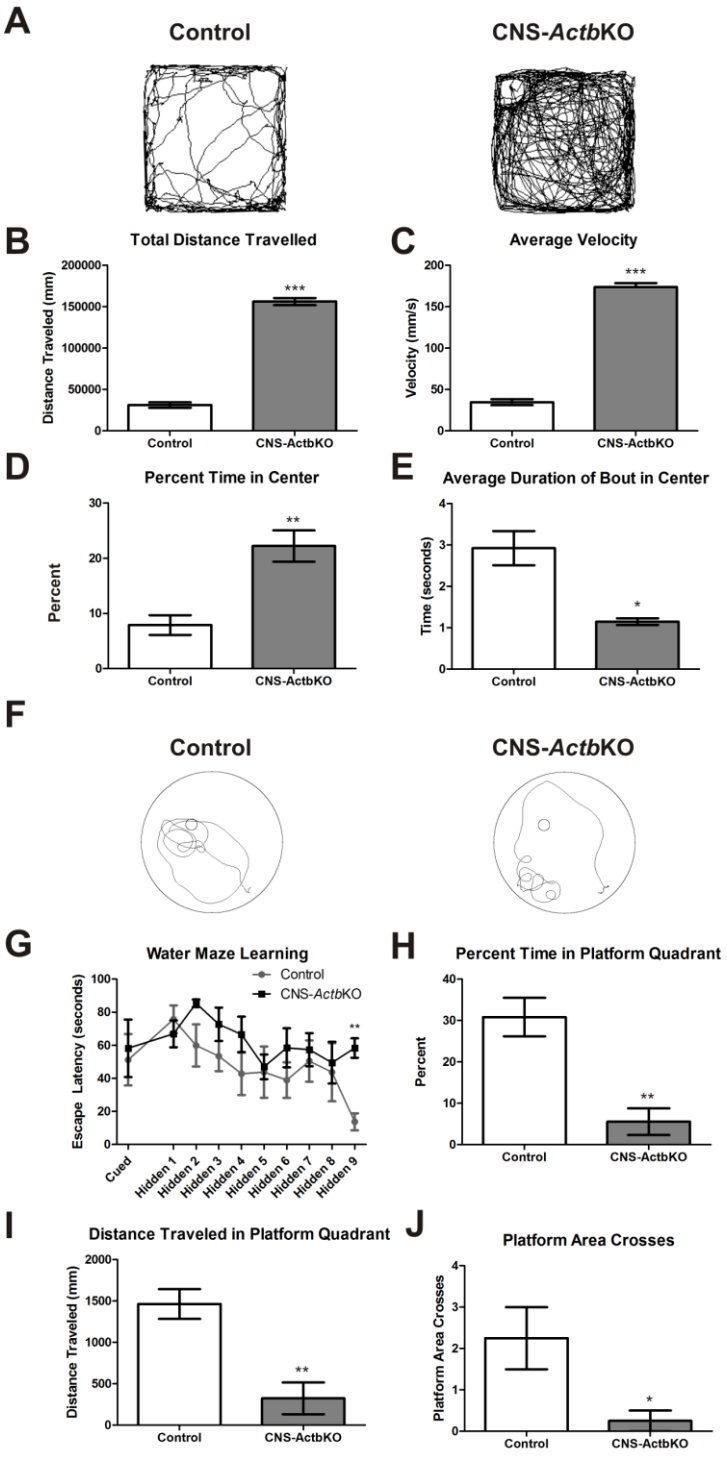
A
Control
CNS-ActbKO
B
Total Distance Travelled
Distance Traveled (mm)
200000
150000
100000
50000
0
***
Control
CNS-ActbKO
C
Average Velocity
Velocity (mm/s)
200
150
100
50
0
***
Control
CNS-ActbKO
D
Percent Time in Center
Percent
30
20
10
0
**
Control
CNS-ActbKO
E
Average Duration of Bout in Center
Time (seconds)
4
3
2
1
0
*
Control
CNS-ActbKO
F
Control
CNS-ActbKO
G
Water Maze Learning
Control
CNS-ActbKO
Escape Latency (seconds)
100
80
60
40
20
0
**
Cued
Hidden 1
Hidden 2
Hidden 3
Hidden 4
Hidden 5
Hidden 6
Hidden 7
Hidden 8
Hidden 9
H
Percent Time in Platform Quadrant
Percent
40
30
20
10
0
**
Control
CNS-ActbKO
I
Distance Traveled in Platform Quadrant
Distance Traveled (mm)
2000
1500
1000
500
0
**
Control
CNS-ActbKO
J
Platform Area Crosses
Platform Area Crosses
4
3
2
1
0
*
Control
CNS-ActbKO

Figure 3.4 CNS-*Actb*KO mice exhibit hyperactivity and decreased performance in the Morris Water Maze. (A) Traces from Control and CNS-*Actb*KO mice from the first 5 minutes of a 15 minute trial in an Open Field Activity Assay. **(B-C)** CNS-*Actb*KO mice traveled significantly greater distances and at significantly greater velocities than control mice. **(D-E)** Although CNS-*Actb*KO mice spent a significantly greater percentage of time in the center of the open field, the average duration of each bout in the center is significantly shorter. **(F)** 30 second traces from control and CNS-*Actb*KO mice during the probe trial of a Morris water maze test. **(G)** CNS-*Actb*KO mice performed similarly to control mice with a cued platform, and followed a similar learning curve until the final day of the hidden platform learning phase, at which time controls found the platform significantly faster. **(H-I)** In the probe trial, CNS-*Actb*KO mice spent a significantly smaller percentage of time in the platform quadrant and traveled significantly less distance in that quadrant. **(J)** CNS-*Actb*KO mice also crossed an area 50% larger than that of the actual platform significantly less time in 30 seconds than control mice. n=4 male mice for each genotype. * indicates $p<0.05$, ** $p<0.01$, *** $p<0.001$.

Figure 3.5

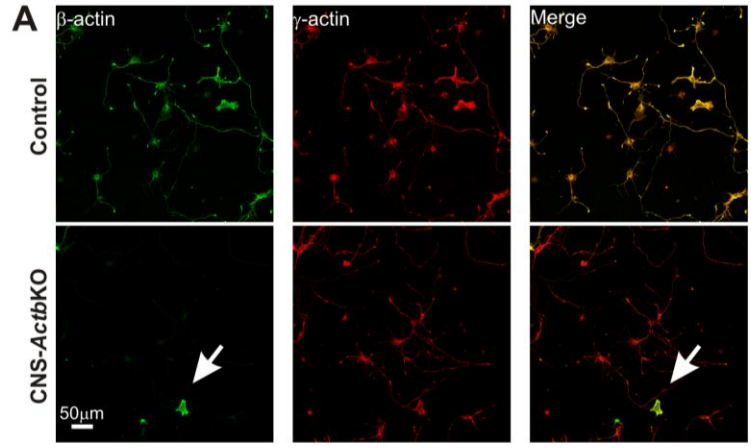

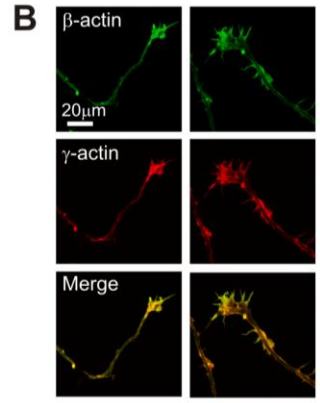

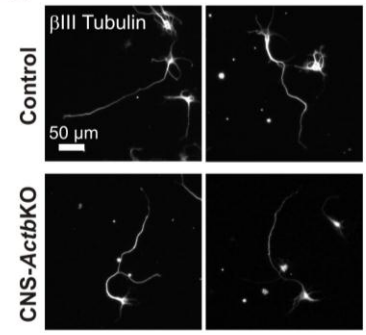

D

	Actb +/+	*Actb* -/-	*p* value
Length of axon (μm)	270.9 ± 7.235	262.6 ± 8.052	0.4404
# of axonal branches	1.468 ± 0.1548	1.315 ± 0.1231	0.4348
Length of axonal branches (μm)	51.68 ± 3.382	55.54 ± 3.198	0.4067
# of dendrites	4.698 ± 0.1296	4.593 ± 0.1266	0.5646
Length of dendrities (μm)	35.35 ± 0.8154	31.23 ± 0.7789	** 0.0003
# of dendritic branches	0.3730 ± 0.0583	0.2333 ± 0.0458	0.0571
Length of dendritic branches (μm)	19.06 ± 1.682	21.68 ± 2.165	0.331

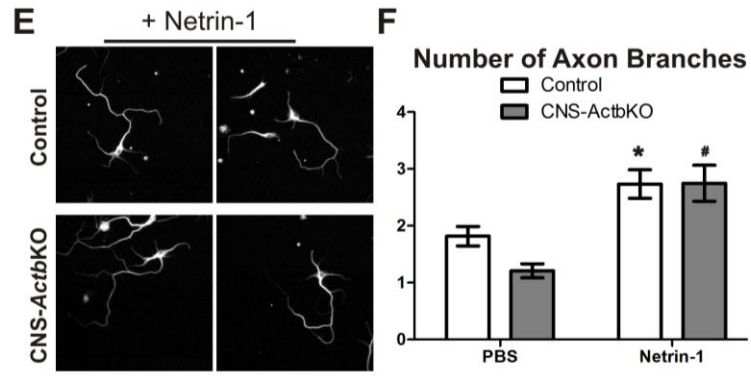

Figure 3.5: Characterization of primary hippocampal neurons from CNS-*Actb*KO mice and response to guidance cues. **(A)** Hippocampal neurons derived from E15.5 control and CNS-*Actb*KO embryos and cultured for 3 days *in vitro*. Neurons were stained with antibodies specific for β- and γ-actin. β-actin was efficiently ablated in hippocampal neurons from CNS-*Actb*KO embryos. Arrow in the bottom left panel indicates a non-neuronal cell expressing β-actin as a positive control. **(B)** β- and γ-actin co-localized in growth cones under the specified conditions (see materials and methods). **(C)** Representative images of control and CNS-*Actb*KO neurons stained with βIII-tubulin for morphological characterization. **(D)** Quantification of neuronal morphology parameters. CNS-*Actb*KO neurons had a significant decrease in the length of primary dendrites but are otherwise similar to control neurons in all measured parameters. **indicates $p<0.001$ **(E)** Representative images of control and CNS-*Actb*KO neurons treated with a bath application of 250ng/ml Netrin-1 for three days and stained with βIII-tubulin. **(F)** CNS-*Actb*KO neurons responded with a comparable increase in axonal branching as controls in response to bath application of netrin-1. * indicates significantly different than control neurons treated with PBS. # indicates significant difference compared to CNS-*Actb*KO neurons treated with PBS. Scale bars in **(A)** and **(C)** 50 μm, 20 μm in **(B)**.

Figure 3S.1

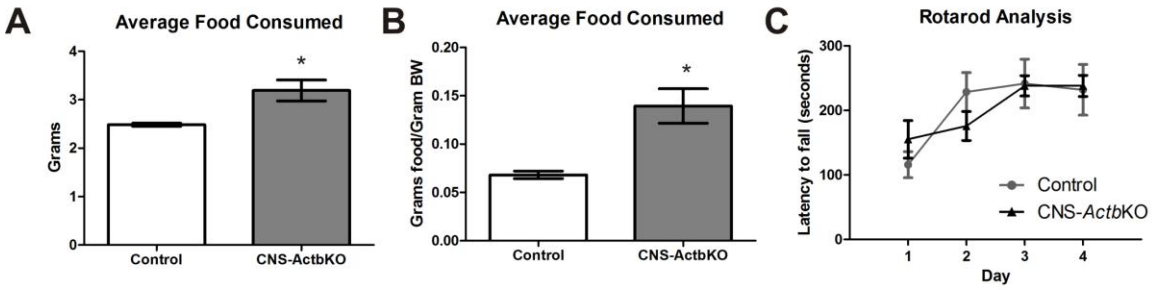

D

Female Genotype	Total Number of Litters	Number of Litters Where All Pups Died	% of Litters Where All Pups Died	*n* (number of mothers analyzed)
flox/flox	26	4	15.38	13
flox/+ ; Cre	21	6	28.57	8
flox/flox ; Cre (CNS-*Actb* KO)	11	11	100.00	3

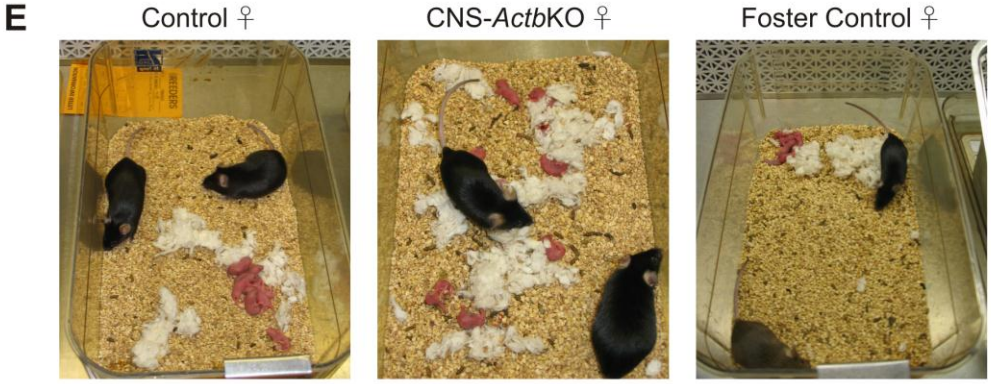

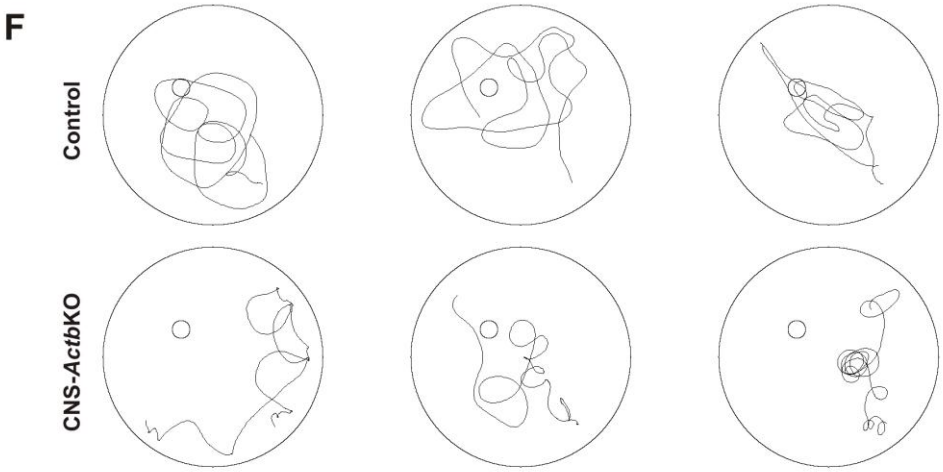

Figure 3S.1: Additional behavioral characterization of CNS-*Actb*KO mice. (A) CNS-*Actb*KO mice consumed significantly more food in a three day period than controls. **(B)** This difference was even more pronounced when normalized to bodyweight to control for the smaller mass of CNS-*Actb*KO mice. *n*=4 mice for each genotype. **(C)** CNS-*Actb*KO mice performed comparably to controls in a four day Rotarod assay experiment. Control and CNS-ActbKO animals were age matched and between 4 and 6 months old. Data plotted as mean ± standard error of the mean. *indicates $p<0.05$. **(D)** Pups born to CNS-*Actb*KO females did not survive longer than one day. (E) CNS-*Actb*KO mothers exhibited a pup retrieval deficit. While control mothers retrieved pups into a nest, pups born to CNS-*Actb*KO females were scattered throughout the cage. The pup retrieval deficit was independent of the pups however, as pups born to CNS-*Actb*KO females were retrieved normally by foster control females. **(F)** Additional traces from 30 second water maze probe trial.

Figure 3S.2

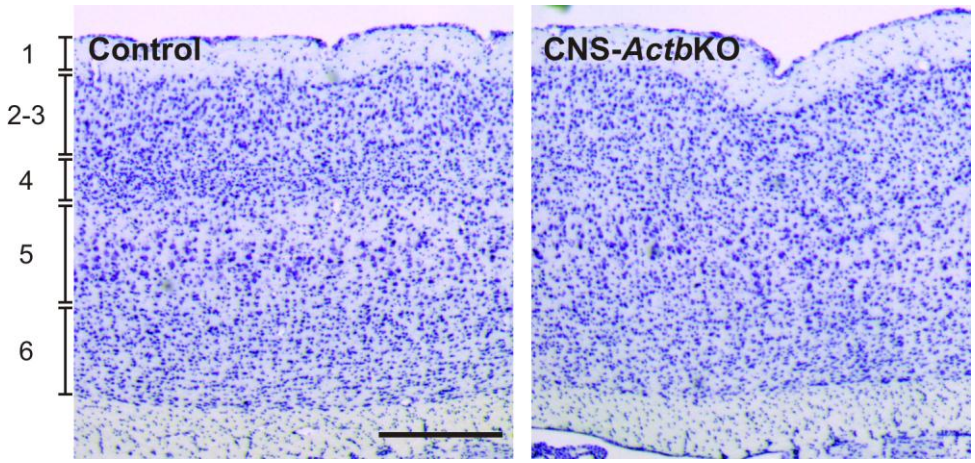

Figure 3S.2: Cortical layer histology in control and CNS-*Actb*KO mice. Saggital sections stained with Cresyl violet reveal cortical layer organization was preserved in 6 month old control and CNS-*Actb*KO mice. Scale bar 0.5mm.

DISCUSSION

Here we report the role of β-actin in the mammalian brain and identify distinct contributions of β-actin in normal brain structure and function. Although β-actin is believed to comprise one-half to two-thirds of the cytoplasmic actin in the mammalian brain (Choo and Bray, 1978; Otey et al., 1987), we showed that total actin levels are maintained during development in CNS-*Actb*KO embryos due to an upregulation of γ- and α_{sm}-actin. However, CNS-*Actb*KO mice presented with significant perinatal lethality, with only 32% surviving to adulthood. Characterization of brain histology in CNS-*Actb*KO mice revealed dramatic perturbations in the structure of the cerebellum and hippocampus that correlated with behavioral abnormalities. Finally, although CNS-*Actb*KO mice exhibited partial agenesis of the corpus callosum, cultured neurons from CNS-*Actb*KO mice had largely normal morphology and responded appropriately to guidance cues, suggesting neuronal extrinsic factors are perturbed and represent the primary cause of the corpus callosum agenesis.

The most prominent phenotype we identified in CNS-*Actb*KO mice was the disrupted architecture of the hippocampus and cerebellum. Interestingly, gross neuronal lamination in the hippocampus, cerebellum, and cortex (Figure 3.3 and Figure 3S.2) was normal, indicating neuronal migration along radial tracts is not likely β-actin dependent. Instead, the morphological abnormalities observed appear to stem primarily from defects in tissue architecture, suggesting impaired regulation of localized cell-cell or cell-extracellular matrix interactions. Alternatively, the outgrowth of cerebellar folia (Sudarov and Joyner, 2007) and folding of the developing hippocampus (Smart, 1982; Eckenhoff

and Rakic, 1984) are reminiscent of the complex tissue remodeling that occurs during neural tube closure in embryonic development. Hinge points at developing tissue folds form when select cells undergo apical constriction mediated by localized actin-myosin contraction (Copp et al., 2003; Martin, 2010). A longstanding question in the field has been how actin and myosin are localized to the apical domain of hing epoint cells (Lecuit and Lenne, 2007; Martin, 2010). One intriguing hypothesis is that perhaps the local translation of β-actin may facilitate the localized accumulation of actin. Interestingly, Dugina and colleagues (2009) previously reported β-actin was strongly enriched at the cleavage furrow in dividing cells in culture while γ-actin was localized ubiquitously along the cortical cytoskeleton, providing precedent for such a role for β-actin in a similar cellular process. The fact that CNS-*Actb*KO embryos do not present with neural tube closure defects is most likely because formation of hinge points during neurulation occurs between E8.5 and E11, while Nestin-Cre expression commences at approximately E10.5 (Graus-Porta et al., 2001; Copp et al., 2003; Schwander et al., 2004). Pre-existing β-actin mRNA and protein present before Cre expression are thus likely sufficient to facilitate proper neural tube development.

The actin filaments involved in mediating tissue morphogenic movements must be dynamic to facilitate cellular shape changes, but at other times more stable to endure mechanical strain encountered during these movements (Maruthamuthu et al., 2010). Although actin binding proteins are hypothesized to play the primary role in regulating the dynamics and stability of actin filaments, the composition of actin itself within filaments may also contribute. A recent study by Bergeron et al. (2010) characterized the

biochemical properties of individual actin isoforms and found that β-actin exhibits more rapid polymerization, phosphate release, and depolymerization than γ-actin, suggesting β-actin may be the more dynamic cytoplasmic actin isoform. Thus, it is plausible that cells may also spatiotemporally regulate the properties of actin filaments by controlling their relative composition of β- and γ-actin, with filaments more rich in β-actin being relatively more dynamic. It also warrants mention however that α-actin filaments are reported to be more stable than β- or γ-actin filaments (Allen et al., 1996; Nyman et al., 2002). Given the significant upregulation of α_{sm}-actin in CNS-*Actb*KO brains (Figure 3.1C), the incorporation of the more stable α_{sm}-actin into otherwise more dynamic filaments could also perturb tissue morphogenesis and lead to the abnormal brain architecture seen in CNS-*Actb*KO mice.

Intriguingly, the altered morphology of specifically the hippocampus may also inform on the mechanism of the partial corpus callosum agenesis in CNS-*Actb*KO mice. Corpus callosum agenesis is a relatively complex phenomenon with significant contributions derived from neuronal axon guidance as well as glial support populations such as the glial wedge and indusium griseum (Shu and Richards, 2001; Richards et al., 2004). The apparently normal crossing of the corpus callosum in rostral regions but failure to cross in areas overlying the hippocampus suggests that the perturbed hippocampal architecture may be influencing the corpus callosum phenotype. Pioneer callosal axons begin crossing the midline in most regions of the brain at E15.5 (Rash and Richards, 2001). Importantly, brains from CNS-*Actb*KO embryos at E13.5 already showed a 53.8% reduction in β-actin (Figure 3.1A-B), indicating that intracellular stores

of pre-existing β-actin mRNA and protein have been exhausted leading to the turnover of β-actin protein. Thus, the pioneer callosal axons in the rostral portion of the CNS-*Actb*KO brain appear to be able to respond to guidance cues and cross the midline independent of the local translation of β-actin (Figure 3.3E).

Axonal growth cones in more caudal regions of the corpus callosum are believed to utilize different sets of guidance mechanisms than more rostrally located growth cones however. Growth cones from callosal axons overlying the hippocampus are hypothesized to follow the pre-existing hippocampal commissures to facilitate midline crossing, which form one day earlier at E14 (Livy and Wahlsten, 1997; Richards et al., 2004). The dorsal hippocampal commissure, which lies immediately ventral to the corpus callosum in the region depicted in Figure 3.3D, also does not cross the midline in CNS-*Actb*KO brains, and thus the later arriving callosal axons may fail to cross because their normal growth substrate is not present. The finding that hippocampal neurons respond normally to netrin-1 (Figure 3.5E-F), a major attractive guidance cue in hippocampal commissure formation (Serafini et al., 1996; Barallobre et al., 2000; Steup et al., 2000), provides further evidence that axonal responses to guidance cues may not strictly require local β-actin translation, and that β-actin may have important neuronal extrinsic roles perhaps in the proper formation of the surrounding glial populations.

The data presented here along with our previous report characterizing the role of β-actin in motor neuron function and axonal regeneration (Cheever et al., 2011) further suggests that distinct roles for β-actin may be unexpectedly confined to select CNS

populations. By using a CNS-wide conditional knock-out approach as described here with a Nestin-Cre line, we were able to identify cell populations where β-actin appears to be particularly important. Although CNS-*Actb*KO mice exhibit significant perinatal lethality hindering studies in adult mice, future studies could take advantage of more selective Cre lines to help further define the molecular mechanisms of the phenotypes described here and the role of β-actin and other actin isoforms in cytoskeletal regulation *in vivo*.

Chapter 4

Conclusions and Future Directions

The actin cytoskeleton has critical functions in a wide variety of basic cell biological processes. In addition, actin is also one of the key mediators underlying the physiological functions of specialized tissues such as skeletal muscle, auditory hair cells, and the central nervous system (CNS). Intriguingly, the composition of the actin cytoskeleton in all three of these cell types and tissues differs dramatically from a vast predominance of $\alpha_{skeleltal}$-actin in skeletal muscle, to an excess of cytoplasmic γ-actin in auditory hair cells, to a prevalence or balance of β- to γ-actin in the nervous system (Choo and Bray, 1978; Flanagan and Lin, 1979; Otey et al., 1987; Hofer et al., 1997; Hanft et al., 2006). While *in vitro* and recent *in vivo* studies have now begun to elucidate the functional significance of actin isoform composition in skeletal muscle and auditory hair cells (Sonnemann et al., 2006; Perrin et al., 2010; Prins et al., 2011), the role of actin isoforms in the mammalian CNS is virtually unexplored. The goal of this thesis work was to characterize the role of the cytoplasmic actins, and specifically β-actin, in the mammalian CNS. The findings described in the previous chapters indicate that β-actin indeed plays an essential role in CNS development and function, but in a strikingly more restricted manner than anticipated that likely has implications for how actin isoforms are viewed in the CNS.

The second chapter of this thesis explores the role of β-actin in motor neuron function and development. Previously, β-actin mRNA and protein were found to be decreased in the growth cones of motor neurons cultured from a mouse model of spinal muscular atrophy (SMA) (Rossoll et al., 2003). The protein deficient in SMA, survival motor neuron 1 (SMN), is known to associate with proteins that bind the zipcode

sequence of β-actin mRNA and has been shown to rapidly translocate from the cell body of motor neurons to growth cones (Rossoll et al., 2002; Rossoll et al., 2003; Zhang et al., 2003; Tadesse et al., 2008). Knock-down of SMN in zebrafish or various cell culture models revealed putative roles for SMN in motor axon elongation and guidance (Jablonka et al., 2004; Briese et al., 2005; Dahm and Macchi, 2007). Collectively, these studies supported the hypothesis that mislocalization or decreased levels of β-actin in motor neuron axons leads to defective outgrowth or guidance, ultimately resulting in SMA. We tested this hypothesis by determining whether β-actin loss-of-function in motor neurons leads to motor neuron disease in an *in vivo* context. Surprisingly, motor neuron specific β-actin knock-out mice (*Actb*-MNsKO) exhibited no evidence of motor axon guidance or neuromuscular junction defects, consistent with the normal muscle function and histology observed. Because the conditional nature of the knock-out precluded analysis of early motor axon outgrowth, we used a motor axon regeneration model that shares similarities with embryonic axonal development to assess whether β-actin may contribute to motor axon outgrowth and synaptic formation. Intriguingly, *Actb*-MNsKO mice regenerated functional motor axons and neuromuscular junctions in a manner indistinguishable from controls. Thus, although a prominent and appealing model based on previous studies, loss-of-function of β-actin in motor neurons and motor axon growth cones likely does not contribute to SMA pathogenesis.

Motor neurons comprise only one small population in an incredibly diverse and complex mammalian nervous system. In order to investigate the role of β-actin in other cell types of the CNS, we analyzed brain structure and function in CNS-specific β-actin

knock-out mice (CNS-*Actb*KO). The results of this study are reported in Chapter 3 and revealed that β-actin has critical but surprisingly restricted roles in the morphogenesis of the hippocampus, cerebellum and corpus callosum, which correlated with a number of behavioral abnormalities. Despite a large body of literature indicating essential roles for β-actin in axon guidance, we found that β-actin null neurons in culture responded normally to attractive guidance cues, and that the partial corpus callosum agenesis was likely due to neuronal extrinsic factors.

The apparent dispensability of β-actin in significant portions of the CNS and axonal responses to guidance cues is in contrast to a body of *in vitro* work reporting critical roles for the local translation of β-actin in directed cell motility and axon guidance (Condeelis and Singer, 2005; Leung et al., 2006; Yao et al., 2006). In these studies, knock-down of ZBP1 or treatment with anti-sense oligonucleotides to the zipcode sequence were used to determine the functional significance of β-actin localization. However, while β-actin is by far the most commonly studied substrate of ZBP1, it is not the only substrate (Nielsen et al., 2001; Yisraeli, 2005). IGF-II (Nielsen et al., 1999), H19 (Runge et al., 2000), c-myc (Doyle et al., 1998), βTrCP1 (Noubissi et al., 2006), tau (Atlas et al., 2004), and semaphorin3F (Rackham and Brown, 2004) have all been identified as mRNA binding partners of ZBP1 and its various homologs, with the latter two of significant importance to neuronal development and function. Additionally, molecular analysis of IMP1 (the mammalian ortholog of ZBP1) ribonucleoprotein graunles in cultured cells identified approximately 3% of the transcriptome as mRNA components. This included a number of mRNAs coding for proteins crucial for actin and

neuronal cytoskeletal regulation including cofilin 1, neuritin 1, profilin 1, paxilin, rhoA, and zyxin, among others (Jonson et al., 2007). Thus, it is possible that during the manipulation of ZBP1 levels or binding to β-actin mRNA that the localization of additional functionally relevant mRNAs may also be perturbed and contribute to the phenotypes observed.

The hypothesis described above could potentially explain β-actin independent phenotypes observed due to ZBP1 knock-down, but it is more difficult to reconcile with experiments where anti-sense oligonucleotides specific to the β-actin zipcode sequence were used. Interfering with β-actin mRNA binding to ZBP1 may disrupt the binding of other mRNA cargos however which may be more functionally relevant than β-actin. Alternatively, the β–actin zipcode anti-sense oligonucleotides could have off target effects inhibiting binding of the large number of other ZBP1 mRNA substrates. It also warrants mention that IMP1 knock-down in HeLa cells has no effect on β-actin protein or mRNA expression or distribution, and an IMP1 knock-out mouse was characterized with no CNS abnormalities reported (Hansen et al., 2004; Vikesaa et al., 2006). Instead, *Imp1*$^{-/-}$ mice presented with impaired intestinal development and dwarfism that likely contributed to partial perinatal lethality. Thus, while the zipcode and ZBP1-mediated localization of β-actin is one of the most commonly cited examples of the functional importance of mRNA localization and local translation, this mechanism may not be conserved across different cell types or species *in vivo*, and caution is warranted when extrapolating findings.

Similarly, the SMN-mediated localization of β-actin in motor neurons is one prominent hypothesis in the SMA field to explain why decreased levels of a ubiquitous, essential protein leads to disease predominantly confined to motor neurons. One cannot ignore however that while a small number of reports have identified SMN transport in axons and growth cones, the most well characterized and supported role for SMN is in snRNP biogenesis (Burghes and Beattie, 2009). mRNA splicing is dependent on an array of snRNPs to facilitate intron removal, and thus it is difficult to comprehend how disruption of such a widespread process as mRNA splicing could lead to pathology in only a small subset of cells. Yet recent studies have now shown that assembly of specific snRNPs is indeed impaired in SMA mice, with the extent of snRNP disruption positively correlating with phenotypic severity (Gabanella et al., 2007). Additional work has confirmed and expanded on these reports indicating that SMN deficiency causes tissue-specific defects in splicing, and that restoration of snRNP assembly significantly rescues SMA mice (Zhang et al., 2008; Workman et al., 2009). In conjunction with the work described in Chapter 2 and multiple studies showing normal motor axon growth and guidance in SMA mice, current data suggests disrupted splicing of mRNAs critical for motor neuron function or survival is the most likely primary pathogenic mechanism in SMA.

While β-actin functions in motor neurons and motor axon regeneration appear to be nonessential (Chapter 2), the prominent but restricted phenotypes in CNS-*Actb*KO mice (Chapter 3) indicate that β-actin does indeed have some essential functions in discrete CNS cell populations. The next most pressing question is whether these

phenotypes are due to unique post-transcriptional regulation of β-actin, most likely involving the localization of β-actin mRNA, or unique functions of β-actin protein itself, potentially involving differences in polymerization kinetics. To address this question, a number of transgenic mice will need to be generated due to the lack of any major phenotype in cultured neurons. The simplest experiment would be to determine whether a transgenic mouse expressing β-actin with the zipcode sequence could rescue CNS-*Actb*KO mice. If it could, an additional transgenic line expressing γ-actin with the β-actin zipcode sequence could be generated and crossed to CNS-*Actb*KO mice. If this line could also rescue, there would be strong evidence that the zipcode sequence is critical for β-actin function while the primary amino acid sequence is not. One caveat to these experiments is that transgene expression would not be driven by endogenous regulatory elements at the *Actb* locus. A significantly more challenging but better controlled experiment would be to knock γ-actin coding sequences into the *Actb* locus. Although labor intensive and costly, the mouse models described above would allow for the definitive determination of whether the essential functions of β-actin are mediated by unique regulatory elements, primary amino acid sequence, or some combination of the two.

There is also the possibility that the significant upregulation of α_{smooth}-actin may confound interpretation of the experiments described above. In order to determine if the upregulation of α_{smooth}-actin is detrimental, compensatory, or has no effect on the CNS-*Actb*KO mice, a β-actin-α_{smooth}-actin double knock-out mouse could be generated. If the α_{smooth}-actin upregulation in CNS-*Actb*KO mice is contributing to the phenotypes

observed or has no effect, then CNS-*Actb*KO mice should be at least partially rescued or show no effect. If α_{smooth}-actin upregulation is partially compensatory in CNS-*Actb*KO mice, then the resulting double knock-out mice should have a more severe phenotype. Because α_{smooth}-actin knock-out mice have only a limited phenotype (Schildmeyer et al., 2000), the chances for a compound phenotype are minimized. Similarly, β-actin-γ-actin double knock-out mice could also be generated to determine the effect of γ-actin upregulation in CNS-*Actb*KO mice. However, there is some precedent that at least one cytoplasmic actin is required for non-muscle actin based structures *in vivo* (Perrin et al., 2010).

The extent of histological and behavioral rescue by the various transgenic mouse lines described above would likely shed a great deal of light on the mechanisms behind the phenotypes observed in CNS-*Actb*KO mice. However, further studies would need to be conducted to determine the temporal contribution of β-actin to the various histological and behavioral phenotypes observed. For example, establishing more precisely when the hippocampus and cerebellar morphological defects manifest would likely be beneficial for more precisely defining the contribution of β-actin to these processes. Unfortunately, these two brain structures develop to a significant extent postnatally, meaning the use of CNS-*Actb*KO mice would be prohibitive due to their high perinatal lethality. However, there are a number of more specific Cre-lines that could be used to target the hippocampus (CaMKII-Cre; Dragatsis and Zeitlin, 2000) or cerebellar populations (Pcp2-Cre; Purkinje Cells (Zhang et al., 2004), GluRε3-Cre, Granule Cells (Tsujita et al., 1999)) with expression patterns that may be restricted enough to circumvent the perinatal

lethality observed with Nestin-Cre mediated β-actin knock-out. In addition, comparison of CNS-wide knock-out mice with neuron specific knock-out lines (*Nex*-Cre) could inform on the relative contribution of neuronal versus glial populations to the phenotypes observed in CNS-*Actb*KO mice (Goebbels et al., 2006; Satz et al., 2010).

The relationship between the histological and behavioral phenotypes in CNS-*Actb*KO mice is also at present not known. Although the significant morphological abnormalities in the hippocampus for example could disrupt hippocampal circuits *en masse*, it is also possible that the behavioral phenotypes observed could be due to individual synaptic deficits rather than disruption of whole pathways. Given the prominent role of actin in remodeling dendritic spines and synaptic plasticity, there is significant precedent for the latter mechanism (Okamoto et al., 2004; Dillon and Goda, 2005; Cingolani and Goda, 2008; Hotulainen and Hoogenraad, 2010). One way to assess the relative contribution of tissue morphological defects or individual synaptic dysfunction to the observed behavioral phenotypes would be to cross floxed *Actb* mice with an inducible Cre line such as the CaMKII-Cre^{ER} transgenic line (Erdmann et al., 2007). Cre recombinase activity could be induced by tamoxifen treatment in adult animals followed by behavioral and histological analysis. If similar behavioral phenotypes but no histological abnormalities were present in inducible β-actin knock-out lines, than impaired synaptic function or plasticity at individual synapses would be a likely mediator of the behavioral phenotypes observed. This hypothesis could be further tested using electrophysiology experiments while dendritic spine morphology could be examined in Golgi-stained brain sections or in cultured neurons.

One confounding factor to the experiments described above is that although most major morphogenic processes involved in brain formation are completed in the early postnatal period, there is still continued neurogenesis, neural migration, and neurite guidance that occur throughout adult life although to a significantly limited extent (Ming and Song, 2005). Nonetheless, recent studies are now beginning to establish critical roles for adult neurogenesis in normal learning and potentially other behaviors (Moreno et al., 2009; Deng et al., 2010). The two sites of neurogenesis in the adult mammalian brain are in the subventricular zone and the dentate gyrus of the hippocampus (Lledo et al., 2006), with the latter one of the few regions morphologically perturbed in CNS-*Actb*KO mice. Neurons derived from the subventricular zone migrate significant distances to the olfactory bulb along a path known as the rostral migratory stream (Alvarez-Buylla and Garcia-Verdugo, 2002). Although the functional significance of these newly generated neurons is controversial, some studies suggest that it is important in odor discrimination (Gheusi et al., 2000; Enwere et al., 2004). Interestingly, increased neurogenesis in the subventricular zone has been observed during late pregnancy in mice, and may be important for proper recognition and retrieval of pups (Shingo et al., 2003).

Adult neurogenesis in the dentate gyrus of the hippocampus can be enhanced following exercise (van Praag et al., 1999; Brown et al., 2003) and has been shown to positively correlate with hippocampal dependent learning paradigms (Shors et al., 2001; Clelland et al., 2009; Deng et al., 2010). Intriguingly, the profound hyperactivity of CNS-*Actb*KO mice coupled with their poor performance in a hippocampal learning dependent assay may corroborate these findings. Injections of BrdU could be used to label newly

generated neurons in the subventricular zone and dentate gyrus followed by quantification and histological analysis to determine if the location and number of newly born neurons in CNS-*Actb*KO mice are comparable to controls. A specific role for β-actin in adult neurogenesis could be more definitively demonstrated by inducing Cre activity in adult Nestin-Cre^{ER} mice (Chen et al., 2009) crossed to the floxed *Actb* line, where Cre activity would be restricted to adult neural progenitors.

Summary

Prior to the work described in this thesis, a number of studies in various cell culture models had reported important or essential roles for β-actin in cell division, directed cell migration, axon guidance, and synaptic formation, suggesting that β-actin is a key mediator of neuronal development and function. However, whether these functions are conserved in higher vertebrates or in *in vivo* was unknown. The work described here has taken the next fundamental step in expanding our understanding of actin isoform functions by assessing their role in the mammalian CNS. Although it is often difficult to obtain mechanistic detail with *in vivo* studies, allowing cells of interest to be maintained in their endogenous environment presents a valuable method to parse through conflicting results from *in vitro* studies. *In vivo* experiments are also the only way to determine whether phenomena observed *in vitro* or in cell culture are biologically relevant. While the proposed experiments above outline a large body of further work that needs to be done, the work described here has established a model to help translate exciting *in vitro* and in cell culture findings to an intact, mammalian system. Given the fundamental role

of actin in CNS function, it is my hope that this work could someday help the millions affected by neurological disorders with limited or no current therapeutic options.

References

Alberti, S., S.M. Krause, O. Kretz, U. Philippar, T. Lemberger, E. Casanova, F.F. Wiebel, H. Schwarz, M. Frotscher, G. Schutz, and A. Nordheim. 2005. Neuronal migration in the murine rostral migratory stream requires serum response factor. *Proc.Natl.Acad.Sci.U.S.A.* 102:6148-6153. doi: 10.1073/pnas.0501191102.

Allan, D.W., and J.J. Greer. 1997. Embryogenesis of the phrenic nerve and diaphragm in the fetal rat. *J.Comp.Neurol.* 382:459-468.

Allen, P.G., C.B. Shuster, J. Kas, C. Chaponnier, P.A. Janmey, and I.M. Herman. 1996. Phalloidin binding and rheological differences among actin isoforms. *Biochemistry.* 35:14062-14069. doi: 10.1021/bi961326g.

Alvarez-Buylla, A., and J.M. Garcia-Verdugo. 2002. Neurogenesis in adult subventricular zone. *J.Neurosci.* 22:629-634.

Atlas, R., L. Behar, E. Elliott, and I. Ginzburg. 2004. The insulin-like growth factor mRNA binding-protein IMP-1 and the Ras-regulatory protein G3BP associate with tau mRNA and HuD protein in differentiated P19 neuronal cells. *J.Neurochem.* 89:613-626. doi: 10.1111/j.1471-4159.2004.02371.x.

Augustine, G.J., F. Santamaria, and K. Tanaka. 2003. Local calcium signaling in neurons. *Neuron.* 40:331-346.

Ayala, R., T. Shu, and L.H. Tsai. 2007. Trekking across the brain: the journey of neuronal migration. *Cell.* 128:29-43. doi: 10.1016/j.cell.2006.12.021.

Bagri, A., H.J. Cheng, A. Yaron, S.J. Pleasure, and M. Tessier-Lavigne. 2003. Stereotyped pruning of long hippocampal axon branches triggered by retraction inducers of the semaphorin family. *Cell.* 113:285-299.

Baloh, R.H., W. Rakowicz, R. Gardner, and A. Pestronk. 2007. Frequent atrophic groups with mixed-type myofibers is distinctive to motor neuron syndromes. *Muscle Nerve.* 36:107-110.

Barallobre, M.J., J.A. Del Rio, S. Alcantara, V. Borrell, F. Aguado, M. Ruiz, M.A. Carmona, M. Martin, M. Fabre, R. Yuste, M. Tessier-Lavigne, and E. Soriano. 2000. Aberrant development of hippocampal circuits and altered neural activity in netrin 1-deficient mice. *Development.* 127:4797-4810.

Bassell, G.J., H. Zhang, A.L. Byrd, A.M. Femino, R.H. Singer, K.L. Taneja, L.M. Lifshitz, I.M. Herman, and K.S. Kosik. 1998. Sorting of beta-actin mRNA and protein to neurites and growth cones in culture. *J.Neurosci.* 18:251-265.

Ben Hamida, C., N. Soussi-Yanicostas, G.S. Butler-Browne, K. Bejaoui, F. Hentati, and M. Ben Hamida. 1994. Biochemical and immunocytochemical analysis in chronic proximal spinal muscular atrophy. *Muscle Nerve.* 17:400-410.

Bergeron, S.E., M. Zhu, S.M. Thiem, K.H. Friderici, and P.A. Rubenstein. 2010. Ion-dependent polymerization differences between mammalian beta- and gamma-nonmuscle actin isoforms. *J.Biol.Chem.* 285:16087-16095. doi: 10.1074/jbc.M110.110130.

Bettinger, B.T., D.M. Gilbert, and D.C. Amberg. 2004. Actin up in the nucleus. *Nat.Rev.Mol.Cell Biol.* 5:410-415. doi: 10.1038/nrm1370.

Blanchoin, L., and T.D. Pollard. 2002. Hydrolysis of ATP by polymerized actin depends on the bound divalent cation but not profilin. *Biochemistry.* 41:597-602.

Bloom, O., E. Evergren, N. Tomilin, O. Kjaerulff, P. Low, L. Brodin, V.A. Pieribone, P. Greengard, and O. Shupliakov. 2003. Colocalization of synapsin and actin during synaptic vesicle recycling. *J.Cell Biol.* 161:737-747.

Bolis, A., S. Coviello, S. Bussini, G. Dina, C. Pardini, S.C. Previtali, M. Malaguti, P. Morana, U. Del Carro, M.L. Feltri, A. Quattrini, L. Wrabetz, and A. Bolino. 2005. Loss of Mtmr2 phosphatase in Schwann cells but not in motor neurons causes Charcot-Marie-Tooth type 4B1 neuropathy with myelin outfoldings. *J.Neurosci.* 25:8567-8577.

Bowerman, M., D. Shafey, and R. Kothary. 2007. Smn depletion alters profilin II expression and leads to upregulation of the RhoA/ROCK pathway and defects in neuronal integrity. *J.Mol.Neurosci.* 32:120-131.

Brandon, E.P., W. Lin, K.A. D'Amour, D.P. Pizzo, B. Dominguez, Y. Sugiura, S. Thode, C.P. Ko, L.J. Thal, F.H. Gage, and K.F. Lee. 2003. Aberrant patterning of neuromuscular synapses in choline acetyltransferase-deficient mice. *J.Neurosci.* 23:539-549.

Briese, M., B. Esmaeili, and D.B. Sattelle. 2005. Is spinal muscular atrophy the result of defects in motor neuron processes? *Bioessays.* 27:946-957. doi: 10.1002/bies.20283.

Brown, J., C.M. Cooper-Kuhn, G. Kempermann, H. Van Praag, J. Winkler, F.H. Gage, and H.G. Kuhn. 2003. Enriched environment and physical activity stimulate hippocampal but not olfactory bulb neurogenesis. *Eur.J.Neurosci.* 17:2042-2046.

Buck, K.B., and J.Q. Zheng. 2002. Growth cone turning induced by direct local modification of microtubule dynamics. *J.Neurosci.* 22:9358-9367.

Burgess, S., M. Walker, P.J. Knight, J. Sparrow, S. Schmitz, G. Offer, B. Bullard, K. Leonard, J. Holt, and J. Trinick. 2004. Structural studies of arthrin: monoubiquitinated actin. *J.Mol.Biol.* 341:1161-1173. doi: 10.1016/j.jmb.2004.06.077.

Burghes, A.H., and C.E. Beattie. 2009. Spinal muscular atrophy: why do low levels of survival motor neuron protein make motor neurons sick? *Nat.Rev.Neurosci.* 10:597-609.

Carlier, M.F., D. Pantaloni, and E.D. Korn. 1986. Fluorescence measurements of the binding of cations to high-affinity and low-affinity sites on ATP-G-actin. *J.Biol.Chem.* 261:10778-10784.

Chaponnier, C., and G. Gabbiani. 2004. Pathological situations characterized by altered actin isoform expression. *J.Pathol.* 204:386-395. doi: 10.1002/path.1635.

Cheever, T.R., E.A. Olson, and J.M. Ervasti. 2011. Axonal regeneration and neuronal function are preserved in motor neurons lacking ss-actin in vivo. *PLoS One.* 6:e17768. doi: 10.1371/journal.pone.0017768.

Chen, J., C.H. Kwon, L. Lin, Y. Li, and L.F. Parada. 2009. Inducible site-specific recombination in neural stem/progenitor cells. *Genesis.* 47:122-131. doi: 10.1002/dvg.20465.

Chen, J., H. Li, N. SundarRaj, and J.H. Wang. 2007. Alpha-smooth muscle actin expression enhances cell traction force. *Cell Motil.Cytoskeleton.* 64:248-257. doi: 10.1002/cm.20178.

Chipman, P.H., C.K. Franz, A. Nelson, M. Schachner, and V.F. Rafuse. 2010. Neural cell adhesion molecule is required for stability of reinnervated neuromuscular junctions. *Eur.J.Neurosci.* 31:238-249.

Choo, Q.L., and D. Bray. 1978. Two forms of neuronal actin. *J.Neurochem.* 31:217-224.

Chow, L.M., Y. Tian, T. Weber, M. Corbett, J. Zuo, and S.J. Baker. 2006. Inducible Cre recombinase activity in mouse cerebellar granule cell precursors and inner ear hair cells. *Dev.Dyn.* 235:2991-2998.

Cifuentes-Diaz, C., S. Nicole, M.E. Velasco, C. Borra-Cebrian, C. Panozzo, T. Frugier, G. Millet, N. Roblot, V. Joshi, and J. Melki. 2002. Neurofilament accumulation at the motor endplate and lack of axonal sprouting in a spinal muscular atrophy mouse model. *Hum.Mol.Genet.* 11:1439-1447.

Cingolani, L.A., and Y. Goda. 2008a. Actin in action: the interplay between the actin cytoskeleton and synaptic efficacy. *Nat.Rev.Neurosci.* 9:344-356.

Clelland, C.D., M. Choi, C. Romberg, G.D. Clemenson Jr, A. Fragniere, P. Tyers, S. Jessberger, L.M. Saksida, R.A. Barker, F.H. Gage, and T.J. Bussey. 2009. A functional role for adult hippocampal neurogenesis in spatial pattern separation. *Science.* 325:210-213. doi: 10.1126/science.1173215.

Cole, J.C., B.R. Villa, and R.S. Wilkinson. 2000. Disruption of actin impedes transmitter release in snake motor terminals. *J.Physiol.* 525 Pt 3:579-586.

Condeelis, J. 1993. Life at the leading edge: the formation of cell protrusions. *Annu.Rev.Cell Biol.* 9:411-444. doi: 10.1146/annurev.cb.09.110193.002211.

Condeelis, J., and R.H. Singer. 2005. How and why does beta-actin mRNA target? *Biol.Cell.* 97:97-110. doi: 10.1042/BC20040063.

Copp, A.J., N.D. Greene, and J.N. Murdoch. 2003. The genetic basis of mammalian neurulation. *Nat.Rev.Genet.* 4:784-793. doi: 10.1038/nrg1181.

Crawford, K., R. Flick, L. Close, D. Shelly, R. Paul, K. Bove, A. Kumar, and J. Lessard. 2002. Mice lacking skeletal muscle actin show reduced muscle strength and growth deficits and die during the neonatal period. *Mol.Cell.Biol.* 22:5887-5896.

Dahm, R., and P. Macchi. 2007. Human pathologies associated with defective RNA transport and localization in the nervous system. *Biol.Cell.* 99:649-661. doi: 10.1042/BC20070045.

Darby, I., O. Skalli, and G. Gabbiani. 1990. Alpha-smooth muscle actin is transiently expressed by myofibroblasts during experimental wound healing. *Lab.Invest.* 63:21-29.

De La Cruz, E.M. 2005. Cofilin binding to muscle and non-muscle actin filaments: isoform-dependent cooperative interactions. *J.Mol.Biol.* 346:557-564. doi: 10.1016/j.jmb.2004.11.065.

Deng, W., J.B. Aimone, and F.H. Gage. 2010. New neurons and new memories: how does adult hippocampal neurogenesis affect learning and memory? *Nat.Rev.Neurosci.* 11:339-350. doi: 10.1038/nrn2822.

Dent, E.W., A.M. Barnes, F. Tang, and K. Kalil. 2004. Netrin-1 and semaphorin 3A promote or inhibit cortical axon branching, respectively, by reorganization of the cytoskeleton. *J.Neurosci.* 24:3002-3012. doi: 10.1523/JNEUROSCI.4963-03.2004.

Dent, E.W., and F.B. Gertler. 2003. Cytoskeletal dynamics and transport in growth cone motility and axon guidance. *Neuron.* 40:209-227.

Dent, E.W., F. Tang, and K. Kalil. 2003. Axon guidance by growth cones and branches: common cytoskeletal and signaling mechanisms. *Neuroscientist.* 9:343-353.

Devineni, N., L.S. Minamide, M. Niu, D. Safer, R. Verma, J.R. Bamburg, and V.T. Nachmias. 1999. A quantitative analysis of G-actin binding proteins and the G-actin pool in developing chick brain. *Brain Res.* 823:129-140.

Dillon, C., and Y. Goda. 2005. The actin cytoskeleton: integrating form and function at the synapse. *Annu.Rev.Neurosci.* 28:25-55. doi: 10.1146/annurev.neuro.28.061604.135757.

Doyle, G.A., N.A. Betz, P.F. Leeds, A.J. Fleisig, R.D. Prokipcak, and J. Ross. 1998. The c-myc coding region determinant-binding protein: a member of a family of KH domain RNA-binding proteins. *Nucleic Acids Res.* 26:5036-5044.

Dragatsis, I., and S. Zeitlin. 2000. CaMKIIalpha-Cre transgene expression and recombination patterns in the mouse brain. *Genesis.* 26:133-135.

Dugina, V., I. Zwaenepoel, G. Gabbiani, S. Clement, and C. Chaponnier. 2009. Beta and gamma-cytoplasmic actins display distinct distribution and functional diversity. *J.Cell.Sci.* 122:2980-2988.

Eckenhoff, M.F., and P. Rakic. 1984. Radial organization of the hippocampal dentate gyrus: a Golgi, ultrastructural, and immunocytochemical analysis in the developing rhesus monkey. *J.Comp.Neurol.* 223:1-21. doi: 10.1002/cne.902230102.

Engle, E.C. 2010. Human genetic disorders of axon guidance. *Cold Spring Harb Perspect.Biol.* 2:a001784. doi: 10.1101/cshperspect.a001784.

Enwere, E., T. Shingo, C. Gregg, H. Fujikawa, S. Ohta, and S. Weiss. 2004. Aging results in reduced epidermal growth factor receptor signaling, diminished olfactory neurogenesis, and deficits in fine olfactory discrimination. *J.Neurosci.* 24:8354-8365. doi: 10.1523/JNEUROSCI.2751-04.2004.

Eom, T., L.N. Antar, R.H. Singer, and G.J. Bassell. 2003. Localization of a beta-actin messenger ribonucleoprotein complex with zipcode-binding protein modulates the density of dendritic filopodia and filopodial synapses. *J.Neurosci.* 23:10433-10444.

Erdmann, G., G. Schutz, and S. Berger. 2007. Inducible gene inactivation in neurons of the adult mouse forebrain. *BMC Neurosci.* 8:63. doi: 10.1186/1471-2202-8-63.

Fan, L., and L.R. Simard. 2002. Survival motor neuron (SMN) protein: role in neurite outgrowth and neuromuscular maturation during neuronal differentiation and development. *Hum.Mol.Genet.* 11:1605-1614.

Flanagan, M.D., and S. Lin. 1979. Comparative studies on the characteristic properties of two forms of brain actin separable by isoelectric focussing. *J.Neurochem.* 32:1037-1046.

Forscher, P., and S.J. Smith. 1988. Actions of cytochalasins on the organization of actin filaments and microtubules in a neuronal growth cone. *J.Cell Biol.* 107:1505-1516.

Fox, M.A., and H. Umemori. 2006. Seeking long-term relationship: axon and target communicate to organize synaptic differentiation. *J.Neurochem.* 97:1215-1231. doi: 10.1111/j.1471-4159.2006.03834.x.

Franz, C.K., U. Rutishauser, and V.F. Rafuse. 2008. Intrinsic neuronal properties control selective targeting of regenerating motoneurons. *Brain.* 131:1492-1505.

Fu, A.K., F.C. Ip, W.Y. Fu, J. Cheung, J.H. Wang, W.H. Yung, and N.Y. Ip. 2005. Aberrant motor axon projection, acetylcholine receptor clustering, and neurotransmission in cyclin-dependent kinase 5 null mice. *Proc.Natl.Acad.Sci.U.S.A.* 102:15224-15229.

Gabanella, F., M.E. Butchbach, L. Saieva, C. Carissimi, A.H. Burghes, and L. Pellizzoni. 2007. Ribonucleoprotein assembly defects correlate with spinal muscular atrophy severity and preferentially affect a subset of spliceosomal snRNPs. *PLoS One.* 2:e921. doi: 10.1371/journal.pone.0000921.

George, L.T., T.M. Myckatyn, J.N. Jensen, D.A. Hunter, and S.E. Mackinnon. 2003. Functional recovery and histomorphometric assessment following tibial nerve injury in the mouse. *J.Reconstr.Microsurg.* 19:41-48.

Gibson, D.A., and L. Ma. 2011. Developmental regulation of axon branching in the vertebrate nervous system. *Development.* 138:183-195. doi: 10.1242/dev.046441.

Gimona, M., J. Vandekerckhove, M. Goethals, M. Herzog, Z. Lando, and J.V. Small. 1994. Beta-actin specific monoclonal antibody. *Cell Motil.Cytoskeleton.* 27:108-116. doi: 10.1002/cm.970270203.

Glinka, M., T. Herrmann, N. Funk, S. Havlicek, W. Rossoll, C. Winkler, and M. Sendtner. 2010. The heterogeneous nuclear ribonucleoprotein-R is necessary for axonal {beta}-actin mRNA translocation in spinal motor neurons. *Hum.Mol.Genet.*

Goebbels, S., I. Bormuth, U. Bode, O. Hermanson, M.H. Schwab, and K.A. Nave. 2006. Genetic targeting of principal neurons in neocortex and hippocampus of NEX-Cre mice. *Genesis.* 44:611-621. doi: 10.1002/dvg.20256.

Grantham, J., L.W. Ruddock, A. Roobol, and M.J. Carden. 2002. Eukaryotic chaperonin containing T-complex polypeptide 1 interacts with filamentous actin and reduces the initial rate of actin polymerization in vitro. *Cell Stress Chaperones.* 7:235-242.

Graus-Porta, D., S. Blaess, M. Senften, A. Littlewood-Evans, C. Damsky, Z. Huang, P. Orban, R. Klein, J.C. Schittny, and U. Muller. 2001. Beta1-class integrins regulate the development of laminae and folia in the cerebral and cerebellar cortex. *Neuron.* 31:367-379.

Greer, J.J., D.W. Allan, M. Martin-Caraballo, and R.P. Lemke. 1999. An overview of phrenic nerve and diaphragm muscle development in the perinatal rat. *J.Appl.Physiol.* 86:779-786.

Gu, L., H. Zhang, Q. Chen, and J. Chen. 2003. Calyculin A-induced actin phosphorylation and depolymerization in renal epithelial cells. *Cell Motil.Cytoskeleton.* 54:286-295. doi: 10.1002/cm.10099.

Gu, W., F. Pan, H. Zhang, G.J. Bassell, and R.H. Singer. 2002. A predominantly nuclear protein affecting cytoplasmic localization of beta-actin mRNA in fibroblasts and neurons. *J.Cell Biol.* 156:41-51. doi: 10.1083/jcb.200105133.

Hanft, L.M., I.N. Rybakova, J.R. Patel, J.A. Rafael-Fortney, and J.M. Ervasti. 2006. Cytoplasmic gamma-actin contributes to a compensatory remodeling response in dystrophin-deficient muscle. *Proc.Natl.Acad.Sci.U.S.A.* 103:5385-5390. doi: 10.1073/pnas.0600980103.

Hansen, T.V., N.A. Hammer, J. Nielsen, M. Madsen, C. Dalbaeck, U.M. Wewer, J. Christiansen, and F.C. Nielsen. 2004. Dwarfism and impaired gut development in insulin-like growth factor II mRNA-binding protein 1-deficient mice. *Mol.Cell.Biol.* 24:4448-4464.

Hess, D.M., M.O. Scott, S. Potluri, E.V. Pitts, C. Cisterni, and R.J. Balice-Gordon. 2007. Localization of TrkC to Schwann cells and effects of neurotrophin-3 signaling at neuromuscular synapses. *J.Comp.Neurol.* 501:465-482.

Hill, M.A., and P. Gunning. 1993. Beta and gamma actin mRNAs are differentially located within myoblasts. *J.Cell Biol.* 122:825-832.

Hinz, B., G. Gabbiani, and C. Chaponnier. 2002. The NH2-terminal peptide of alpha-smooth muscle actin inhibits force generation by the myofibroblast in vitro and in vivo. *J.Cell Biol.* 157:657-663. doi: 10.1083/jcb.200201049.

Hofer, D., W. Ness, and D. Drenckhahn. 1997. Sorting of actin isoforms in chicken auditory hair cells. *J.Cell.Sci.* 110 (Pt 6):765-770.

Hofmann, W.A., A. Arduini, S.M. Nicol, C.J. Camacho, J.L. Lessard, F.V. Fuller-Pace, and P. de Lanerolle. 2009. SUMOylation of nuclear actin. *J.Cell Biol.* 186:193-200. doi: 10.1083/jcb.200905016.

Hofmann, W.A., L. Stojiljkovic, B. Fuchsova, G.M. Vargas, E. Mavrommatis, V. Philimonenko, K. Kysela, J.A. Goodrich, J.L. Lessard, T.J. Hope, P. Hozak, and P. de Lanerolle. 2004. Actin is part of pre-initiation complexes and is necessary for transcription by RNA polymerase II. *Nat.Cell Biol.* 6:1094-1101. doi: 10.1038/ncb1182.

Holtmaat, A., and K. Svoboda. 2009. Experience-dependent structural synaptic plasticity in the mammalian brain. *Nat.Rev.Neurosci.* 10:647-658. doi: 10.1038/nrn2699.

Honkura, N., M. Matsuzaki, J. Noguchi, G.C. Ellis-Davies, and H. Kasai. 2008. The subspine organization of actin fibers regulates the structure and plasticity of dendritic spines. *Neuron.* 57:719-729. doi: 10.1016/j.neuron.2008.01.013.

Hoock, T.C., P.M. Newcomb, and I.M. Herman. 1991. Beta actin and its mRNA are localized at the plasma membrane and the regions of moving cytoplasm during the cellular response to injury. *J.Cell Biol.* 112:653-664.

Hotulainen, P., and C.C. Hoogenraad. 2010. Actin in dendritic spines: connecting dynamics to function. *J.Cell Biol.* 189:619-629. doi: 10.1083/jcb.201003008.

Huttelmaier, S., D. Zenklusen, M. Lederer, J. Dictenberg, M. Lorenz, X. Meng, G.J. Bassell, J. Condeelis, and R.H. Singer. 2005. Spatial regulation of beta-actin translation by Src-dependent phosphorylation of ZBP1. *Nature.* 438:512-515.

Inserra, M.M., D.A. Bloch, and D.J. Terris. 1998. Functional indices for sciatic, peroneal, and posterior tibial nerve lesions in the mouse. *Microsurgery.* 18:119-124.

Jablonka, S., M. Beck, B.D. Lechner, C. Mayer, and M. Sendtner. 2007. Defective Ca2+ channel clustering in axon terminals disturbs excitability in motoneurons in spinal muscular atrophy. *J.Cell Biol.* 179:139-149.

Jablonka, S., S. Wiese, and M. Sendtner. 2004. Axonal defects in mouse models of motoneuron disease. *J.Neurobiol.* 58:272-286. doi: 10.1002/neu.10313.

Jaeger, M.A., K.J. Sonnemann, D.P. Fitzsimons, K.W. Prins, and J.M. Ervasti. 2009. Context-dependent functional substitution of alpha-skeletal actin by gamma-cytoplasmic actin. *FASEB J.* 23:2205-2214.

Jevsek, M., A. Jaworski, L. Polo-Parada, N. Kim, J. Fan, L.T. Landmesser, and S.J. Burden. 2006. CD24 is expressed by myofiber synaptic nuclei and regulates synaptic transmission. *Proc.Natl.Acad.Sci.U.S.A.* 103:6374-6379.

Jonson, L., J. Vikesaa, A. Krogh, L.K. Nielsen, T. Hansen, R. Borup, A.H. Johnsen, J. Christiansen, and F.C. Nielsen. 2007. Molecular composition of IMP1 ribonucleoprotein granules. *Mol.Cell.Proteomics.* 6:798-811.

Kabsch, W., H.G. Mannherz, D. Suck, E.F. Pai, and K.C. Holmes. 1990. Atomic structure of the actin:DNase I complex. *Nature.* 347:37-44. doi: 10.1038/347037a0.

Kaech, S., M. Fischer, T. Doll, and A. Matus. 1997. Isoform specificity in the relationship of actin to dendritic spines. *J.Neurosci.* 17:9565-9572.

Karakozova, M., M. Kozak, C.C. Wong, A.O. Bailey, J.R. Yates 3rd, A. Mogilner, H. Zebroski, and A. Kashina. 2006. Arginylation of beta-actin regulates actin cytoskeleton and cell motility. *Science.* 313:192-196. doi: 10.1126/science.1129344.

Kariya, S., R. Mauricio, Y. Dai, and U.R. Monani. 2009. The neuroprotective factor Wld(s) fails to mitigate distal axonal and neuromuscular junction (NMJ) defects in mouse models of spinal muscular atrophy. *Neurosci.Lett.* 449:246-251. doi: 10.1016/j.neulet.2008.10.107.

Kariya, S., G.H. Park, Y. Maeno-Hikichi, O. Leykekhman, C. Lutz, M.S. Arkovitz, L.T. Landmesser, and U.R. Monani. 2008. Reduced SMN protein impairs maturation of the neuromuscular junctions in mouse models of spinal muscular atrophy. *Hum.Mol.Genet.* 17:2552-2569.

Kim, N., and S.J. Burden. 2008. MuSK controls where motor axons grow and form synapses. *Nat.Neurosci.* 11:19-27.

Kislauskis, E.H., Z. Li, R.H. Singer, and K.L. Taneja. 1993. Isoform-specific 3'-untranslated sequences sort alpha-cardiac and beta-cytoplasmic actin messenger RNAs to different cytoplasmic compartments. *J.Cell Biol.* 123:165-172.

Kislauskis, E.H., X. Zhu, and R.H. Singer. 1997. beta-Actin messenger RNA localization and protein synthesis augment cell motility. *J.Cell Biol.* 136:1263-1270.

Kislauskis, E.H., X. Zhu, and R.H. Singer. 1994. Sequences responsible for intracellular localization of beta-actin messenger RNA also affect cell phenotype. *J.Cell Biol.* 127:441-451.

Knoll, B., O. Kretz, C. Fiedler, S. Alberti, G. Schutz, M. Frotscher, and A. Nordheim. 2006. Serum response factor controls neuronal circuit assembly in the hippocampus. *Nat.Neurosci.* 9:195-204. doi: 10.1038/nn1627.

Knoll, B., and A. Nordheim. 2009. Functional versatility of transcription factors in the nervous system: the SRF paradigm. *Trends Neurosci.* 32:432-442. doi: 10.1016/j.tins.2009.05.004.

Kong, L., X. Wang, D.W. Choe, M. Polley, B.G. Burnett, M. Bosch-Marce, J.W. Griffin, M.M. Rich, and C.J. Sumner. 2009. Impaired synaptic vesicle release and immaturity of neuromuscular junctions in spinal muscular atrophy mice. *J.Neurosci.* 29:842-851.

Kramer, E.R., L. Knott, F. Su, E. Dessaud, C.E. Krull, F. Helmbacher, and R. Klein. 2006. Cooperation between GDNF/Ret and ephrinA/EphA4 signals for motor-axon pathway selection in the limb. *Neuron.* 50:35-47.

Kudryashova, E., D. Kudryashov, I. Kramerova, and M.J. Spencer. 2005. Trim32 is a ubiquitin ligase mutated in limb girdle muscular dystrophy type 2H that binds to skeletal muscle myosin and ubiquitinates actin. *J.Mol.Biol.* 354:413-424. doi: 10.1016/j.jmb.2005.09.068.

Kueh, H.Y., W.M. Brieher, and T.J. Mitchison. 2008. Dynamic stabilization of actin filaments. *Proc.Natl.Acad.Sci.U.S.A.* 105:16531-16536. doi: 10.1073/pnas.0807394105.

Kumar, A., K. Crawford, L. Close, M. Madison, J. Lorenz, T. Doetschman, S. Pawlowski, J. Duffy, J. Neumann, J. Robbins, G.P. Boivin, B.A. O'Toole, and J.L. Lessard. 1997. Rescue of cardiac alpha-actin-deficient mice by enteric smooth muscle gamma-actin. *Proc.Natl.Acad.Sci.U.S.A.* 94:4406-4411.

Lafont, F., M. Rouget, A. Rousselet, C. Valenza, and A. Prochiantz. 1993. Specific responses of axons and dendrites to cytoskeleton perturbations: an in vitro study. *J.Cell.Sci.* 104 (Pt 2):433-443.

Larsson, H., and U. Lindberg. 1988. The effect of divalent cations on the interaction between calf spleen profilin and different actins. *Biochim.Biophys.Acta.* 953:95-105.

Lecuit, T., and P.F. Lenne. 2007. Cell surface mechanics and the control of cell shape, tissue patterns and morphogenesis. *Nat.Rev.Mol.Cell Biol.* 8:633-644. doi: 10.1038/nrm2222.

Lefebvre, S., L. Burglen, S. Reboullet, O. Clermont, P. Burlet, L. Viollet, B. Benichou, C. Cruaud, P. Millasseau, and M. Zeviani. 1995. Identification and characterization of a spinal muscular atrophy-determining gene. *Cell.* 80:155-165.

Leslie, K.O., J.J. Mitchell, J.L. Woodcock-Mitchell, and R.B. Low. 1990. Alpha smooth muscle actin expression in developing and adult human lung. *Differentiation.* 44:143-149.

Letourneau, P.C., and A.H. Ressler. 1984. Inhibition of neurite initiation and growth by taxol. *J.Cell Biol.* 98:1355-1362.

Leung, K.M., F.P. van Horck, A.C. Lin, R. Allison, N. Standart, and C.E. Holt. 2006. Asymmetrical beta-actin mRNA translation in growth cones mediates attractive turning to netrin-1. *Nat.Neurosci.* 9:1247-1256.

Li, X.M., X.P. Dong, S.W. Luo, B. Zhang, D.H. Lee, A.K. Ting, H. Neiswender, C.H. Kim, E. Carpenter-Hyland, T.M. Gao, W.C. Xiong, and L. Mei. 2008. Retrograde regulation of motoneuron differentiation by muscle beta-catenin. *Nat.Neurosci.* 11:262-268.

Lin, C.H., C.A. Thompson, and P. Forscher. 1994. Cytoskeletal reorganization underlying growth cone motility. *Curr.Opin.Neurobiol.* 4:640-647.

Lin, W., H.B. Sanchez, T. Deerinck, J.K. Morris, M. Ellisman, and K.F. Lee. 2000. Aberrant development of motor axons and neuromuscular synapses in erbB2-deficient mice. *Proc.Natl.Acad.Sci.U.S.A.* 97:1299-1304.

Livy, D.J., and D. Wahlsten. 1997. Retarded formation of the hippocampal commissure in embryos from mouse strains lacking a corpus callosum. *Hippocampus.* 7:2-14. doi: 2-R.

Lledo, P.M., M. Alonso, and M.S. Grubb. 2006. Adult neurogenesis and functional plasticity in neuronal circuits. *Nat.Rev.Neurosci.* 7:179-193. doi: 10.1038/nrn1867.

Lowery, L.A., and D. Van Vactor. 2009. The trip of the tip: understanding the growth cone machinery. *Nat.Rev.Mol.Cell Biol.* 10:332-343. doi: 10.1038/nrm2679.

Lund, L.M., and I.G. McQuarrie. 1996. Axonal regrowth upregulates beta-actin and Jun D mRNA expression. *J.Neurobiol.* 31:476-486.

Lunn, M.R., and C.H. Wang. 2008. Spinal muscular atrophy. *Lancet.* 371:2120-2133. doi: 10.1016/S0140-6736(08)60921-6.

Luo, L. 2002. Actin cytoskeleton regulation in neuronal morphogenesis and structural plasticity. *Annu.Rev.Cell Dev.Biol.* 18:601-635. doi: 10.1146/annurev.cellbio.18.031802.150501.

Luria, V., and E. Laufer. 2007. Lateral motor column axons execute a ternary trajectory choice between limb and body tissues. *Neural Dev.* 2:13.

Mantilla, C.B., and G.C. Sieck. 2008. Key aspects of phrenic motoneuron and diaphragm muscle development during the perinatal period. *J.Appl.Physiol.* 104:1818-1827.

Marsh, L., and P.C. Letourneau. 1984. Growth of neurites without filopodial or lamellipodial activity in the presence of cytochalasin B. *J.Cell Biol.* 99:2041-2047.

Marsick, B.M., K.C. Flynn, M. Santiago-Medina, J.R. Bamburg, and P.C. Letourneau. 2010. Activation of ADF/cofilin mediates attractive growth cone turning toward nerve growth factor and netrin-1. *Dev.Neurobiol.* 70:565-588. doi: 10.1002/dneu.20800.

Martin, A.C. 2010. Pulsation and stabilization: contractile forces that underlie morphogenesis. *Dev.Biol.* 341:114-125. doi: 10.1016/j.ydbio.2009.10.031.

Maruthamuthu, V., Y. Aratyn-Schaus, and M.L. Gardel. 2010. Conserved F-actin dynamics and force transmission at cell adhesions. *Curr.Opin.Cell Biol.* 22:583-588. doi: 10.1016/j.ceb.2010.07.010.

McGovern, V.L., T.O. Gavrilina, C.E. Beattie, and A.H. Burghes. 2008. Embryonic motor axon development in the severe SMA mouse. *Hum.Mol.Genet.* 17:2900-2909.

McHugh, K.M., K. Crawford, and J.L. Lessard. 1991. A comprehensive analysis of the developmental and tissue-specific expression of the isoactin multigene family in the rat. *Dev.Biol.* 148:442-458.

McHugh, K.M., and J.L. Lessard. 1988. The development expression of the rat alpha-vascular and gamma-enteric smooth muscle isoactins: isolation and characterization of a rat gamma-enteric actin cDNA. *Mol.Cell.Biol.* 8:5224-5231.

McWhorter, M.L., U.R. Monani, A.H. Burghes, and C.E. Beattie. 2003. Knockdown of the survival motor neuron (Smn) protein in zebrafish causes defects in motor axon outgrowth and pathfinding. *J.Cell Biol.* 162:919-931. doi: 10.1083/jcb.200303168.

Medeiros, N.A., D.T. Burnette, and P. Forscher. 2006. Myosin II functions in actin-bundle turnover in neuronal growth cones. *Nat.Cell Biol.* 8:215-226. doi: 10.1038/ncb1367.

Meijering, E., M. Jacob, J.C. Sarria, P. Steiner, H. Hirling, and M. Unser. 2004. Design and validation of a tool for neurite tracing and analysis in fluorescence microscopy images. *Cytometry A.* 58:167-176. doi: 10.1002/cyto.a.20022.

Mejat, A., V. Decostre, J. Li, L. Renou, A. Kesari, D. Hantai, C.L. Stewart, X. Xiao, E. Hoffman, G. Bonne, and T. Misteli. 2009. Lamin A/C-mediated neuromuscular junction defects in Emery-Dreifuss muscular dystrophy. *J.Cell Biol.* 184:31-44.

Mende, Y., M. Jakubik, M. Riessland, F. Schoenen, K. Rossbach, A. Kleinridders, C. Kohler, T. Buch, and B. Wirth. 2010. Deficiency of the splicing factor Sfrs10 results in early embryonic lethality in mice and has no impact on full-length SMN /Smn splicing. *Hum.Mol.Genet.*

Micheva, K.D., A. Vallee, C. Beaulieu, I.M. Herman, and N. Leclerc. 1998. beta-Actin is confined to structures having high capacity of remodelling in developing and adult rat cerebellum. *Eur.J.Neurosci.* 10:3785-3798.

Mignogna, P., and D. Viggiano. 2010. Brain distribution of genes related to changes in locomotor activity. *Physiol.Behav.* 99:618-626. doi: 10.1016/j.physbeh.2010.01.026.

Ming, G.L. 2006. Turning by asymmetric actin. *Nat.Neurosci.* 9:1201-1203. doi: 10.1038/nn1006-1201.

Ming, G.L., and H. Song. 2005. Adult neurogenesis in the mammalian central nervous system. *Annu.Rev.Neurosci.* 28:223-250. doi: 10.1146/annurev.neuro.28.051804.101459.

Monani, U.R. 2005. Spinal muscular atrophy: a deficiency in a ubiquitous protein; a motor neuron-specific disease. *Neuron.* 48:885-896. doi: 10.1016/j.neuron.2005.12.001.

Monani, U.R., M.T. Pastore, T.O. Gavrilina, S. Jablonka, T.T. Le, C. Andreassi, J.M. DiCocco, C. Lorson, E.J. Androphy, M. Sendtner, M. Podell, and A.H. Burghes. 2003. A transgene carrying an A2G missense mutation in the SMN gene modulates phenotypic severity in mice with severe (type I) spinal muscular atrophy. *J.Cell Biol.* 160:41-52.

Moreno, M.M., C. Linster, O. Escanilla, J. Sacquet, A. Didier, and N. Mandairon. 2009. Olfactory perceptual learning requires adult neurogenesis. *Proc.Natl.Acad.Sci.U.S.A.* 106:17980-17985. doi: 10.1073/pnas.0907063106.

Murray, L.M., L.H. Comley, D. Thomson, N. Parkinson, K. Talbot, and T.H. Gillingwater. 2008. Selective vulnerability of motor neurons and dissociation of pre- and post-synaptic pathology at the neuromuscular junction in mouse models of spinal muscular atrophy. *Hum.Mol.Genet.* 17:949-962.

Murray, L.M., S. Lee, D. Baumer, S.H. Parson, K. Talbot, and T.H. Gillingwater. 2010. Pre-symptomatic development of lower motor neuron connectivity in a mouse model of severe spinal muscular atrophy. *Hum.Mol.Genet.* 19:420-433.

Namba, Y., M. Ito, Y. Zu, K. Shigesada, and K. Maruyama. 1992. Human T cell L-plastin bundles actin filaments in a calcium-dependent manner. *J.Biochem.* 112:503-507.

Nielsen, F.C., J. Nielsen, and J. Christiansen. 2001. A family of IGF-II mRNA binding proteins (IMP) involved in RNA trafficking. *Scand.J.Clin.Lab.Invest.Suppl.* 234:93-99.

Nielsen, J., J. Christiansen, J. Lykke-Andersen, A.H. Johnsen, U.M. Wewer, and F.C. Nielsen. 1999. A family of insulin-like growth factor II mRNA-binding proteins represses translation in late development. *Mol.Cell.Biol.* 19:1262-1270.

Nimchinsky, E.A., B.L. Sabatini, and K. Svoboda. 2002. Structure and function of dendritic spines. *Annu.Rev.Physiol.* 64:313-353. doi: 10.1146/annurev.physiol.64.081501.160008.

Nishimune, H., J.R. Sanes, and S.S. Carlson. 2004. A synaptic laminin-calcium channel interaction organizes active zones in motor nerve terminals. *Nature.* 432:580-587. doi: 10.1038/nature03112.

Niu, Z., W. Yu, S.X. Zhang, M. Barron, N.S. Belaguli, M.D. Schneider, M. Parmacek, A. Nordheim, and R.J. Schwartz. 2005. Conditional mutagenesis of the murine serum response factor gene blocks cardiogenesis and the transcription of downstream gene targets. *J.Biol.Chem.* 280:32531-32538. doi: 10.1074/jbc.M501372200.

Noubissi, F.K., I. Elcheva, N. Bhatia, A. Shakoori, A. Ougolkov, J. Liu, T. Minamoto, J. Ross, S.Y. Fuchs, and V.S. Spiegelman. 2006. CRD-BP mediates stabilization of betaTrCP1 and c-myc mRNA in response to beta-catenin signalling. *Nature.* 441:898-901. doi: 10.1038/nature04839.

Nowak, K.J., G. Ravenscroft, C. Jackaman, A. Filipovska, S.M. Davies, E.M. Lim, S.E. Squire, A.C. Potter, E. Baker, S. Clement, C.A. Sewry, V. Fabian, K. Crawford, J.L. Lessard, L.M. Griffiths, J.M. Papadimitriou, Y. Shen, G. Morahan, A.J. Bakker, K.E. Davies, and N.G. Laing. 2009. Rescue of skeletal muscle alpha-actin-null mice by cardiac (fetal) alpha-actin. *J.Cell Biol.* 185:903-915. doi: 10.1083/jcb.200812132.

Nyman, T., H. Schuler, E. Korenbaum, C.E. Schutt, R. Karlsson, and U. Lindberg. 2002. The role of MeH73 in actin polymerization and ATP hydrolysis. *J.Mol.Biol.* 317:577-589. doi: 10.1006/jmbi.2002.5436.

O'Connor, T.P., and D. Bentley. 1993. Accumulation of actin in subsets of pioneer growth cone filopodia in response to neural and epithelial guidance cues in situ. *J.Cell Biol.* 123:935-948.

Oda, T., M. Iwasa, T. Aihara, Y. Maeda, and A. Narita. 2009. The nature of the globular- to fibrous-actin transition. *Nature.* 457:441-445. doi: 10.1038/nature07685.

Okamoto, K., T. Nagai, A. Miyawaki, and Y. Hayashi. 2004. Rapid and persistent modulation of actin dynamics regulates postsynaptic reorganization underlying bidirectional plasticity. *Nat.Neurosci.* 7:1104-1112. doi: 10.1038/nn1311.

Oprea, G.E., S. Krober, M.L. McWhorter, W. Rossoll, S. Muller, M. Krawczak, G.J. Bassell, C.E. Beattie, and B. Wirth. 2008. Plastin 3 is a protective modifier of autosomal recessive spinal muscular atrophy. *Science.* 320:524-527. doi: 10.1126/science.1155085.

Otey, C.A., M.H. Kalnoski, and J.C. Bulinski. 1987. Identification and quantification of actin isoforms in vertebrate cells and tissues. *J.Cell.Biochem.* 34:113-124. doi: 10.1002/jcb.240340205.

Otey, C.A., M.H. Kalnoski, J.L. Lessard, and J.C. Bulinski. 1986. Immunolocalization of the gamma isoform of nonmuscle actin in cultured cells. *J.Cell Biol.* 102:1726-1737.

Pagliardini, S., A. Giavazzi, V. Setola, C. Lizier, M. Di Luca, S. DeBiasi, and G. Battaglia. 2000. Subcellular localization and axonal transport of the survival motor neuron (SMN) protein in the developing rat spinal cord. *Hum.Mol.Genet.* 9:47-56.

Pak, C.W., K.C. Flynn, and J.R. Bamburg. 2008. Actin-binding proteins take the reins in growth cones. *Nat.Rev.Neurosci.* 9:136-147. doi: 10.1038/nrn2236.

Palazzolo, I., C. Stack, L. Kong, A. Musaro, H. Adachi, M. Katsuno, G. Sobue, J.P. Taylor, C.J. Sumner, K.H. Fischbeck, and M. Pennuto. 2009. Overexpression of IGF-1 in muscle attenuates disease in a mouse model of spinal and bulbar muscular atrophy. *Neuron.* 63:316-328.

Pantaloni, D., C. Le Clainche, and M.F. Carlier. 2001. Mechanism of actin-based motility. *Science.* 292:1502-1506.

Pappenberger, G., E.A. McCormack, and K.R. Willison. 2006. Quantitative actin folding reactions using yeast CCT purified via an internal tag in the CCT3/gamma subunit. *J.Mol.Biol.* 360:484-496. doi: 10.1016/j.jmb.2006.05.003.

Penzes, P., M.E. Cahill, K.A. Jones, J.E. VanLeeuwen, and K.M. Woolfrey. 2011. Dendritic spine pathology in neuropsychiatric disorders. *Nat.Neurosci.* 14:285-293. doi: 10.1038/nn.2741.

Perrin, B.J., K.J. Sonnemann, and J.M. Ervasti. 2010. beta-actin and gamma-actin are each dispensable for auditory hair cell development but required for Stereocilia maintenance. *PLoS Genet.* 6:e1001158. doi: 10.1371/journal.pgen.1001158.

Pollard, T.D. 1986a. Assembly and dynamics of the actin filament system in nonmuscle cells. *J.Cell.Biochem.* 31:87-95. doi: 10.1002/jcb.240310202.

Pollard, T.D. 1986b. Rate constants for the reactions of ATP- and ADP-actin with the ends of actin filaments. *J.Cell Biol.* 103:2747-2754.

Pollard, T.D., and G.G. Borisy. 2003. Cellular motility driven by assembly and disassembly of actin filaments. *Cell.* 112:453-465.

Pollard, T.D., and J.A. Cooper. 2009. Actin, a central player in cell shape and movement. *Science.* 326:1208-1212. doi: 10.1126/science.1175862.

Popko, J., A. Fernandes, D. Brites, and L.M. Lanier. 2009. Automated analysis of NeuronJ tracing data. *Cytometry A.* 75:371-376. doi: 10.1002/cyto.a.20660.

Porter, B.E., J. Weis, and J.R. Sanes. 1995. A motoneuron-selective stop signal in the synaptic protein S-laminin. *Neuron.* 14:549-559.

Prins, K.W., J.A. Call, D.A. Lowe, and J.M. Ervasti. 2011. Quadriceps myopathy caused by skeletal muscle-specific ablation of beta(cyto)-actin. *J.Cell.Sci.* 124:951-957. doi: 10.1242/jcs.079848.

Prins, K.W., D.A. Lowe, and J.M. Ervasti. 2008. Skeletal muscle-specific ablation of gamma(cyto)-actin does not exacerbate the mdx phenotype. *PLoS One.* 3:e2419.

Rackham, O., and C.M. Brown. 2004. Visualization of RNA-protein interactions in living cells: FMRP and IMP1 interact on mRNAs. *EMBO J.* 23:3346-3355. doi: 10.1038/sj.emboj.7600341.

Rash, B.G., and L.J. Richards. 2001. A role for cingulate pioneering axons in the development of the corpus callosum. *J.Comp.Neurol.* 434:147-157.

Richards, L.J., C. Plachez, and T. Ren. 2004. Mechanisms regulating the development of the corpus callosum and its agenesis in mouse and human. *Clin.Genet.* 66:276-289. doi: 10.1111/j.1399-0004.2004.00354.x.

Roche, F.K., B.M. Marsick, and P.C. Letourneau. 2009. Protein synthesis in distal axons is not required for growth cone responses to guidance cues. *J.Neurosci.* 29:638-652. doi: 10.1523/JNEUROSCI.3845-08.2009.

Ross, A.F., Y. Oleynikov, E.H. Kislauskis, K.L. Taneja, and R.H. Singer. 1997. Characterization of a beta-actin mRNA zipcode-binding protein. *Mol.Cell.Biol.* 17:2158-2165.

Rossoll, W., S. Jablonka, C. Andreassi, A.K. Kroning, K. Karle, U.R. Monani, and M. Sendtner. 2003. Smn, the spinal muscular atrophy-determining gene product, modulates axon growth and localization of beta-actin mRNA in growth cones of motoneurons. *J.Cell Biol.* 163:801-812.

Rossoll, W., A.K. Kroning, U.M. Ohndorf, C. Steegborn, S. Jablonka, and M. Sendtner. 2002. Specific interaction of Smn, the spinal muscular atrophy determining gene product, with hnRNP-R and gry-rbp/hnRNP-Q: a role for Smn in RNA processing in motor axons? *Hum.Mol.Genet.* 11:93-105.

Rubenstein, P.A. 1990. The functional importance of multiple actin isoforms. *Bioessays.* 12:309-315. doi: 10.1002/bies.950120702.

Rubenstein, P.A., and D.J. Martin. 1983. NH2-terminal processing of actin in mouse L-cells in vivo. *J.Biol.Chem.* 258:3961-3966.

Runge, S., F.C. Nielsen, J. Nielsen, J. Lykke-Andersen, U.M. Wewer, and J. Christiansen. 2000. H19 RNA binds four molecules of insulin-like growth factor II mRNA-binding protein. *J.Biol.Chem.* 275:29562-29569. doi: 10.1074/jbc.M001156200.

Sanes, J.R., and J.W. Lichtman. 1999. Development of the vertebrate neuromuscular junction. *Annu.Rev.Neurosci.* 22:389-442.

Sasaki, Y., K. Welshhans, Z. Wen, J. Yao, M. Xu, Y. Goshima, J.Q. Zheng, and G.J. Bassell. 2010. Phosphorylation of zipcode binding protein 1 is required for brain-derived neurotrophic factor signaling of local beta-actin synthesis and growth cone turning. *J.Neurosci.* 30:9349-9358. doi: 10.1523/JNEUROSCI.0499-10.2010.

Satz, J.S., A.P. Ostendorf, S. Hou, A. Turner, H. Kusano, J.C. Lee, R. Turk, H. Nguyen, S.E. Ross-Barta, S. Westra, T. Hoshi, S.A. Moore, and K.P. Campbell. 2010. Distinct functions of glial and neuronal dystroglycan in the developing and adult mouse brain. *J.Neurosci.* 30:14560-14572. doi: 10.1523/JNEUROSCI.3247-10.2010.

Schevzov, G., C. Lloyd, and P. Gunning. 1992. High level expression of transfected beta- and gamma-actin genes differentially impacts on myoblast cytoarchitecture. *J.Cell Biol.* 117:775-785.

Schildmeyer, L.A., R. Braun, G. Taffet, M. Debiasi, A.E. Burns, A. Bradley, and R.J. Schwartz. 2000. Impaired vascular contractility and blood pressure homeostasis in the smooth muscle alpha-actin null mouse. *FASEB J.* 14:2213-2220. doi: 10.1096/fj.99-0927com.

Schmidt, H., and F.G. Rathjen. 2010. Signalling mechanisms regulating axonal branching in vivo. *Bioessays.* 32:977-985. doi: 10.1002/bies.201000054; 10.1002/bies.201000054.

Schwander, M., R. Shirasaki, S.L. Pfaff, and U. Muller. 2004. Beta1 integrins in muscle, but not in motor neurons, are required for skeletal muscle innervation. *J.Neurosci.* 24:8181-8191.

Serafini, T., S.A. Colamarino, E.D. Leonardo, H. Wang, R. Beddington, W.C. Skarnes, and M. Tessier-Lavigne. 1996. Netrin-1 is required for commissural axon guidance in the developing vertebrate nervous system. *Cell.* 87:1001-1014.

Shawlot, W., J.M. Deng, L.E. Fohn, and R.R. Behringer. 1998. Restricted beta-galactosidase expression of a hygromycin-lacZ gene targeted to the beta-actin locus and embryonic lethality of beta-actin mutant mice. *Transgenic Res.* 7:95-103.

Sheng, M., and C.C. Hoogenraad. 2007. The postsynaptic architecture of excitatory synapses: a more quantitative view. *Annu.Rev.Biochem.* 76:823-847. doi: 10.1146/annurev.biochem.76.060805.160029.

Shestakova, E.A., R.H. Singer, and J. Condeelis. 2001. The physiological significance of beta -actin mRNA localization in determining cell polarity and directional motility. *Proc.Natl.Acad.Sci.U.S.A.* 98:7045-7050. doi: 10.1073/pnas.121146098.

Shimada, A., C.A. Mason, and M.E. Morrison. 1998. TrkB signaling modulates spine density and morphology independent of dendrite structure in cultured neonatal Purkinje cells. *J.Neurosci.* 18:8559-8570.

Shmerling, D., C.P. Danzer, X. Mao, J. Boisclair, M. Haffner, M. Lemaistre, V. Schuler, E. Kaeslin, R. Korn, K. Burki, B. Ledermann, B. Kinzel, and M. Muller. 2005. Strong and ubiquitous expression of transgenes targeted into the beta-actin locus by Cre/lox cassette replacement. *Genesis.* 42:229-235.

Shors, T.J., G. Miesegaes, A. Beylin, M. Zhao, T. Rydel, and E. Gould. 2001. Neurogenesis in the adult is involved in the formation of trace memories. *Nature.* 410:372-376. doi: 10.1038/35066584.

Shu, T., and L.J. Richards. 2001. Cortical axon guidance by the glial wedge during the development of the corpus callosum. *J.Neurosci.* 21:2749-2758.

Shupliakov, O., O. Bloom, J.S. Gustafsson, O. Kjaerulff, P. Low, N. Tomilin, V.A. Pieribone, P. Greengard, and L. Brodin. 2002. Impaired recycling of synaptic vesicles after acute perturbation of the presynaptic actin cytoskeleton. *Proc.Natl.Acad.Sci.U.S.A.* 99:14476-14481.

Shuster, C.B., A.Y. Lin, R. Nayak, and I.M. Herman. 1996. Beta cap73: a novel beta actin-specific binding protein. *Cell Motil.Cytoskeleton.* 35:175-187. doi: 2-8.

Smart, I.H. 1982. Radial unit analysis of hippocampal histogenesis in the mouse. *J.Anat.* 135:763-793.

Sonnemann, K.J., D.P. Fitzsimons, J.R. Patel, Y. Liu, M.F. Schneider, R.L. Moss, and J.M. Ervasti. 2006. Cytoplasmic gamma-actin is not required for skeletal muscle development but its absence leads to a progressive myopathy. *Dev.Cell.* 11:387-397.

Steup, A., M. Lohrum, N. Hamscho, N.E. Savaskan, O. Ninnemann, R. Nitsch, H. Fujisawa, A.W. Puschel, and T. Skutella. 2000. Sema3C and netrin-1 differentially affect axon growth in the hippocampal formation. *Mol.Cell.Neurosci.* 15:141-155. doi: 10.1006/mcne.1999.0818.

Strasser, G.A., N.A. Rahim, K.E. VanderWaal, F.B. Gertler, and L.M. Lanier. 2004. Arp2/3 is a negative regulator of growth cone translocation. *Neuron.* 43:81-94. doi: 10.1016/j.neuron.2004.05.015.

Sudarov, A., and A.L. Joyner. 2007. Cerebellum morphogenesis: the foliation pattern is orchestrated by multi-cellular anchoring centers. *Neural Dev.* 2:26. doi: 10.1186/1749-8104-2-26.

Suter, D.M., and P. Forscher. 2000. Substrate-cytoskeletal coupling as a mechanism for the regulation of growth cone motility and guidance. *J.Neurobiol.* 44:97-113.

Tadesse, H., J. Deschenes-Furry, S. Boisvenue, and J. Cote. 2008. KH-type splicing regulatory protein interacts with survival motor neuron protein and is misregulated in spinal muscular atrophy. *Hum.Mol.Genet.* 17:506-524.

Telerman-Toppet, N., and C. Coers. 1978. Motor innervation and fiber type pattern in amyotrophic lateral sclerosis and in Charcot-Marie-Tooth disease. *Muscle Nerve.* 1:133-139.

Tessier-Lavigne, M., and C.S. Goodman. 1996. The molecular biology of axon guidance. *Science.* 274:1123-1133.

Tiruchinapalli, D.M., Y. Oleynikov, S. Kelic, S.M. Shenoy, A. Hartley, P.K. Stanton, R.H. Singer, and G.J. Bassell. 2003. Activity-dependent trafficking and dynamic localization of zipcode binding protein 1 and beta-actin mRNA in dendrites and spines of hippocampal neurons. *J.Neurosci.* 23:3251-3261.

Tizzano, E.F., C. Cabot, and M. Baiget. 1998. Cell-specific survival motor neuron gene expression during human development of the central nervous system: implications for the pathogenesis of spinal muscular atrophy. *Am.J.Pathol.* 153:355-361. doi: 10.1016/S0002-9440(10)65578-2.

Tondeleir, D., D. Vandamme, J. Vandekerckhove, C. Ampe, and A. Lambrechts. 2009. Actin isoform expression patterns during mammalian development and in pathology: insights from mouse models. *Cell Motil.Cytoskeleton.* 66:798-815. doi: 10.1002/cm.20350.

Tronche, F., C. Kellendonk, O. Kretz, P. Gass, K. Anlag, P.C. Orban, R. Bock, R. Klein, and G. Schutz. 1999. Disruption of the glucocorticoid receptor gene in the nervous system results in reduced anxiety. *Nat.Genet.* 23:99-103.

Tsujita, M., H. Mori, M. Watanabe, M. Suzuki, J. Miyazaki, and M. Mishina. 1999. Cerebellar granule cell-specific and inducible expression of Cre recombinase in the mouse. *J.Neurosci.* 19:10318-10323.

van Bergeijk, J., K. Rydel-Konecke, C. Grothe, and P. Claus. 2007. The spinal muscular atrophy gene product regulates neurite outgrowth: importance of the C terminus. *FASEB J.* 21:1492-1502. doi: 10.1096/fj.06-7136com.

Van Damme, P., M. Leyssen, G. Callewaert, W. Robberecht, and L. Van Den Bosch. 2003. The AMPA receptor antagonist NBQX prolongs survival in a transgenic mouse model of amyotrophic lateral sclerosis. *Neurosci.Lett.* 343:81-84.

van Praag, H., G. Kempermann, and F.H. Gage. 1999. Running increases cell proliferation and neurogenesis in the adult mouse dentate gyrus. *Nat.Neurosci.* 2:266-270. doi: 10.1038/6368.

Vandekerckhove, J., and K. Weber. 1978. At least six different actins are expressed in a higher mammal: an analysis based on the amino acid sequence of the amino-terminal tryptic peptide. *J.Mol.Biol.* 126:783-802.

Vandermoere, F., I. El Yazidi-Belkoura, Y. Demont, C. Slomianny, J. Antol, J. Lemoine, and H. Hondermarck. 2007. Proteomics exploration reveals that actin is a signaling target of the kinase Akt. *Mol.Cell.Proteomics.* 6:114-124. doi: 10.1074/mcp.M600335-MCP200.

Varejao, A.S., P. Melo-Pinto, M.F. Meek, V.M. Filipe, and J. Bulas-Cruz. 2004. Methods for the experimental functional assessment of rat sciatic nerve regeneration. *Neurol.Res.* 26:186-194.

Viggiano, D. 2008. The hyperactive syndrome: metanalysis of genetic alterations, pharmacological treatments and brain lesions which increase locomotor activity. *Behav.Brain Res.* 194:1-14. doi: 10.1016/j.bbr.2008.06.033.

Vikesaa, J., T.V. Hansen, L. Jonson, R. Borup, U.M. Wewer, J. Christiansen, and F.C. Nielsen. 2006. RNA-binding IMPs promote cell adhesion and invadopodia formation. *EMBO J.* 25:1456-1468. doi: 10.1038/sj.emboj.7601039.

Vogelaar, C.F., N.M. Gervasi, L.F. Gumy, D.J. Story, R. Raha-Chowdhury, K.M. Leung, C.E. Holt, and J.W. Fawcett. 2009. Axonal mRNAs: characterisation and role in the

growth and regeneration of dorsal root ganglion axons and growth cones. *Mol.Cell.Neurosci.* 42:102-115.

Wang, J., E.S. Boja, W. Tan, E. Tekle, H.M. Fales, S. English, J.J. Mieyal, and P.B. Chock. 2001. Reversible glutathionylation regulates actin polymerization in A431 cells. *J.Biol.Chem.* 276:47763-47766. doi: 10.1074/jbc.C100415200.

Wang, X.H., J.Q. Zheng, and M.M. Poo. 1996. Effects of cytochalasin treatment on short-term synaptic plasticity at developing neuromuscular junctions in frogs. *J.Physiol.* 491 (Pt 1):187-195.

Wanger, M., and A. Wegner. 1983. Similar affinities of ADP and ATP for G-actin at physiological salt concentrations. *FEBS Lett.* 162:112-116.

Weinberger, R., G. Schevzov, P. Jeffrey, K. Gordon, M. Hill, and P. Gunning. 1996. The molecular composition of neuronal microfilaments is spatially and temporally regulated. *J.Neurosci.* 16:238-252.

Whittemore, L.A., K. Song, X. Li, J. Aghajanian, M. Davies, S. Girgenrath, J.J. Hill, M. Jalenak, P. Kelley, A. Knight, R. Maylor, D. O'Hara, A. Pearson, A. Quazi, S. Ryerson, X.Y. Tan, K.N. Tomkinson, G.M. Veldman, A. Widom, J.F. Wright, S. Wudyka, L. Zhao, and N.M. Wolfman. 2003. Inhibition of myostatin in adult mice increases skeletal muscle mass and strength. *Biochem.Biophys.Res.Commun.* 300:965-971.

Workman, E., L. Saieva, T.L. Carrel, T.O. Crawford, D. Liu, C. Lutz, C.E. Beattie, L. Pellizzoni, and A.H. Burghes. 2009. A SMN missense mutation complements SMN2 restoring snRNPs and rescuing SMA mice. *Hum.Mol.Genet.* 18:2215-2229. doi: 10.1093/hmg/ddp157.

Yang, X., S. Arber, C. William, L. Li, Y. Tanabe, T.M. Jessell, C. Birchmeier, and S.J. Burden. 2001. Patterning of muscle acetylcholine receptor gene expression in the absence of motor innervation. *Neuron.* 30:399-410.

Yao, J., Y. Sasaki, Z. Wen, G.J. Bassell, and J.Q. Zheng. 2006. An essential role for beta-actin mRNA localization and translation in Ca2+-dependent growth cone guidance. *Nat.Neurosci.* 9:1265-1273.

Yao, X., L. Cheng, and J.G. Forte. 1996. Biochemical characterization of ezrin-actin interaction. *J.Biol.Chem.* 271:7224-7229.

Yisraeli, J.K. 2005. VICKZ proteins: a multi-talented family of regulatory RNA-binding proteins. *Biol.Cell.* 97:87-96.

Yoshihara, Y., M. De Roo, and D. Muller. 2009. Dendritic spine formation and stabilization. *Curr.Opin.Neurobiol.* 19:146-153. doi: 10.1016/j.conb.2009.05.013.

Zebda, N., O. Bernard, M. Bailly, S. Welti, D.S. Lawrence, and J.S. Condeelis. 2000. Phosphorylation of ADF/cofilin abolishes EGF-induced actin nucleation at the leading edge and subsequent lamellipod extension. *J.Cell Biol.* 151:1119-1128.

Zhang, F., S. Saha, S.A. Shabalina, and A. Kashina. 2010. Differential arginylation of actin isoforms is regulated by coding sequence-dependent degradation. *Science.* 329:1534-1537. doi: 10.1126/science.1191701.

Zhang, H.L., T. Eom, Y. Oleynikov, S.M. Shenoy, D.A. Liebelt, J.B. Dictenberg, R.H. Singer, and G.J. Bassell. 2001. Neurotrophin-induced transport of a beta-actin mRNP complex increases beta-actin levels and stimulates growth cone motility. *Neuron.* 31:261-275.

Zhang, H.L., F. Pan, D. Hong, S.M. Shenoy, R.H. Singer, and G.J. Bassell. 2003. Active transport of the survival motor neuron protein and the role of exon-7 in cytoplasmic localization. *J.Neurosci.* 23:6627-6637.

Zhang, X.M., A.H. Ng, J.A. Tanner, W.T. Wu, N.G. Copeland, N.A. Jenkins, and J.D. Huang. 2004. Highly restricted expression of Cre recombinase in cerebellar Purkinje cells. *Genesis.* 40:45-51. doi: 10.1002/gene.20062.

Zhang, Z., F. Lotti, K. Dittmar, I. Younis, L. Wan, M. Kasim, and G. Dreyfuss. 2008. SMN deficiency causes tissue-specific perturbations in the repertoire of snRNAs and widespread defects in splicing. *Cell.* 133:585-600. doi: 10.1016/j.cell.2008.03.031.

Zigmond, S.H. 1996. Signal transduction and actin filament organization. *Curr.Opin.Cell Biol.* 8:66-73.

Appendix

Actg1$^{-/-}$ Neurons do not exhibit morphological abnormalities in culture

While most evidence suggests β-actin performs critical functions in neuronal development, a distinct role for γ-actin has never been directly investigated. E15.5 *Actg1*$^{-/-}$ embryos are viable (Bunnell and Ervasti, 2010), unlike *Actb*$^{-/-}$ embryos (Bunnell, 2011, under review), allowing for the culture and characterization of hippocampal neurons null for γ-actin. *Actg1*$^{-/-}$ and control hippocampal neurons were cultured and analyzed as described in Chapter 3. Although γ-actin is present throughout the neuronal cell body, axon, and growth cone of control neurons, we observed no morphological abnormalities except for a small increase in the dendrite length of *Actg1*$^{-/-}$ neurons. The lack of any dramatic phenotypes is consistent with *in vivo* findings where brains from *Actg1*$^{-/-}$ mice are histologically normal. Thus, γ-actin does not play an essential role in neuronal development.

Figure A.1

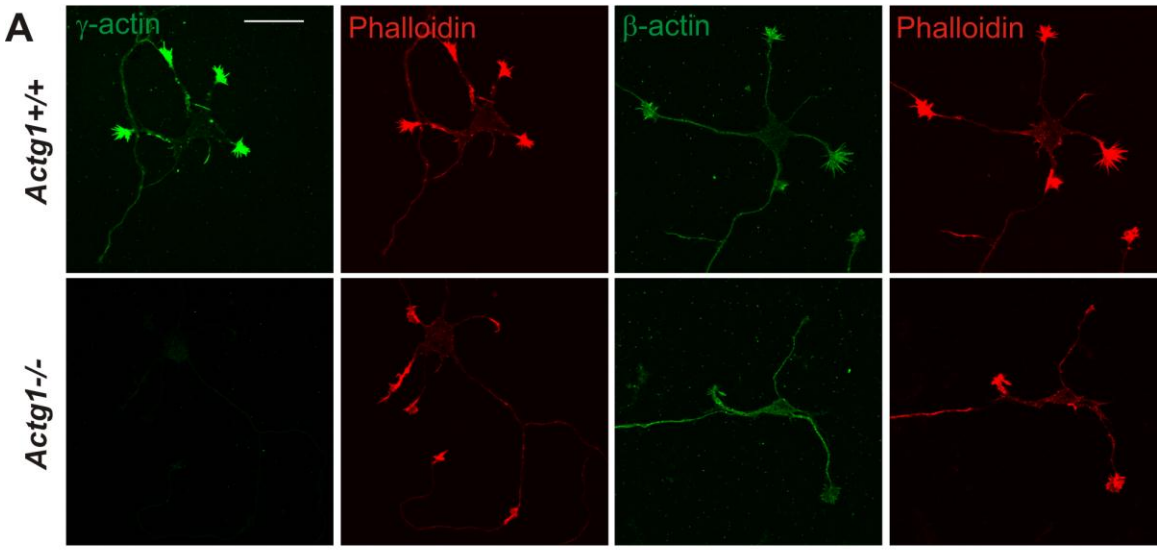

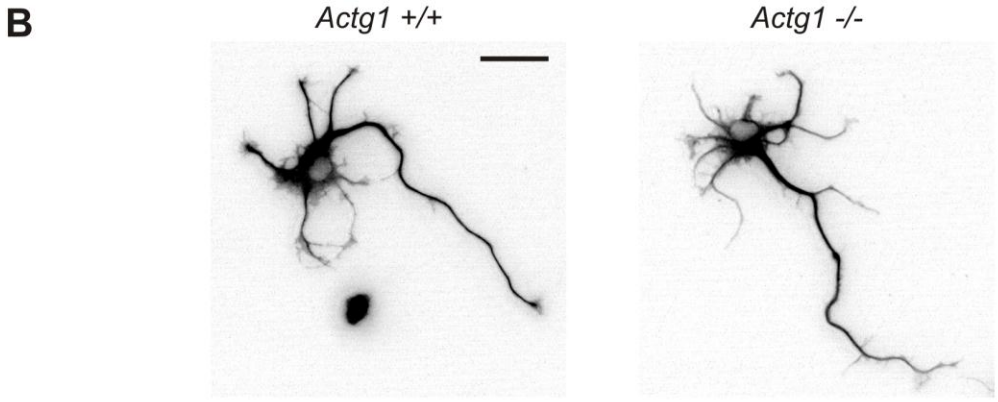

	Control	*Actg1 -/-*	*p* value
Length of axon (μm)	140.9 ± 4.803	150.9 ± 7.179	0.2487
# of axonal branches	0.8860 ± 0.1018	0.9103 ± 0.1213	0.8786
Length of axonal branches (μm)	26.92 ± 1.634	34.08 ± 3.253	0.0517
# of dendrites	3.579 ± 0.1536	3.705 ± 0.1723	0.5904
Length of dendrities (μm)	23.21 ± 0.5597	26.23 ± 0.7899	** 0.0019
# of dendritic branches	0.1964 ± 0.04718	0.3590 ± 0.0815	0.0869
Length of dendritic branches (μm)	15.26 ± 1.385	18.70 ± 2.274	0.2032

Figure A.1: *Actg1*$^{-/-}$ hippocampal neurons do not exhibit morphological abnormalities. (A) Primary hippocampal neurons from *Actg1*$^{+/+}$ and *Actg1*$^{-/-}$ embryos were cultured for three days and double-labeled with the indicated isoform specific antibody and fluorescently labeled phalloidin. γ-actin staining is absent from *Actg1*$^{-/-}$ neurons while β-actin staining appears more diffusely localized as compared to control neurons. Scale bar 30 μm. **(B)** Morphological analysis of *Actg1*$^{+/+}$ and *Actg1*$^{-/-}$ hippocampal neurons at three days *in vitro*. Neurons from at least two independent cultures were labeled with βIII-tubulin and measured using the NeuronJ plugin for NIH ImageJ software. Data from *Actg1*$^{+/+}$ and $^{+/-}$ neurons were pooled together as controls. n=114 control and 78 *Actg1*$^{-/-}$ neurons. The axon was defined as the neurite at least twice as long as the next longest neurite. Data is represented as the mean ± standard error of the mean. Statistical significance was assessed using the Student's T-test. ** indicates p<0.01 Scale bar 30 μm.

Localization of cytoplasmic actin isoforms in the adult mouse brain

Unique functions of the cytoplasmic actin isoforms have often been attributed to distinct localization patterns in different tissues (Weinberger et al., 1996; Micheva et al., 1998; Hofer et al., 1997; Rybakova et al., 2000; Belyantseva et al., 2009). However, there are some limitations to these studies. First, some of the antibodies used have not been validated on tissue from knock-out animals, raising the possibility of cross-reactivity with other proteins or actin isoforms. Second, it was recently shown that some actin based structures may be inaccessible to secondary antibodies. For example, a previous study reported that β-actin was distributed throughout the stereocilia of auditory hair cells while γ-acitn was localized to the periphery (Belyantseva et al., 2009). However, when stereocilia were re-examined with primary antibodies specific for β- and γ-actin that were directly conjugated to fluorescent dyes, both β- and γ-actin were found to be uniformly distributed throughout the stereocilia (Perrin et al., 2010). Finally, a recent study has confirmed our own findings that isoform-specific epitopes may be masked when in tightly bundled structures or following formaldehyde fixation (Dugina et al., 2009). Antigen unmasking with methanol appears to significantly alleviate these effects and promotes robust signals from actin isoform-specific antibodies whose specificity has been verified with knock-out tissue.

A small number of reports have examined the localization of the cytoplasmic actins in adult brain tissue. In one study, γ-actin was reported to be ubiquitously expressed in cell bodies and neurites while β-actin expression was reported to be

decreased dramatically during development and predominantly restricted to dendritic spines in adults based on immunogold electron microscopy experiments (Micheva et al., 1998).Additional studies also observed restriction of β-actin expression as animals mature, with one study noting a loss of β-actin immunoreactivy in medulla axons during CNS maturation (Weinberger et al., 1996). Yet another somewhat conflicting study reported β-actin immunoreactivity was higher in microglial cells than any other CNS cell type, including neurons and astrocytes (Plantier et al., 1998). However, none of these studies used a methanol antigen retrieval step that we and others have since found is critical for strong isoform-specific reactivity, while the specificity of the γ-actin antibodies used in these studies is also questionable.

Using antibodies and conditions validated on knock-out tissue, the localization of the cytoplasmic actin isoforms was examined in three different regions of adult control and CNS-*Actb*KO brain sections. In the hippocampus, β- and γ-actin staining is most prominent in the stratum radiatum and stratum lacunosum moleculare, both areas with a high density of synapses. Neither β- nor γ-actin was observed in nuclei under these staining conditions. The localization of the cytoplasmic actins in the cerebellum is comparable to that of the hippocampus, with both isoforms present in the synapse-rich molecular layer and absent from nuclei concentrated in the granule cell layer. Interestingly, β-actin is absent from large axonal bundles in the white matter of the cerebellum while γ-actin is still present (arrows), consistent with the previously reported absence of β-actin in axonal bundles. The exclusion of β-actin from axonal tracts was also apparent in the striatum. These experiments show the localization of the cytoplasmic

actin isoforms in brain sections for the first time with antibodies and conditions validated on knock-out tissue, and have confirmed previous reports indicating β-actin is absent from large axonal bundles in some adult brain regions. However, β-actin expression appears to be much more widespread in the adult brain than previously reported. Whether the distinct localization of the cytoplasmic actins in axonal tracts has any functional significance is unclear at present however.

Figure A.2

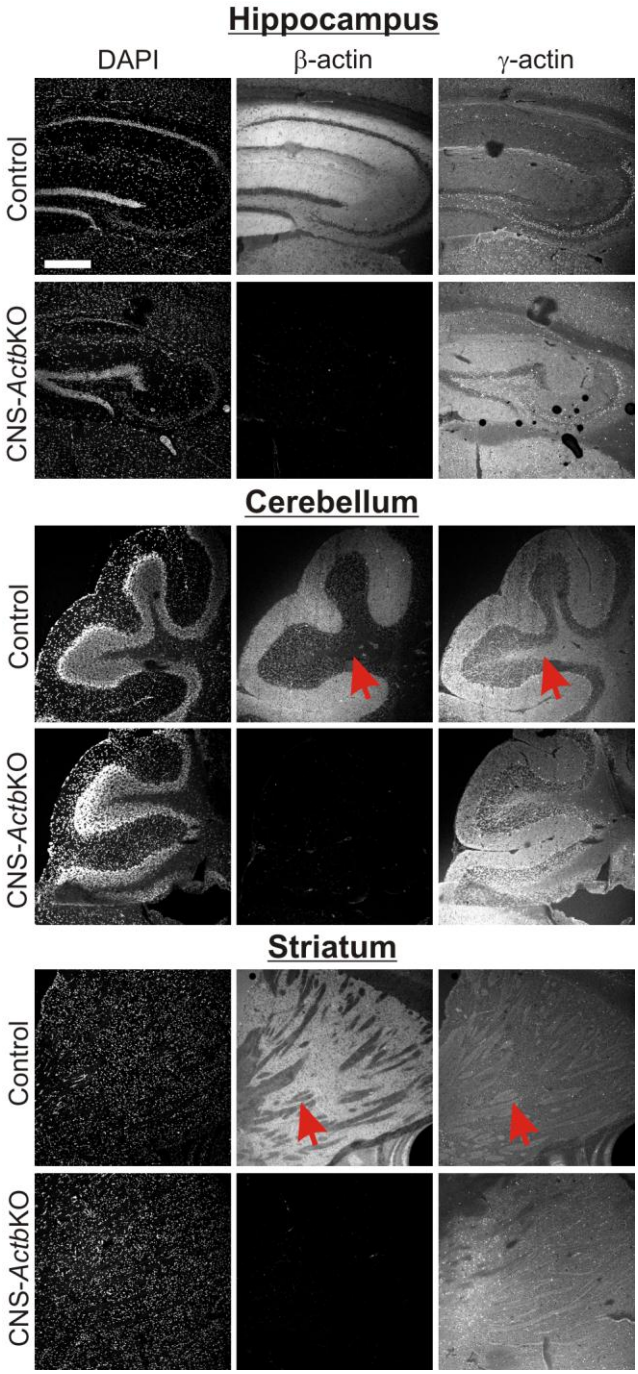
Hippocampus
DAPI
β-actin
γ-actin
Control
CNS-ActbKO
Cerebellum
Control
CNS-ActbKO
Striatum
Control
CNS-ActbKO

Figure A.2: Localization of cytoplasmic actin isoforms in the adult mouse brain. Saggital sections through the hippocampus, cerebellum, and striatum were co-labeled with DAPI to label nuclei and directly conjugated primary antibodies to β- and γ-actin. In the hippocampus, β- and γ-actin were both expressed in the synapse-rich stratum radiatum and stratum lacunosum moleculare regions. The expression of β- and γ-actin in synapse-rich regions was also consistent with the localization of both cytoplasmic actins in the cerebellum, where β- and γ-actin were expressed throughout the molecular layer but absent from the nuclei-dense granule cell layer. β-actin immunoreactivity was absent from large axonal bundles in the cerebellar white matter while γ-actin expression was still present (arrows). The absence of β-actin from large axonal bundles was also apparent in the striatum (arrows). Scale bar 300 μm.

Activity levels of CNS-*Actb*KO mice over a 24-hour period

In Chapter 3, profound hyperactivity of CNS-*Actb*KO mice was reported using a 15 minute Open Field Assay. In order to confirm and expand upon these findings, control and CNS-*Actb*KO mice were also analyzed for a 24-hour time period to determine the timespan of hyperactive behavior and whether CNS-*Actb*KO mice exhibited normal circadian rhythm patterns in relation to activity. Following acclimation to a mock chamber for 24 hours, control and CNS-*Actb*KO mice were placed into activity cages and monitored for 24 hours as described previously (Greising et al., 2011). CNS-*Actb*KO mice traveled significantly farther than control mice throughout the entire testing period. Interestingly, CNS-*Actb*KO mice appeared to have a normal circadian rhythm however, as they were most active during the dark cycle and least active during the light cycle. Thus, the profound hyperactivity of CNS-*Actb*KO mice was not an artifact of a novel environment and follows the normal circadian rhythm of mice.

Figure A.3

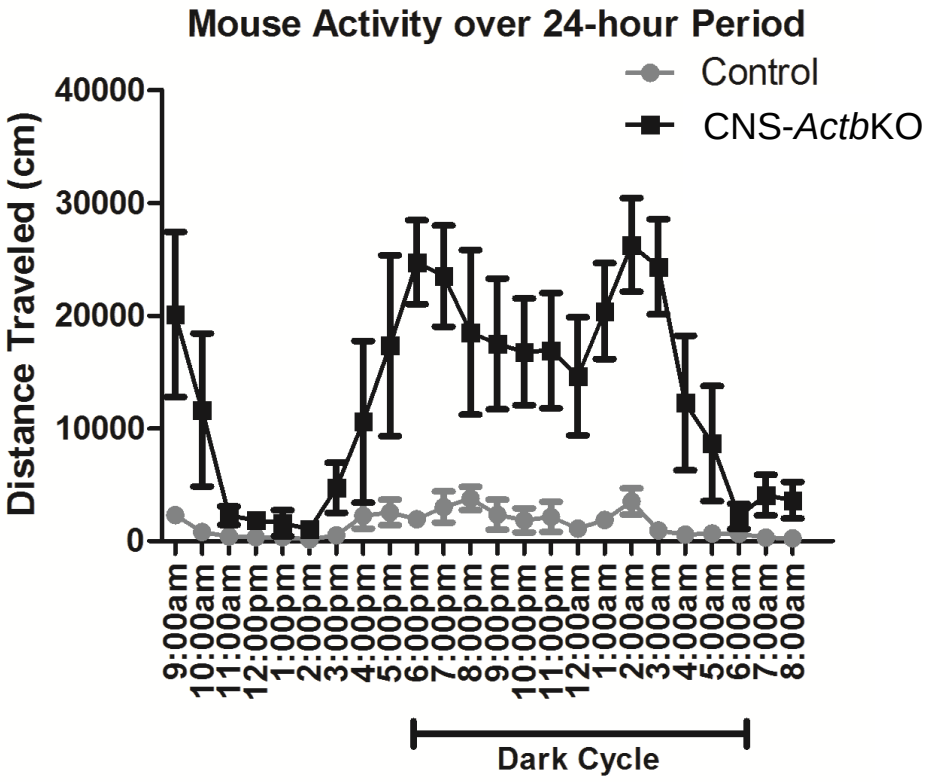

Figure A.3: Activity of control and CNS-*Actb*KO over a 24-hour period CNS-*Actb*KO mice were significantly more active than controls over a 24-hour time period but showed fluctuations in activity consistent with the normal circadian rhythm of mice. Data represents mean ± standard error of the mean (S.E.M.). *n*=4 mice per genotype.

Analysis of Olfactory Discrimination in CNS-*Actb*KO mice

Maternal behavior is a complex behavioral paradigm in mice involving multiple cognitive and physical aspects (Leckman and Herman, 2002; Gammie, 2005; Numan, 2007). However, olfactory function in particular is believed to be a critical component of pup recognition and proper maternal behavior (Kinsley and Bridges, 1990; Kendrick et al., 1997). Given that neurogenesis and remodeling of olfactory circuits are dramatically increased during pregnancy (Shingo et al., 2003), and that β-actin is thought to have important functions in cell division and directed cell migration (Shestakova et al., 2001; Dugina et al., 2009), it is possible that perturbed olfactory neurogenesis during pregnancy adversely effects neural circuits responsible for pup recognition, which together may explain the impaired pup retrieval and high pup mortality observed with CNS-*Actb*KO females (Chapter 3).

Olfactory discrimination is thought to be one physiological function of adult neurogenesis and olfactory circuit remodeling (Gheusi et al., 2000). Therefore, olfactory discrimination was assessed in CNS-*Actb*KO by examining habituation and dishabituation to novel and social odor cues following a protocol previously described (Yang and Crawley, 2009). In this assay, CNS-*Actb*KO mice showed comparable habituation and dishabituation to multiple novel cues and a social odor cue, suggesting that olfactory discrimination is normal in CNS-*Actb*KO mice. Intriguingly, CNS-*Actb*KO mice did not show significant dishabituation to the water control, suggesting that CNS-*Actb*KO mice are not able to recognize the scent of water or that they have a heightened

attraction to it. Given the dramatically increased activity and caloric intake of CNS-*Actb*KO the latter explanation is most likely responsible for the lack of dishabituation of CNS-*Actb*KO mice to water. However, further behavioral and histological experiments will be required to definitively rule out possible olfactory deficits in CNS-*Actb*KO mice.

Figure A.4

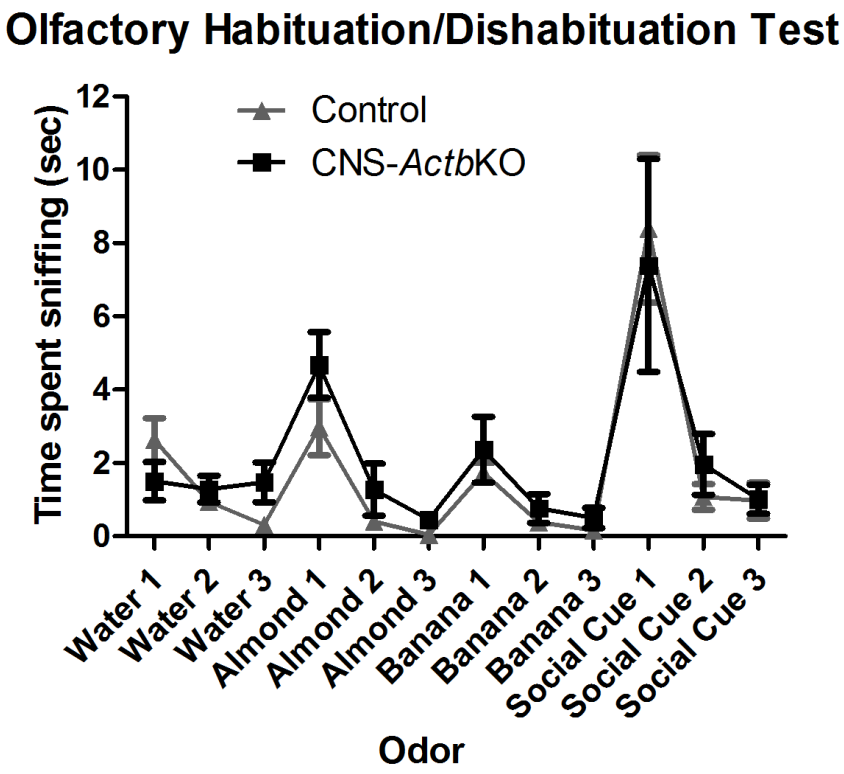

Figure A.4: Analysis of Olfactory Discrimination in CNS-*Actb*KO mice. Control and CNS-*Actb*KO were exposed to novel and social odor cues for three consecutive trials to assess the rate of habituation following repeated exposure to identical odors. Following the third trial, a novel cue was presented to examine dishabituation and recognition of a novel odor. CNS-*Actb*KO mice showed comparable habituation and dishabituation to multiple novel and one social odor cue. However, CNS-*Actb*KO mice failed to show habituation to the water control, indicating an inability to recognize the odor cue or a heightened attraction to it. Date represents mean ± standard error of the mean. *n*=9 animals per genotype.

References

Belyantseva, I.A., B.J. Perrin, K.J. Sonnemann, M. Zhu, R. Stepanyan, J. McGee, G.I. Frolenkov, E.J. Walsh, K.H. Friderici, T.B. Friedman, and J.M. Ervasti. 2009. Gamma-actin is required for cytoskeletal maintenance but not development. *Proc.Natl.Acad.Sci.U.S.A.* 106:9703-9708. doi: 10.1073/pnas.0900221106.

Bunnell, T.M., and J.M. Ervasti. 2010. Delayed embryonic development and impaired cell growth and survival in Actg1 null mice. *Cytoskeleton (Hoboken).* 67:564-572. doi: 10.1002/cm.20467.

Dugina, V., I. Zwaenepoel, G. Gabbiani, S. Clement, and C. Chaponnier. 2009. Beta and gamma-cytoplasmic actins display distinct distribution and functional diversity. *J.Cell.Sci.* 122:2980-2988.

Gammie, S.C. 2005. Current models and future directions for understanding the neural circuitries of maternal behaviors in rodents. *Behav.Cogn.Neurosci.Rev.* 4:119-135. doi: 10.1177/1534582305281086.

Gheusi, G., H. Cremer, H. McLean, G. Chazal, J.D. Vincent, and P.M. Lledo. 2000. Importance of newly generated neurons in the adult olfactory bulb for odor discrimination. *Proc.Natl.Acad.Sci.U.S.A.* 97:1823-1828.

Greising, S.M., R.S. Carey, J.E. Blackford, L.E. Dalton, A.M. Kosir, and D.A. Lowe. 2011. Estradiol treatment, physical activity, and muscle function in ovarian-senescent mice. *Exp.Gerontol.* doi: 10.1016/j.exger.2011.04.006.

Hofer, D., W. Ness, and D. Drenckhahn. 1997. Sorting of actin isoforms in chicken auditory hair cells. *J.Cell.Sci.* 110 (Pt 6):765-770.

Kendrick, K.M., A.P. Da Costa, K.D. Broad, S. Ohkura, R. Guevara, F. Levy, and E.B. Keverne. 1997. Neural control of maternal behaviour and olfactory recognition of offspring. *Brain Res.Bull.* 44:383-395.

Kinsley, C.H., and R.S. Bridges. 1990. Morphine treatment and reproductive condition alter olfactory preferences for pup and adult male odors in female rats. *Dev.Psychobiol.* 23:331-347. doi: 10.1002/dev.420230405.

Leckman, J.F., and A.E. Herman. 2002. Maternal behavior and developmental psychopathology. *Biol.Psychiatry.* 51:27-43.

Micheva, K.D., A. Vallee, C. Beaulieu, I.M. Herman, and N. Leclerc. 1998. beta-Actin is confined to structures having high capacity of remodelling in developing and adult rat cerebellum. *Eur.J.Neurosci.* 10:3785-3798.

Numan, M. 2007. Motivational systems and the neural circuitry of maternal behavior in the rat. *Dev.Psychobiol.* 49:12-21. doi: 10.1002/dev.20198.

Plantier, M., E. Der Terrossian, and A. Represa. 1998. Beta-actin immunoreactivity in rat microglial cells: developmental pattern and participation in microglial reaction after kainate injury. *Neurosci.Lett.* 247:49-52.

Rybakova, I.N., J.R. Patel, and J.M. Ervasti. 2000. The dystrophin complex forms a mechanically strong link between the sarcolemma and costameric actin. *J.Cell Biol.* 150:1209-1214.

Shestakova, E.A., R.H. Singer, and J. Condeelis. 2001. The physiological significance of beta -actin mRNA localization in determining cell polarity and directional motility. *Proc.Natl.Acad.Sci.U.S.A.* 98:7045-7050. doi: 10.1073/pnas.121146098.

Shingo, T., C. Gregg, E. Enwere, H. Fujikawa, R. Hassam, C. Geary, J.C. Cross, and S. Weiss. 2003. Pregnancy-stimulated neurogenesis in the adult female forebrain mediated by prolactin. *Science.* 299:117-120. doi: 10.1126/science.1076647.

Weinberger, R., G. Schevzov, P. Jeffrey, K. Gordon, M. Hill, and P. Gunning. 1996. The molecular composition of neuronal microfilaments is spatially and temporally regulated. *J.Neurosci.* 16:238-252.

Yang, M., and J.N. Crawley. 2009. Simple behavioral assessment of mouse olfaction. *Curr.Protoc.Neurosci.* Chapter 8:Unit 8.24. doi: 10.1002/0471142301.ns0824s48.